JPRS L/9524

4 February 1981

USSR Report

METEOROLOGY AND HYDROLOGY

No. 9, September 1980

FBIS FOREIGN BROADCAST INFORMATION SERVICE

FOR OFFICIAL USE ONLY

APPROVED FOR RELEASE: 2007/02/08: CIA-RDP82-00850R000300080007-3

NOTE

JPRS publications contain information primarily from foreign newspapers, periodicals and books, but also from news agency transmissions and broadcasts. Materials from foreign-language sources are translated; those from English-language sources are transcribed or reprinted, with the original phrasing and other characteristics retained.

Headlines, editorial reports, and material enclosed in brackets [] are supplied by JPRS. Processing indicators such as [Text] or [Excerpt] in the first line of each item, or following the last line of a brief, indicate how the original information was processed. Where no processing indicator is given, the information was summarized or extracted.

Unfamiliar names rendered phonetically or transliterated are enclosed in parentheses. Words or names preceded by a question mark and enclosed in parentheses were not clear in the original but have been supplied as appropriate in context. Other unattributed parenthetical notes within the body of an item originate with the source. Times within items are as given by source.

The contents of this publication in no way represent the policies, views or attitudes of the U.S. Government.

APPROVED FOR RELEASE: 2007/02/08: CIA-RDP82-00850R000300080007-3

JPRS L/9524

4 February 1981

USSR REPORT

METEOROLOGY AND HYDROLOGY

No. 9, September 1980

Translation of the Russian-language monthly journal METEOROLOGIYA I GIDROLOGIYA published in Moscow by Gidrometeoizdat.

CONTENTS

UDC 551.50(212.7)(575)

GLOBAL AEROSOL-RADIATION EXPERIMENT

Moscow METEOROLOGIYA I GIDROLOGIYA in Russian No 9, Sep 80 pp 5-11

[Article by K. Ya. Kondrat'yev, Corresponding Member USSR Academy of Sciences, Candidates of Physical and Mathematical Sciences V. I. Binenko, L. R. Dmitriyeva-Arrago and N. Ye. Ter-Markaryants, Candidate of Geographical Sciences V. F. Zhvalev, V. A. Ivanov and M. A. Prokof'yev, Main Geophysical Observatory, manuscript submitted 5 Feb 80]

[Text]

Abstract: On the basis of the results of the CAENEX, GATE and BOMEX experiments the authors formulate a multisided program for the Global Aerosol-Radiation Experiment (GAAREX) and its scientific objectives. The article presents the first results of expeditions carried out under the GAAREX program in 1977-1979 and presents the plan for implementation of GAAREX in three principal directions: "Desert," "Volcano" and "Cloud."

Introduction. An analysis of the present-day status of the theory of climate shows that an adequate theory can be formulated only on the basis of correct modeling of general circulation of the atmosphere (GCA) with allowance for different forms of heat and moisture exchange in the atmosphere [1-3, 10].

At the center of the problem of present-day changes in global climate is the question of the influence exerted on climate by variations in atmospheric composition. The physical content of the problem is reduced to the task of ascertaining the influence of variations of composition on the radiant heat influx, in which the main role is played by aspects of the problem related to the study of cloud cover, aerosol and optically active gas components of the atmosphere.

The present-day status of the theory of radiation transfer in the atmosphere is characterized by an abundance of diverse methods, from very approximate to virtually precise, allowing "standard" computations of the fluxes and influxes of radiant energy. However, the complexity of the real atmosphere, determined by the irregularity of spatial structure and variability of the properties of aerosol and cloud cover, makes it very difficult to take into account radiation factors on the

basis of "pure" theory and makes it necessary to develop methods for a semi-empirical parameterization. A solution of this problem is possible on the basis of regularization of computation methods by their comparison with experimental data and development of methods for the parameterization of radiation effects.

This problem is becoming particularly timely in connection with the development of the physical theory of climate transpiring within the framework of the World Climatic Research Program and the necessity for ascertaining the factors determining recent climatic changes, including anthropogenic influences.

In the further development of the physical theory of climate the use of experimentally validated data on the radiation properties of clouds, atmospheric aerosol and their interrelationships is of fundamentally great importance. Such a well-known fact that the atmosphere is a colloid and not a purely gas medium has not yet found adequate reflection in investigations of the thermal regime and dynamics of the atmosphere.

The results of investigations of recent years indicate a strong variability of the field of concentration of aerosol in the free atmosphere and great variations in the optical characteristics of aerosol. At the same time, a fact which has become very clear is that aerosol, like cloud cover, is one of the principal factors determining radiation transfer in the atmosphere, especially short-wave radiation.

The noted variability of the concentration field and the optical properties of aerosol at a global scale complicates the development of the theory of formation of global aerosol and the possibility of adequate parameterization of its climatic effects. The development of this type of parameterization methods is possible only on the basis of obtaining considerably more complete information on the concentration field and the properties of global aerosol.

Specialists in the USSR and in the United States have now carried out a series of experiments partially satisfying the goals of aerosol-radiation research [7, 11, 14-16]. The first truly multisided investigation of this type was the Complex Energy Experiment (CAENEX), carried out in 1970-1975 by a number of scientific institutes of the State Committee on Hydrometeorology, USSR Academy of Sciences and USSR Ministry of Higher Education under the direction of and with the participation of the Main Geophysical Observatory imeni A. I. Voyeykov. The pioneering character of these investigations was widely recognized abroad and the CAENEX experiment now serves as a basis in the planning and organization of multisided experiments for the study of atmospheric energetics. However, the results obtained in the mentioned experiments can be regarded only as a first approximation in solving the formulated problem as a result of their incompleteness and the difficulties sometimes arising in comparing the results. In particular, the experience in carrying out GATE indicated how important methodological problems (ensuring completeness and comparability of the results) are in complex experiments of this type.

Principal Results of Aerosol-Radiation Research Under the CAENEX, GATE and BOMEX Programs

The distinguishing characteristic of the mentioned national and international experiments of recent years was their multisided character, which made it possible to obtain simultaneous data on both the aerosol and radiation characteristics of the atmosphere.

Laboratory experiments and chemical analysis of samples of atmospheric aerosol made it possible to determine the optical constants of matter in the disperse phase of an aerosol and the limits of variability of these constants in dependence on the chemical composition of the aerosol and relative humidity [4-6, 11].

The investigations which have been made yielded much material on the spatial-temporal structure, chemical composition and microstructure of aerosol [7, 8, 12]. Estimates have been made of the intensity of different sources of atmospheric aerosol [15, 16]. Unfortunately, it must be noted once again that the indicated materials are rather contradictory due to their selective character and the lack of unified methods.

Radiation measurements have confirmed the presence of selective aerosol absorption of short-wave radiation. Under definite conditions its value is comparable to the absorption of radiation by optically active gas components or even exceeds it. Data have been obtained on the transformation of the vertical profiles of radiation heat influxes in the atmosphere in the presence of an absorbing aerosol, continuous and partial cloud cover. These results were obtained for a number of typical underlying surfaces and some climatic zones.

The problem of ascertaining the influence of aerosol on climate requires the collection of data on all the principal types of atmospheric aerosol, including its macro- and microphysical characteristics over typical underlying surfaces during different seasons. The mentioned data must meet the requirements of completeness and closure from the point of view of the problem of atmospheric energetics in general and radiation transfer in an atmosphere containing aerosol, in particular. Types of aerosol having a global or extensive regional propagation and exerting an appreciable influence on the atmospheric radiation field are of particular interest in this respect: arid aerosol, volcanic aerosol, anthropogenic aerosol, stratiform cloud cover.

Since at the present time many available data do not have adequate completeness and closure, the statistical support of the results is low, and no observations have been made at all under some typical conditions. For example, there is a total lack of data on the spatial structure and properties of atmospheric aerosol during winter. There is extremely limited information on the radiation properties of arctic stratiform cloud cover, on the interaction between cloud cover and aerosol, on the possible mechanisms of modulation of cloud cover as a result of the spatial variability of radiation heat influxes in the free atmosphere.

Program of Global Atmospheric Aerosol-Radiation Experiment (GAAREX)

Taking into account what has been said above, in the coming years it seems desirable, within the framework of the World Climatic Research Program, to develop a broad complex program of aerosol-radiation investigations whose scientific goals can be formulated in the following way:

1. Investigations of the radiation characteristics of the "underlying surface-atmosphere" system (especially the albedo of the system, the distribution of absorbed radiation between the atmosphere and the underlying surface, radiant heat

exchange, etc.) and their variability in different climatic zones, bearing in mind the objective of creating an empirical basis for the parameterization of radiation processes.

2. Investigations of the field of concentration of atmospheric aerosol, microstructure, chemical composition, complex refractive index and variability of these characteristics in different climatic zones; estimation of the contribution of different factors to the formation of the principal components of global aerosol; construction of a model of global aerosol.

3. Investigations of atmospheric composition (optically active small gas components and aerosol), its influence on radiation transfer and possible climatic effects (a joint allowance for the influence of aerosol and associates of water molecules is of great importance).

4. Laboratory and theoretical investigations of the formation of the spectrum of aerosol particles, their optical characteristics.

5. Laboratory and theoretical investigations of the processes of formation of the gas and aerosol composition of the stratosphere.

6. Development and use of ground, aircraft and satellite methods for the remote sensing of aerosol with the intention of the most complete determination of its properties.

7. Development and use of direct and indirect methods for investigating the microphysical and optical parameters of clouds (particular attention must be devoted to the problem of cirrus clouds).

8. Comparison of the results of field and laboratory investigations of different aerosol systems.

9. Development of approximate methods for computing the radiation characteristics of the real atmosphere, intended for the parameterization of radiation processes in the numerical modeling of general circulation of the atmosphere and the theory of climate.

In this connection there must be:

a) development of models of the vertical distribution of the optical properties of aerosol systems characteristic for regions with different properties of the underlying surface;
b) determination of the integral transmission functions for the aerosol component of the atmosphere on the basis of measurements under real and laboratory conditions;
c) development of methods for computing radiation of heat influxes attributable to the influence of aerosol suitable for inclusion in a model of general circulation of the atmosphere and climate;
d) implementation of numerical experiments with models of general circulation of the atmosphere and climate for study of their response to variations of aerosol properties of the atmosphere.

10. Theoretical investigations of radiation transfer in the real atmosphere on the basis of use of "precise" methods and comparison of the results of computations with experimental data.

11. Numerical modeling of general circulation of the atmosphere and climate for the purpose of evaluating response to radiation factors and development of optimum schemes for their parameterization.

Similar proposals were formulated earlier in the review [9], in which the proposed program was called the Global Aerosol-Radiation Experiment (GAAREX).

It is understandable that solution of the scientific tasks of GAAREX is not within the capabilities of any single institute, but possibly only on the basis of a broad and effective cooperation among a whole series of institutes of the State Committee on Hydrometeorology, USSR Academy of Sciences and the USSR Ministry of Higher Education. Considerable experience in such cooperation has been accumulated by the Main Geophysical Observatory during the time of carrying out of CAENEX, when field investigations were carried out at agreed-upon times by groups of specialists from different scientific institutes of the USSR Academy of Sciences in conformity to a unified program directed to ensuring maximum complexity of the collected set of data. In the mentioned investigations the Main Geophysical Observatory played the role of a methodological and coordinating center for directing the experiment, on its part carrying out a considerable part of the special, particularly aircraft observations.

Taking into account the experience of joint investigations in the CAENEX and GATE expeditions, as well as the scientific specialization of the corresponding institutes and establishments, it is desirable that in GAAREX a role be played by the Arctic and Antarctic Scientific Research Institute, Leningrad State University, Institute of Experimental Meteorology, Institute of Atmospheric Physics USSR Academy of Sciences, Institute of Atmospheric Optics Siberian Department USSR Academy of Sciences, Institute of Atmospheric Physics Kazakh Academy of Sciences and regional scientific research institutes of the State Committee on Hydrometeorology. The Main Geophysical Observatory (Radiation Research Section) can assume the role of the coordinating and directing institute in the organization and implementation of multisided field investigations under the GAAREX program.

The GAAREX program was part of the national efforts of the USSR within the framework of the program of special observations in the global meteorological experiment.

In order to ensure actual global coverage it is necessary that in the future GAAREX assume the character of an international program. Such a need is dictated both by the properties of the object of the proposed investigations itself (in particular, the need for carrying out observations under conditions not encountered in the USSR), but also by the fact that international cooperation will make possible the most complete satisfaction of the requirements of complexity of the measurements carried out.

Such cooperation with specialists in the United States is being carried out by the Soviet-American Working Group VIII on the "Influence of the Environment on Climate." It should be noted that the need for international cooperation in the

field of investigations of atmospheric aerosol and its influence on climate has also been noted by key foreign specialists in the mentioned field [13], and was also expressed during the creation of two working groups of the committe organizing research on global atmospheric processes: "Aerosol and Climate" and "Radiation and Extensive Cloud Cover."

Radiation processes occupy an important place in the program of still another working group of the committee organizing research on global atmospheric processes: "Processes on the Land and Their Parameterization in Models of General Circulation of the Atmosphere."

The specific implementation of the GAAREX program has already been initiated and is being carried out in the following way:

1) The first experiment under the GAAREX program was carried out in the Karakum region in 1977. Extensive, multisided data were obtained on the aerosol composition, radiation and optical characteristics of the atmosphere. The object of the investigations was dust storms as a factor forming the regional climate of arid zones.

2) Two complex expeditions under the GAAREX program were successfully carried out during 1979 when implementing the first and second special observation periods of GARP. The GAAREX-79-I expedition was carried out in February-March in the Karakum region and GAAREX-79-II in May-June in the Arctic, jointly with the SP-22 drifting station, and in the region of Kamchatkan volcanoes.

The principal objective of the GAAREX-79-I expedition was investigations of the influence of the aerosol of deserts on the radiation regime of the atmosphere. The results of this expedition confirmed the conclusions which we drew on the basis of data from earlier experiments carried out in the desert. The desert region is characterized by a stability of the form of size distribution of aerosol particles. With a stability of the form of this distribution there are considerable variations in the concentration of particles. The stability of microstructure facilitates formulation of a model of aerosol for the deserts.

The complex use of the results of aerosol measurements at a ground point and on an IL-18 aircraft laboratory of the Main Geophysical Observatory made it possible to study the peculiarities of the vertical profiles of aerosol concentration under different atmospheric conditions (in clear weather and in the absence of strong winds, in the case of an adequately turbid atmosphere and during dust storms), and also to find the relationship between these distributions and profiles of the components of the radiation heat influx. Analysis of data on the change in the disperse composition of aerosols with altitude indicated a constancy of the bimodal structure of the distribution. A second minimum is common for all the distributions and falls in the size range 8-10 μm.

On the expedition specialists carried out measurements of the chemical composition of aerosol in different ranges of particle sizes with the use of a multicascade impactor which are very important for further theoretical computations.

An investigation of the dependence of the aerosol concentration on wind velocity was also made. The experimental data will be used in carrying out theoretical computations of the transfer of short-wave radiation in the dust-filled atmosphere for the purpose of formulating forms of parameterization of the radiation effects of aerosol, and also for computing the possible diurnal variations of the radiation heat influxes characteristic for the atmosphere in the desert region.

The results of the expedition are of great importance for a sufficiently reliable allowance for the atmosphere as a colloid in models of general circulation of the atmosphere and the theory of climate.

The principal purpose of the second expedition, GAAREX-79-II, was a study of the processes of formation of extensive stratiform cloud cover in the Arctic (over SP-22) in summer and the radiation properties of the products of volcanic eruptions. On Kamchatka experimental investigations of the dynamics of fog and low cloud cover were supplemented by numerical modeling on the basis of the collected data. Investigations of the ice-water radiation contrasts were made in this experiment. On Kamchatka, in the neighborhood of Aldair and Cheringotan Islands, the radiation regime of the atmosphere was investigated on Chepurachek volcano during a period of fumarole activity of volcanoes during clear weather and in the presence of a continuous cloud cover.

3) By way of making preparations for the GAAREX-79-II expedition, in December 1978 aircraft measurements were made over the cities of Zaporozh'ye and Donetsk from IL-18 and IL-14 flying laboratories for the purpose of study of the influence of anthropogenic aerosol on the radiation properties of clouds below an inversion.

The following questions were raised in this experiment:
-- How does the aerosol in a cloud exert an influence on the radiation regime of the atmosphere over a city?
-- What is the role of nucleus formation and what aerosols are most important and active in this process?
-- How are the microphysical properties of a cloud transformed as a result of cloud-aerosol interaction?
-- How great are the radiation effects of soluble and hydrophobic aerosol in comparison with molecular absorption in a cloud?
-- What properties of aerosol are most important to take into account in models of the climate of a city?

The results of this experiment, together with data from investigations of the role of anthropogenic and volcanic aerosol on Kamchatka made it possible to draw important conclusions on the influence of aerosol of anthropogenic origin on the radiation properties of clouds.

4) In August 1979, at Ryl'sk, specialists carried out comparisons of balloon-borne aerosol instrumentation and investigations of the chemical composition of aerosol (especially stratospheric).

The experience in carrying out this sort of comparisons indicates the importance of developing metrological principles for aerosol measurements, the creation of generators of a polydisperse aerosol with known physicochemical properties, the need for carrying out laboratory and field comparisons of aerosol instrumentation. In the future plans call for carrying out the GAAREX program with the

implementation of complex experimental investigations in three principal directions:

1) September-October 1980-1981 -- "Desert" experiment. The planned experiment will make possible a more complete understanding of the factors exerting an influence on the formation of climate in arid zones, as well as a comparison of Soviet and American aerosol instrumentation.

2) 1981-1983 -- "Cloud" experiment. Investigations under this subprogram will make it possible to carry out a thorough comparison of the radiation fields for an atmosphere with pure clouds and clouds subjected to an anthropogenic influence; these will make it possible to formulate a unified approach to the use of experimental and theoretical data in the parameterization of the interaction between clouds and radiation.

3) 1981-1985 -- "Volcano" experiment. The implementation of investigations under this subprogram will make possible:
a) a fuller understanding of the influence of aerosol of volcanic origin on the radiation field in the atmosphere and an evaluation, in particular, of the reliability of the hypothesis of volcanically induced changes in paleoclimate;
b) on the basis of systematic satellite tracking of the state of the stratosphere conclusions can be drawn on the possible reaction of the atmosphere to artificial contamination of the stratosphere by aerosol particles.

The practical implementation of the research programs will be accomplished on the basis of Soviet-American cooperation within the framework of the agreement on preservation of the environment. (Working Group VIII. Project 0.2.08-12 "Influence of Atmospheric Contamination on Climate.")

BIBLIOGRAPHY

1. Blinova, Ye. N., "Hydrodynamic Long-Range Weather Forecasting," METEOROLOGIYA I GIDROLOGIYA (Meteorology and Hydrology), No 11, 1974.

2. GIDRODINAMICHESKAYA MODEL' OBSHCHEY TSIRKULYATSII ATMOSFERY I OKEANA (Hydrodynamic Model of Circulation of the Atmosphere and Ocean), edited by G. I. Marchuk, Novosibirsk, Computation Center Siberian Department USSR Academy of Sciences, 1975.

3. Zuyev, V. Ye., LAZER-METEOROLOG (Laser Meteorologist), 1974.

4. Kondrat'yev, K. Ya., "Aerosol and Climate," TRUDY GGO (Transactions of the Main Geophysical Observatory), No 381, 1976.

5. Kondrat'yev, K. Ya., "Modern Changes in Climate and the Factors Determining Them," ITOGI NAUKI I TEKHNIKI. METEOROLOGIYA I KLIMATOLOGII (Results of Science and Technology. Meteorology and Climatology), Vol 4, VINITI, Moscow, 1977.

6. Kondrat'yev, K. Ya., SPUTNIKOVYY MONITORING KLIMATA: OBZOR VNIIGMI-MTsD (Satellite Monitoring of Climate: Review of the All-Union Scientific Research Institute of Hydrometeorological Information-World Data Center), Obninsk, 1978.

7. Kondrat'yev, K. Ya., et al., KOMPLEKSNYY ENERGETICHESKIY EKSPERIMENT (KENEKS): OBZOR VNIIGMI-MTsD (Complex Energy Experiment (CAENEX): Review of the All-Union Scientific Research Institute of Hydrometeorological Information-World Data Center), Obninsk, 1975.

8. Kondrat'yev, K. Ya., et al., VLIYANIYE AEROZOLYA NA PERENOS IZLUCHENIYA: VOZMOZHNYYE KLIMATICHESKIYE POSLEDSTVIYA (Influence of Aerosol on Radiation Transfer: Possible Climatic Consequences), Leningrad, Izd-vo LGU, 1973.

9. Kondrat'yev, K. Ya., Vasil'yev, O. B., Ivlev, L. S., GLOBAL'NYY AEROZOL'NO-RADIATSIONNYY EKSPERIMENT (GAAREX): OBZOR VNIIGMI-MTsD (Global Aerosol-Radiation Experiment (GAAREX): Review of the All-Union Scientific Research Institute of Hydrometeorological Information-World Data Center), Obninsk, 1976.

10. Marchuk, G. I., Musayelyan, Sh. A., "Methods for Computing Variations of the Total Flux of Radiant Energy for Long-Range Forecasting of Large-Scale Meteorological Fields," METEOROLOGIYA I GIDROLOGIYA (Meteorology and Hydrology), No 8, 1974.

11. POLNYY RADIATSIONNYY EKSPERIMENT (Full Radiation Experiment), edited by K. Ya. Kondrat'yev and Ye. N. Ter-Markaryants, Leningrad, Gidrometeoizdat, 1976.

12. CIAP MONOGRAPHS, CIAP Office, Washington, D. C., Vols 1, 4, 1975.

13. CLIMATE DYNAMICS BOARD. WORKING GROUP ON AEROSOLS AND CLIMATE, Report of the Meeting 7-11 August 1978, NCAR, Boulder, Colorado.

14. Cox, S. K., Kraus, M., THE GATE RADIATION SUBPROGRAM, Field Phase Report, Dept. of Atm. Sci., CSU, Fort Collins, Colorado, January 1975.

15. GLOBAL ATMOSPHERIC AEROSOL RADIATION STUDY, Research Plan. NCAR, Univ. Arizona, Univ. Wisconsin, Univ. Washington, NOAA, 1973.

16. Kuhn, P. M., Stearns, L., "Radiative Transfer Observations During BOMEX," NOAA TECHN. REPT. ERL 203-APCL 19, Boulder, Colorado, 1971.

UDC 551.576(100)

CALCULATION OF THE GLOBAL DISTRIBUTION OF THREE-LEVEL MACROSCALE CLOUD COVER

Moscow METEOROLOGIYA I GIDROLOGIYA in Russian No 9, Sep 80 pp 12-23

[Article by Candidate of Physical and Mathematical Sciences V. P. Meleshko, Main Geophysical Observatory, submitted for publication 2 Apr 80]

[Text]

Abstract: In this article an attempt is made to calculate three-level cloud cover for the entire earth. A method is proposed for calculating cloud cover at three levels in the atmosphere based on solution of the inverse problem for the transport of long-wave radiation. On the basis of use of climatic data on total cloud cover, temperature, humidity and outgoing radiation at the boundary of the atmosphere it was possible to calculate the distributions of the quantity of clouds at three levels in the atmosphere for the conditions prevailing in July. The determined distribution of cloud cover agrees well with both the actual zonal data and with the principal macroscale cloud formations in some regions of the earth, in particular, in the region of the Indian monsoon, ICZ and zone of baroclinic instability.

Introduction. In the modeling of general circulation of the atmosphere and climate by means of hydrodynamic models of the atmosphere it is necessary to have information on the three-dimensional distribution of cloud cover, which in turn is needed for calculating radiation heat influxes. At the present time cloud cover in the models is calculated using relatively simple empirical expressions in which the tenths of cloud cover at a priori stipulated levels is usually related to relative humidity. The corresponding coefficients in these expressions are selected in such a way that the computed mean seasonal distribution of the quantity of clouds will agree with the similar actual distribution. In a number of investigations such a matching was accomplished with the zonal data published by London [9].

The question as to what degree the quantity of clouds computed in the model agrees with the real quantity at different levels in the atmosphere and in different geographical regions of the earth remains open because at the present time there are no climatic data on the three-dimensional distribution of cloud cover. However, a knowledge of the three-dimensional structure of the actual cloud cover is extremely important for improving schemes of its parametric description and for refining methods for calculating heat influxes in atmospheric models.

Information on cloud cover obtained using data from the ground network of stations and using meteorological satellites has been generalized and published in a whole series of investigations [2, 6, 13, 14]. The television images of cloud cover collected during recent years made it possible to supplement and refine available materials from surface observations over the waters of the oceans and in inaccessible regions of the earth. In most cases these data are the mean monthly values of total cloud cover, estimated in tenths or fractions of sky coverage. Source [13] also contains information on the frequency of recurrence of cloud cover of different quantitative gradations, expressed in relative brightnesses.

With respect to data on the quantity of clouds at different levels, they are extremely scarce, and if they exist, are available only for individual, adequately well-studied regions of the northern hemisphere. For example, maps of the seasonal distribution of the ratio of lower cloud cover to total cloud cover over the territory of the USSR are given in [1]. An extensive set of parameters describing the spatial-temporal structure of cloud cover for individual points in the territory of the USSR is given in [3]. Some ideas concerning the vertical extent of large-scale formations can be obtained from [6, 12], which give information on the geographical distribution of the predominant types of clouds. Using information on the frequency of recurrence of clouds of different types, London [9] constructed the zonal distribution of their quantity for the four seasons. At the present time this is, indeed, the only source of climatic data which includes information on both the quantity of clouds and on their vertical extent.

The development of satellite systems for making such observations served as a stimulus for the development and improvement of methods for determining not only total cloud cover, but also the altitude of its upper boundary, as well as other characteristics, on the basis of data from measurements of outgoing long-wave radiation in the transparency window and cloud brightness in the visible spectral region. The methods for determining the temperature of the upper cloud boundary are based on the idea of registry of the thermal contrasts in the field of outgoing radiation between the boundary of the clouds and the underlying surface. The visible spectral range is usually used in evaluating the total quantity, thickness and phase state of the clouds on the basis of an analysis of the brightness contrasts. A thorough review of investigations in this direction is given in the two monographs of K. Ya. Kondrat'yev and Yu. M. Timofeyev [4, 5]. It must be noted that existing satellite methods for the time being are in the testing stage and therefore no other generalized data have yet been published for the earth (or even for the northern hemisphere) other than for total cloud cover.

In this study an attempt has been made to compute the vertical distribution of large-scale cloud cover, using for this purpose climatic data on total cloud cover, outgoing radiation at the upper boundary of the atmosphere, temperature and humidity.

The quantity of clouds is computed for three altitudes, which on the average correspond to the upper boundary of clouds of the upper, middle and lower levels. The computation method is based on the identification of the thermal contrasts in the field of outgoing radiation between the clouds, situated at stipulated

levels in the troposphere, and the underlying surface.

In this study we made computations of the global distribution of three-level cloud cover for July.

Method for Computing the Quantity of Clouds

We will examine a column of the atmosphere of a unit area and extent from the ground surface to the upper boundary of the atmosphere. We will assume that in a column at different altitudes from the ground surface there are K layers with incomplete cloud cover, so that the total quantity of clouds (in fractions of a unit area) $\tilde{N}$, visible from the upper boundary of the atmosphere, is equal to

$$\sum_{k=1}^{K} N_k = \tilde{N}. \tag{1}$$

Here N_k is the fraction of a unit area covered by clouds of the k-th layer which the observer could see if he was at the upper boundary of the atmosphere. With $N_k = 1$ the considered area is completely covered by clouds.

The total flux of outgoing radiation at the boundary of the atmosphere $\tilde{R}$ consists of fluxes emanating from the cloud sectors, visible below, situated at different levels, the part of the underlying surface not covered by clouds and the radiation of the atmospheric layers falling between the radiating surfaces and the upper boundary of the atmosphere,

$$\sum_{k=0}^{K} N_k R_k = \tilde{R}. \tag{2}$$

Here $N_0 = 1 - \tilde{N}$ is the fraction of the unit area free of clouds, R_k is the flux of radiation reaching the upper boundary in the presence of total cloud cover at the level k. The expression for the integral flux R_k can be written in the form

$$R_k = B(T_k)\, D(m_k) + \int_0^{m_k} B(T)\, dD(m_k - m), \tag{3}$$

where B(T) is the radiation function at the temperature T, $D(m_k)$ is the integral transmission function with an effective mass m_k.

The first term on the right-hand side describes the part of the radiation from the cloud surface or from the underlying surface reaching the boundaries of the atmosphere. The second characterizes the radiation of the atmospheric layer situated between the radiating surface and the boundary of the atmosphere.

Now we will determine the properties of large-scale cloud formations which in a general case can include several of the considered unit areas.

1. Here and in the text which follows it will be assumed that clouds exist at only three levels in the atmosphere. This corresponds to their generally accepted division into clouds of the upper, middle and lower levels.

2. The altitude of the upper cloud boundary is known. For the cloud cover of the middle and lower levels it is situated at the levels 700 and 925 mb respectively. The boundary of the upper-level clouds is a function of latitude. In both hemispheres from the pole to latitude 48° it is situated at the level 500 mb; then

gradually increases and from a latitude of 28° to the equator is situated at the 300-mb level.

3. The horizontal distribution of cloud cover at each level in an elementary area is random, so that the probability of their mutual overlapping is equal to the product of their quantities at the corresponding levels. Thus, the fraction of cloud cover visible from above is related to their quantity by means of the expressions

$$\begin{aligned} N_1 &= n_1, \\ N_2 &= (1-n_1)\,n_2, \\ N_3 &= (1-n_1)\,(1-n_2)\,n_3. \end{aligned} \tag{4}$$

Here and in the text which follows n_k (k = 1, 2, 3) is the quantity of clouds at the k-th level (in fractions of unity).

4. Clouds of the upper, middle and lower levels radiate as ideally black bodies with the temperature at their upper limits.

5. Clouds of the middle and lower levels are quite dense and do not transmit long-wave radiation from the lower-lying layers of the atmosphere. The upper-level clouds are assumed to be partially transparent.

6. The contribution of the nonlinear errors arising as a result of use of atmospheric characteristics averaged in time and space for computing the mean radiation fluxes is negligible.

The algebraic equations (1) and (2) contain three unknown functions N_k(k = 1, 2, 3). Still another equation is required for closing the system. As such an equation it is possible to use an expression similar to (2) but describing the transfer of fluxes of reflected short-wave radiation. This requires the inclusion of a number of additional assumptions relative to the reflecting and transmitting properties of clouds following from the theory of transfer of short-wave radiation in the cloudy atmosphere.

In this study we examine a simpler approach whose basis is the use of an empirical relationship between the quantity of clouds and relative humidity at the two lowest levels in the atmosphere. In other words, we will assume that the ratio of the quantity of clouds of the middle and lower levels is proportional to the ratio of the relative humidities at the corresponding levels (layers) in the atmosphere:

$$\frac{n_2}{n_3} = \beta \frac{h_2}{h_3}, \tag{5}$$

where h_2, h_3 are the relative humidities in the layers of clouds of the middle and lower levels, β is an empirical proportionality factor ($0<\beta\leqslant 1$).

With allowance for the properties of clouds enumerated above, equations (1), (2) and (5) are rewritten in the form

$$\left.\begin{aligned} &\sum_{k=1}^{3} N_k = \tilde{N} \\ &\sum_{k=1}^{3} \alpha_k (R_k - R_0) N_k = \tilde{R} - R_0 - \sum_{k=1}^{3} \delta R_k \\ &(1 - n_2) \delta \frac{h_2}{h_3} N_2 = N_3 \end{aligned}\right\}, \tag{6}$$

where α_k characterizes the degree of transparency of clouds at the k-th level.

When $\alpha_k = 1$ the clouds are opaque for long-wave radiation.

Since we assume that only upper-level clouds are partially transparent, then

$$\begin{aligned} \delta R_1 &= (1 - \alpha_1)[(R_2 - R_0)\, n_1 n_2 + (R_3 - R_0)(1 - n_2)\, n_1 n_3], \\ \delta R_2 &= \delta R_3 = 0. \end{aligned} \tag{7}$$

The system of equations (6) is closed and can be solved by the iterations method if the fluxes R_0, R_1, R_2, R_3, $\tilde{R}$ and the total quantity of clouds N are known.

The fluxes of outgoing radiation at the boundary of the atmosphere were computed using the radiation scheme developed at the Geophysical Hydrodynamics Laboratory at Princeton in the United States. Its description is given in the studies of Manabe and Strickler [10] and Manabe and Wetherald [11]. Computations of fluxes of long-wave radiation are made using this scheme, taking into account the distribution of water vapor, carbon dioxide and ozone. The mixture ratio for carbon dioxide is assumed equal to $0.456 \cdot 10^{-3}$ in mass. The ozone distribution is also stipulated and is dependent on season, altitude and latitude.

It should be noted that the system of equations (6) is poorly stipulated in the case of temperature gradients close to isothermal or when there is a thick inversion in the lower troposphere. From the physical point of view this means that as a result of small or zero contrasts in long-wave radiation between the cloud cover of different levels it is impossible to make an unambiguous determination of the vertical structure of clouds. On the other hand, numerous observations of cloud cover show (for example, see [3]) that in the middle and high latitudes of the northern hemisphere under conditions close to isothermal or an inversion (as a rule such conditions are observed during the cold season of the year) the cloud cover is formed only in the lowest layer of the atmosphere. Thus, under these conditions it is not necessary to solve the system of equations (6) and it can be assumed that the entire (total) cloud cover is concentrated only at the lowest level.

The algorithm realizing computation of three-level cloud cover includes a number of stages in which there is successive determination of the possibility of the existence or absence of cloud cover at different levels. In the first stage, as a result of solution of the system of equations (6) by the successive approximations method, N_k is found. Choice of the initial approximation exerts virtually no influence on the rate of convergence of the iteration process.

The solution must satisfy the natural condition

$$0 \leq N_k < 1{,}0. \tag{8}$$

If this condition is not satisfied at one of the levels, a solution is sought for two other levels, beginning with the lower levels. In this case the third expression in (6) is not used in the solution. Finally, if once again condition (8) is not satisfied at one of the two levels the quantity of clouds at the other (of the two considered) level is assumed to be equal to their total quantity. Thus, the determined vertical distribution of the quantity of clouds is always equal to the total cloud cover in accordance with condition (4), whereas the long-wave radiation, computed with these clouds taken into account, agrees with that stipulated at the upper boundary of the atmosphere, except for cases of a single-level cloud cover, when the latter condition is satisfied approximately.

Initial Data

The restoration of the vertical distribution of clouds is accomplished over the entire earth for July conditions. As the initial data we used the following.

1. The distribution of the total quantity of clouds constructed by T. G. Berlyand and L. A. Strokina [2]. For the latitude zone 60-90°S the data on the total cloud cover were taken from [15]. These data were obtained using materials from long-term observations at stations in the world meteorological network and for individual poorly studied regions of the earth were supplemented by satellite measurements. Figure 1 shows the distribution of total cloud cover used in the computations.

2. Mean monthly data on outgoing long-wave radiation at the upper boundary of the atmosphere at the points of intersection of a regular grid 10°x 10°. These data represent the generalized results of July satellite measurements during 1964-1970 published in [16].

3. Mean monthly temperature and dew point values stipulated at standard levels in the atmosphere (temperature at the levels 100, 200, 300, 500, 700, 850, 1000 mb, but humidity only at the four lower atmospheric levels) at the points of intersection of a regular grid 5° x 5°. Information on this mass of data can be found in [7, 8].

The temperature and humidity values at 13 levels in the atmosphere were used in computing the radiation fluxes. Since climatic data on humidity are available only to the 500-mb level, the values corresponding to them for higher levels were obtained by means of extrapolation. At the level 100 mb and above the humidity values were assumed to be $3 \cdot 10^{-6}$ g/g at all latitudes. The temperature at the additional intermediate levels (50, 250, 400, 600, 775 and 925 mb) was obtained as a result of interpolation from standard levels.

The restoration of the vertical distribution of cloud cover was at the points of intersection of a regular grid with a resolution 5° x 5°.

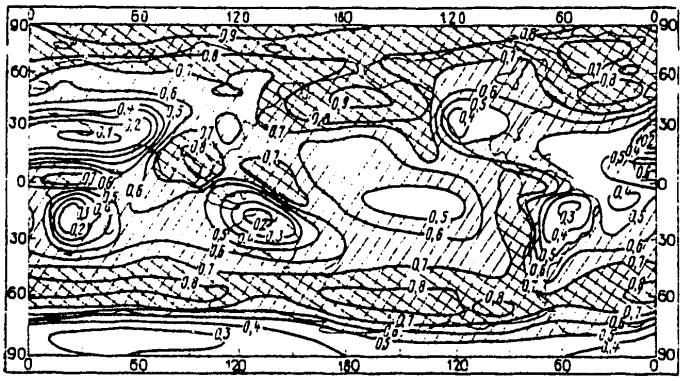

Fig. 1. Observed distribution of total cloud cover (in fractions of unity) in July (data from T. G. Berlyand and L. A. Strokina [2]).

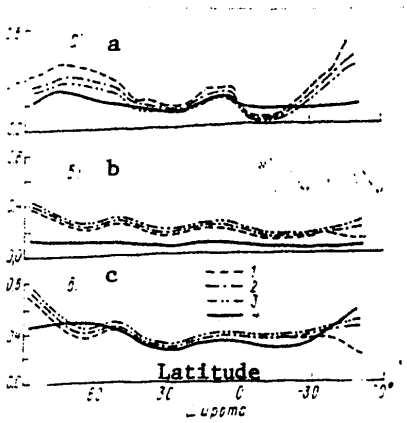

Fig. 2. Zonal distribution of computed and actual cloud cover (in fractions of unity) for upper (a), middle (b) and lower (c) levels. 1) computed cloud cover with $\alpha = 0.75$; 2) with $\alpha = 0.9$; 3) with $\alpha = 1.0$; 4) actual cloud cover according to data published by London [9].

Although the horizontal resolution for satellite radiation fluxes is less in comparison with other stipulated characteristics, we will assume that the field of fluxes contains adequate useful information necessary for restoring the vertical structure of the large-scale cloud cover.

Results of Computations

In solving the system of equations (6) it is necessary to stipulate the parameters α_1 and β. As already noted, the first of these characterizes the degree of transparency of upper-level clouds for long-wave radiation. As a result of the known

uncertainty in its stipulation the computations were first made with α_1 = 0.75, 0.90, 1.0.

Figure 2 shows the zonal distributions of the computed and actual cloud cover of the upper, middle and lower levels. The computations were made using the zonal distributions of outgoing radiation, total cloud cover, temperature and humidity in July. As a comparison, this same figure shows the actual distributions of cloud cover obtained in [9] for the warm season of the year.

It follows from Fig. 2 that the computed cloud covers of the upper and lower levels agree surprisingly well with the actual data published by London [9] for the northern hemisphere with α_1 = 1.0. However, in the southern hemisphere they differ essentially from one another, especially in the latitude zone 30-60°S. The computed middle-level cloud cover was everywhere approximately twice as great as the actual cloud cover. The considerable discrepancies between the computed and actual cloud covers in the middle latitudes of the southern hemisphere are evidently attributable to the presence of systematic errors in the climatic distribution of temperature, humidity and cloud cover (total and at different levels). Errors in the determination of outgoing radiation do not play a significant role because their value in the southern hemisphere is of the same order of magnitude as in the northern hemisphere where the computed cloud cover agrees well with the observed cloud cover.

In order to clarify the possible reasons for the exaggeration of the upper cloud cover in the zone 30-60°S we made estimates of the sensitivity of the computed cloud cover to the possible errors in determining temperature and humidity in this zone. As indicated by the evaluations which were made, a temperature decrease by only 2°C in the entire troposphere leads to a decrease in the quantity of upper clouds by approximately 25%. The sensitivity of the vertical distribution of clouds to variations of humidity is less significant, evidently as a result of the low moisture content of the southern hemisphere atmosphere during the cold season of the year. One gets the impression that the zonal temperature of the troposphere in this latitude zone is exaggerated on the average by 2-3°C.

The distributions of the quantity of clouds with different degrees of transparency of upper cloud cover show that the best agreement with zonal data is with α = 0.9-1.0. Therefore, in all the computations it was assumed that upper cloud cover transmits 10% of the long-wave radiation. In the computations it was assumed that β = 1.0.

Since the temperature distribution in the troposphere to the south of 60°S is of the inversion type, it was assumed that only lower-level cloud cover can exist in this region.

Now we will examine the problem of the sensitivity of the computed cloud cover to the errors in determining outgoing radiation and the quantity of total cloud cover. According to the careful estimates of Ellis and Vonder Haar [16], the uncertainty in estimates of long-wave radiation from satellites is ±5%, which corresponds to an error ±10 W/m^2.

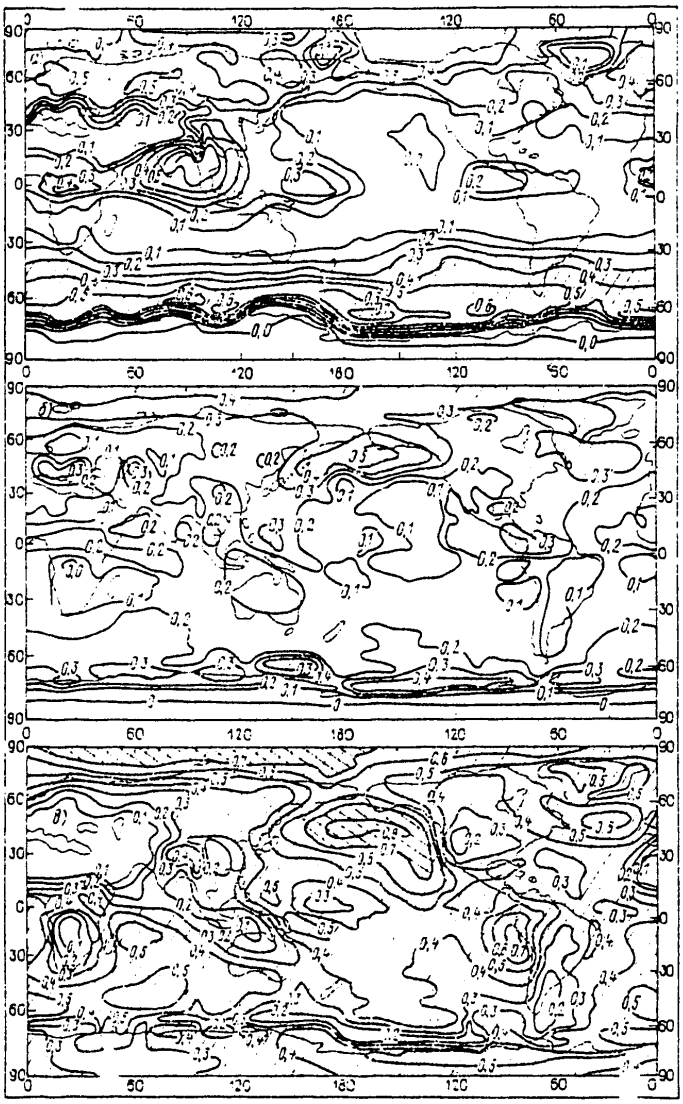

Fig. 3. Geographical distribution of computed cloud cover (in fractions of unity) for the upper (a), middle (b) and lower (c) levels.

Table 1 shows the zonal changes in the quantity of clouds of the upper, middle and lower levels with the mentioned errors superposed on the outgoing radiation. If the error is positive, the upper-level cloud cover decreases, whereas the middle- and lower-level cloud cover increases. The reverse picture is observed in the case of negative errors. Upper-level cloud cover is more sensitive to errors in measuring outgoing radiation than are middle- and lower-level clouds. This is

Table 1

Dependence of Errors in Determining Quantity of Clouds of the Upper, Middle and Lower Levels (in Fractions of Unity) on Error in Determining Outgoing Radiation at the Boundary of the Atmosphere Equal to ±10 W/m^2. (The Numerator Gives the Errors in Determining Cloud Cover Caused by Positive Changes in Radiation, in Denominator -- by Negative Changes)

Cloud level	Latitude, °					
	90	60	30	0	-30	-60
Upper	∓0.22	∓0.21	-0.10/+0.12	-0.10/+0.11	-0.11/+0.33	-0.20/+0.22
Middle	+0.03/-0.06	+0.06/-0.10	+0.03/-0.06	+0.02/-0.05	±0.03	+0.10/-0.13
Lower	+0.04/-0.10	+0.09/-0.15	±0.06	±0.06	+0.06/-0.07	+0.13/-0.27

Table 2

Dependence of Errors in Determining Cloud Cover of Upper, Middle and Lower Levels (in Fractions of Unity) on Error in Determining Total Quantity of Clouds, Equal to ±0.1

Cloud level	Latitude,°					
	90	60	30	0	-30	-60
Upper	∓0.05	∓0.06	∓0.03	∓0.02	∓0.03	∓0.6
Middle	+0.13/-0.11	+0.12/-0.11	±0.07	±0.05	±0.05	+0.10/-0.12
Lower	+0.25/-0.21	+0.18/-0.16	±0.10	±0.11	±0.12	+0.27/-0.30

*The notations are the same as in Table 1.

attributable to the circumstance that the contribution of the lower-lying clouds to the total radiation is less than the contribution of upper-level clouds as a result of the effect of random superpositioning and screening of radiation by upper clouds. With one and the same absolute error in radiation the errors in determining cloud cover increase from the low to the high latitudes. The reason for this is the latitudinal decrease in the mean vertical temperature gradient in the troposphere, which leads to a decrease in the thermal contrasts in the fluxes of outgoing radiation arriving at the boundary of the atmosphere from different layers. For example, the errors in determining the quantity of upper-level clouds are 0.1 in the low latitudes, and gradually increasing, attain 0.2 in the high latitudes. The corresponding errors for middle- and lower-level cloud cover are approximately half as great.

Table 2 gives the mean zonal changes in computed cloud cover as a function of the errors in determining the total quantity of clouds, equal to ± 0.1. The absolute value of the error is the mean northern hemisphere deviation between the distributions of total cloud cover cited in [2, 14]. Comparison with Table 1 shows that in this case the determination of lower cloud cover is more sensitive to errors in determining total cloud cover than upper cloud cover. The magnitude of the change in the quantity of lower clouds is almost twice as great as the error in total cloud cover. With respect to the zonal peculiarities of the change in the quantity of clouds at different levels, they are similar to those shown in Table 1.

The mass of climatic data described in section 3 was used in computing three-level cloud cover for the entire earth.

Figure 3 shows the distribution of the computed quantity of clouds of the upper, middle and lower levels. The figures indicate that the principal large-scale characteristics of the vertical distribution of cloud cover agree well with the known characteristics of general circulation of the atmosphere and available data on the frequency of recurrence of stratus and cumulus forms in individual regions of the earth. We will enumerate some of them.

1. A considerable quantity of upper-level clouds is observed in the middle latitudes of both hemispheres. The formation of cloud cover was associated with the development of baroclinic instability.

2. An extensive maximum of the quantity of upper-level clouds was clearly expressed over Southeast Asia, including India. This maximum agrees with the observed region of formation of thick convective cloud cover caused by the development of southwesterly and southeasterly monsoons during this season of the year.

3. Regions of an increased quantity of clouds of the upper and middle levels are traced along the equator. Their formation is associated with the position of the ICZ.

4. Extensive regions of considerable lower cloud cover are situated in the northern and northeastern parts of the Pacific Ocean and along the western shores of South America. Observational data show that in these regions there is a predominance of clouds of stratus forms [12], forming over the relatively cold water surface of the oceans.

At the same time, some specific peculiarities are also noted in the field of three-level cloud cover. For example, in regions with a considerable upper cloud cover (region of Southeast Asia, equatorial and southern part of the Pacific Ocean) there is a relative decrease in the quantity of lower-level clouds. This was evidently caused by both the errors in the initial data and the use of some of the assumptions adopted in the computation scheme. For example, one of these assumptions is that the cloud cover distribution at each level is random. It can be assumed that such an assumption is satisfied quite rigorously in regions of formation of stratiform clouds. However, it may not be satisfied in those regions where the cloud cover has a considerable vertical extent and is associated with the development of powerful convection. The assumption of a random vertical distribution of clouds should lead to an underestimate of their quantity at the lower levels, as was found in the computations. In addition, the underestimate of lower cloud cover in the ICZ over the Pacific Ocean is in part attributable to another factor. Figure 1 shows that in this region along the equator there is no zone of an increased quantity of total cloud cover, although available satellite observations indicate its existence. It was demonstrated earlier that this sort of error in the quantity of total cloud cover should lead, in particular, to an underestimate of the quantity of lower clouds.

Moreover, the distribution of outgoing radiation used in the computations was stipulated at the points of intersection of a 10° x 10° grid. This means that some fine peculiarities in the radiation field associated with the existence of a narrow cloud zone along the equator was evidently inadequately well expressed in such a relatively thin grid.

In summarizing what has been said above, it can be assumed that except for some of the mentioned shortcomings, relating for the most part to the determination of lower cloud cover, in general the computed three-dimensional distribution of the quantity of clouds agrees well with the principal large-scale peculiarities of general circulation of the atmosphere and can be used in evaluations of the possibilities of schemes for the parameterization of cloud cover used in hydrodynamic models of the atmosphere.

In conclusion the author expresses sincere appreciation to Doctor S. Manabe and R. T. Wetherald (Geophysical Hydrodynamics Laboratory, Princeton, United States) for numerous productive discussions and assistance in carrying out this study.

BIBLIOGRAPHY

1. Berlyand, T. G., "Seasonal Change in the Relationship Between Lower and Total Cloud Cover Over the Territory of the USSR," TRUDY GGO (Transactions of the Main Geophysical Observatory), No 307, 1974.

2. Berlyand, T. G., Strokina, L. A., "Cloud Cover Regime on the Earth. Physical Climatology," TRUDY GGO, No 388, 1974.

3. Dubrovina, L. S., "Statistical Characteristics of the Spatial and Microphysical Structure of Clouds," AVIATSIONNO-KLIMATICHESKIY ATLAS-SPRAVOCHNIK SSSR (Aviation-Climatic Atlas-Reference Book of the USSR), Vol 1, No 3, 1975.

4. Kondrat'yev, K. Ya., Timofeyev, Yu. M., TERMICHESKOYE ZONDIROVANIYE ATMOSFERY SO SPUTNIKOV (Thermal Sounding of the Atmosphere from Satellites), Leningrad, Gidrometeoizdat, 1970.

5. Kondrat'yev, K. Ya., Timofeyev, Yu. M., TERMICHESKOYE ZONDIROVANIYE ATMOSFERY IZ KOSMOSA (Thermal Sounding of the Atmosphere from Space), Leningrad, Gidrometeoizdat, 1978.

6. Lobanova, V. Ya., "Characteristics of the Geographical Distribution of Cloud Cover Over the Northern Hemisphere," TRUDY NIIAK (Transactions of the Scientific Research Institute of Aeroclimatology), No 44, 1967.

7. Crutcher, H. L., Meserve, J. M., SELECTED LEVEL HEIGHTS, TEMPERATURE AND DEW POINT FOR THE NORTHERN HEMISPHERE, NAVAIR 50 IC-52, US Nav. Weather Serv., Washington, D. C., 1970.

8. Jenne, R. L., Crutcher, H. L., van Loon, H., Taljaard, J. J., "A Selected Climatology of the Southern Hemisphere: Computer Methods and Data Availability," NCAR TECHNICAL NOTE, NCAR-TN/STR-92, 1974.

9. London, J. A., "Study of the Atmospheric Heat Balance," College of Engineering, New York University. Final Report. Contract AF 19(122)-165, 1957.

10. Manabe, S., Strickler, R. F., "Thermal Equilibrium of the Atmosphere With a Convective Adjustment," J. AMOS. SCI., Vol 21, 1964.

11. Manabe, S., Wetherald, R. T., "Thermal Equilibrium of the Atmosphere With a Given Distribution of Relative Humidity," J. ATMOS. SCI., Vol 24, 1967.

12. McDonald, W. F. (Editor), ATLAS OF CLIMATIC CHARTS OF THE OCEANS, WB No 1247, US Govt Printing Office, Washington, D. C., 1938.

13. Miller, B. D. (Editor), GLOBAL ATLAS OF RELATIVE CLOUD COVER 1967-1970, US Department of Commerce and USAF, Washington, D. C., 1971.

14. Schuts, C., Gates, W. L., GLOBAL CLIMATIC DATA FOR SURFACE, 800 mb, 400 mb, January, R-915-ARPA, Rand Co., 1972.

15. Van Loon, H., Taljaard, J. J., Sasamori, T., London, J., Hoyt, D. V., Labitzke, K., Newton, C. W., "Meteorology of the Southern Hemisphere," METEOROL. MONOGR., Vol 13, No 35, 1972.

16. Vonder Haar, T. H., Ellis, J. S., ATLAS OF RADIATION BUDGET MEASUREMENTS FROM SATELLITES (1962-1970), Atmos. Sci. Paper No 231, Colorado State University, Fort Collins, Colorado, 1970.

UDC 551.508.769

ACCURACY IN DETERMINING INTEGRAL PARAMETERS FROM THE RESULTS OF MEASUREMENT OF THE MICROSTRUCTURE OF CLOUDS

Moscow METEOROLOGIYA I GIDROLOGIYA in Russian No 9, Sep 80 pp 24-31

[Article by Candidate of Physical and Mathematical Sciences M. Yu. Orlov, Institute of Experimental Meteorology, manuscript submitted 24 Jan 80]

[Text]

Abstract: Formulas are derived for determining the random errors of the values of integral parameters of the spectrum of cloud droplets measured, for example, using a photoelectric instrument for measuring sizes. It is shown that with the present-day characteristics of measuring instruments the principal contribution to the errors in measuring the concentration of droplets, liquid-water content and radar reflectivity is from the error in determining the computation volume (±20%). For the remaining integral parameters the errors are determined for the most part by errors in measuring the radii (widths of the analyzer channels). The errors associated with the randomness of spatial positioning of droplets introduce a small contribution to the total error of the results. It is shown that the errors in measuring the mean radius are 7-8%; the errors of the mean square radius are 10-20%.

Many studies have been devoted to measurements of the microstructure of clouds [3, 8]. The usual methods which have been employed by different authors for determining the size distributions of cloud droplets are the methods associated with the precipitation of droplets on a backing [2, 3, 8] or photoelectric methods (for example, see [7]).

At the present time virtually all studies of the microstructure of clouds are made using photoelectric counters of cloud particles. Emphasis is on determination not only of the spectrum of droplet sizes itself, but also its various integral characteristics (for example, the moments of size distribution of particles).

When using photoelectric counters, especially counters with optical formation of the computation volume, a particle with a given size can be registered either in the analyzer channel corresponding to its radius or in the channel corresponding to a lesser radius. As a result, corrections for the nonuniformity of illumination of the computation volume must be introduced into the instrument spectrum of sizes. During the time of measurements in a channel with the number i there is registry of n_i particles, which is expressed through N_j -- the numbers of particles in the atmosphere with radii corresponding to a channel with the number j, in the following way [7]:

$$n_i = \sum_{j=M}^{i} \alpha_{ji} N_j, \quad \sum_{j=M}^{0} \alpha_{ji} = 1, \tag{1}$$

where α_{ji} is the probability that a particle with a radius corresponding to a channel with the number j will be registered in a channel with the number i ($r_i \leqslant r_j$); M is the total number of analyzer channels in which the particles are registered.

Thus, it can be seen that the errors Δn_i of the n_i values with independent errors of the values N_i -ΔN_i are correlated. The Δn_i distribution will differ from the Poisson distribution and evidently will be close to normal.

Estimates made for typical spectra measured using the cloud droplet counter described in [7] indicated that $\Delta n_i/n_i \leqslant \Delta N_i/N_i$, and the correlation coefficients are equal to

$$\rho_{ik} = \frac{\alpha_{ik}^2}{\sqrt{\alpha_{ii}^2 \alpha_{kk}^2}} \leqslant \frac{\alpha_{ii} N_i}{\alpha_{i-1,i} N_{i-1}} \geqslant 0{,}5.$$

The introduction of corrections for the nonuniformity of illumination of the computation volume essentially involves solution of the system of linear equations (1) with the limitations $N_i \geqslant 0$ (i = 1, 2, 3,...,M). Thus, the errors N'_i obtained using the photoelectric instrument for measuring particle sizes, after introduction of corrections, will also be correlated and will be dependent, in particular, on the intercorrelated errors of the α_{ji} values. By virtue of the normalization condition $\sum \alpha_{ij} \alpha_j = -1$ for all $j \neq i$. However, since usually it is possible to neglect the contributions to the errors in the N'_i values obtained from the system of equations (1) (due to the $\Delta\alpha_{ji}$ errors), the dispersion matrix $D(N_i)$ of the N_i values can be written [6] as follows:

$$D(N_i) = \|\alpha^{-1}\| \times D(n_i) \times \|\tilde{\alpha^{-1}}\|, \tag{2}$$

where $D(n_i)$ is the dispersion matrix of the n_i values, $\|\alpha^{-1}\|$ is a triangular matrix, inverse of the matrix of probabilities $\|\alpha\|$, the sign $\sim$ denotes transpositioning.

However, in a case when it is possible to neglect the contribution to the errors ΔN_i due to the errors $\Delta\alpha_{ji}$, formula (2) leads directly to the identity

$$D(N'_i) \equiv D(N_i).$$

The neglecting of the $\Delta\alpha_{jj}$ errors is all the more justified because the α_{jj} values are the instrument constants for the unit used in measuring the spectrum and at least in principle can be measured as precisely as desired.

In theoretical and experimental studies of cloud microphysics, in addition to the spectrum itself

$$\left(P_i = \frac{N_i}{N}; \quad N = \sum_{i=1}^{n} N_i\right)$$

it is customary to determine some of the following integral parameters of the cloud droplet spectrum:

1. The moments of the size distribution of droplets or the parameters associated with them:

droplet concentration
$$N' = \sum_i N_i V_n, \tag{3}$$

[π = error]

mean radius
$$\bar{r} = \sum_i N_i r_i \Big/ \sum_i N_i, \tag{4}$$

mean square radius
$$\bar{r^2} = \sum_i r_i^2 N_i \Big/ \sum_i N_i, \tag{5}$$

mean cubic radius
$$\bar{r^3} = \sum_i r_i^3 N_i \Big/ \sum_i N_i \tag{6}$$

dispersion of spectrum
$$\bar{s^2} = \bar{r^2} - \bar{r}^2, \tag{7}$$

liquid-water content
$$W = \frac{4\pi}{3} \frac{\rho_0 N \bar{r^3}}{V_n}, \tag{8}$$

the ratio of the standard deviation to the mean radius (so-called relative dispersion)
$$a = \frac{\bar{s}}{\bar{r}} = \sqrt{\frac{\sum_i r_i^6 N_i \cdot \sum_i N_i}{\left(\sum_i N_i r_i^3\right)^2} - 1}, \tag{9}$$

radar reflectivity
$$Z = \frac{B}{V_n} \frac{\sum_i N_i r_i^6}{\sum_i N_i} = \frac{B\bar{r}^6}{V_n}. \tag{10}$$

2. The exponent m in the formula describing the large-droplet part of the spectrum,
$$N_i = \int_{r_i}^{r_{i+1}} A r^{-m}\, dr = \frac{A}{m+1}\left(\frac{1}{r_i^{m+1}} - \frac{1}{r_{i+1}^{m+1}}\right). \tag{11}$$

The exponent can be determined using the description of the large-droplet part of the spectrum by a power-law curve and employing the least squares method. It is asserted in [5] that the value of the exponent is related to the exponent ν in the Junge spectrum of condensation nuclei by the expression $m = 5\nu - 2/3$. Thus, whereas the dispersions of the moments of the size distributions of droplets or the parameters associated with them can be explicitly expressed through the N_i dispersions and the dispersions of the measured radii r_i, the dispersion

of the exponent m, in addition, will also be dependent on the method for processing of the experimental data and obtaining the specific m value.

The sources of errors in determining the integral parameters when using photoelectric instruments for measuring sizes are as follows. The Poisson distribution of droplets introduces its contribution to the accuracy in determining the integral parameters. The error in the volume of air passing through the measuring instrument V_{error} is related to the error in determining the section of the computation volume and the error in the air velocities passing through the measuring instrument. A contribution to the error in the results is made by the errors in the calibration curve of the measuring instrument (relationship between the amplitude of the pulse and particle size) and the errors in the widths of the channels of the recording unit and the errors in tie-in of the scales of the channels to the size scale. A role, although small, is also played by the errors in the corrections introduced into the results of the measurements in order to eliminate the influence of nonuniformity of illumination of the computation volume, especially in its optical formation.

The randomness in arrangement of droplets in space will introduce its contribution in a double fashion. Thus, the total number of droplets counted in a given experiment, $N = \sum_i N_i$, is a random value with a distribution close to normal. The measurements are usually made in such a way that the number N is equal to approximately 10^4. Thus, the error in the result due to the "sampling volume" will be only a few percent [3]. N_i, the numbers of droplets falling in the range of sizes from r_i to r_{i+1}, will have distributions close to normal.

It is also clear from the form of formulas (3)-(10) that the accuracy in measuring the volume of the sample (the quantity of air passing through the instrument) exerts an influence only on the accuracy in determining the concentration of droplets, liquid-water content and radar reflectivity. The accuracy of the remaining parameters is not dependent on the accuracy of knowledge of volume of the sample. The errors in the values of the radii of the channels are attributable to several factors. According to estimates, the greatest contribution to them is introduced by the error in determining the radius of a particle in the pulse analyzer. Most modern multichannel amplitude analyzers determine the pulse amplitude from the time of discharge of a capacitor charged by the pulse to be analyzed. For several different reasons the error in determining amplitude must not exceed one analyzer channel.

Among the other errors of relatively little importance we can mention, for example, the error due to the introduction of corrections for dead time, but dead time is determined quite precisely by the time necessary for the analyzer to find pulse amplitude.

Thus, we will examine the contributions of different sources of errors. We will limit ourselves only to their random components, remembering that so-called systematic errors of the results, as soon as their existence becomes known to the experimenter, can be taken into account by introducing corrections, which, it goes without saying, make their contribution to the increase in the random errors in the final results.

Here we will cite formulas for determining the errors in the above-mentioned integral parameters of the spectrum:

-- concentration of droplets

$$(\Delta N')^2 = (N')^2 \left[\frac{1}{N} + \left(\frac{\Delta V_n}{V_n}\right)^2\right]; \tag{12}$$

-- mean radius

$$(\Delta \bar{r})^2 = \frac{1}{N}(\bar{r}^2 - \bar{r}^2) + \overline{\left[\sum_i p_i \Delta r_i\right]^2}. \tag{13}$$

We note that in this and in subsequent formulas in the case of presence of a correlation between the errors of the radii r_i the terms containing $\overline{\Delta r_i \Delta r_j}$ are not equal to zero. However, in the absence of correlations such terms are equal to zero;

-- mean square radius

$$(\Delta \bar{r}^2) = \frac{1}{N}(\bar{r}^4 - \bar{r}^{2^2}) + \overline{\left[\sum_i 2 p_i r_i \Delta r_i\right]^2}; \tag{14}$$

-- dispersion of spectrum

$$(\Delta \sigma^2)^2 = \frac{1}{N}(\bar{r}^4 - \bar{r}^{2^2} - 4\bar{r}\bar{r}^3 + 8\bar{r}^2\bar{r}^2) + \overline{\left[2\sum_i p_i (r_i - \bar{r})\Delta r_i\right]^2}; \tag{15}$$

-- mean cubic radius

$$(\Delta \bar{r}^3)^2 = \frac{1}{N}(\bar{r}^6 - \bar{r}^{3^2}) + \overline{\left[3\sum_i p_i r_i^2 \Delta r_i\right]^2}; \tag{16}$$

-- liquid-water content

$$\left(\frac{\Delta W}{W}\right)^2 = \frac{1}{N} + \left(\frac{\Delta \bar{r}^3}{\bar{r}^3}\right)^2 + \left(\frac{\Delta V_n}{V_n}\right)^2; \tag{17}$$

-- ratio of the standard deviation to the mean radius (with allowance for the correlations of errors σ^2 and $\bar{r}$)

$$(\Delta a)^2 = \frac{1}{4N\bar{r}^{2^2}}(\bar{r}^2\bar{r}^4 + 4\bar{r}^{2^3} - 4\bar{r}^2\bar{r}\bar{r}^3 - \bar{r}^{2^2}\bar{r}^2) + \frac{1}{\bar{r}^{2^2}}(\bar{r}^2\sum_i p_i^2 r_i^2 \Delta r_i^2 + \bar{r}^{2^2}\sum_i p_i^2 \Delta r_i^2 - 2\bar{r}\bar{r}^2\sum_i p_i^2 r_i \Delta r_i^2); \tag{18}$$

-- radar reflectivity

$$(\Delta Z)^2 = \frac{B^2}{N}(\overline{r^{12}} - \overline{r^2}) + B^2\left[6\sum_i p_i r_i^5 \Delta r_i\right]^2 + B^2\left(\frac{\overline{r^6}}{\overline{r^3}}\right)^2\left(\frac{\Delta V_n}{V_n}\right)^2. \quad (19)$$

It is impossible to express the error of the exponent m explicitly through the errors in the measured parameters due to the nonlinearity in the procedure for finding it. An evaluation of the accuracy m must be made for each specific case separately. Due to the nonlinearity of the system of equations for the least squares method, in order to determine the m value it is necessary to use, for example, the linearization described in [5].

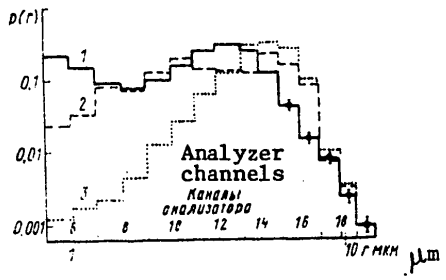

Fig. 1. Typical normalized spectra for cloud droplets obtained using a photoelectric instrument for measuring the size of cloud droplets. The figures on the histograms are the numbers of the spectra (see Tables 1 and 2).

Using the formulas cited above, we will estimate the errors of different measured microstructural parameters. For this purpose we will use the experimental data obtained using a photoelectric counter of cloud droplets [7].

Typical measured normalized spectra of particles in the range size from 0.5 to 12.8 μm are given in Fig. 1.

Table 1 gives the values of the parameters and their errors. [Data on the spectra of droplets were furnished through the kindness of K. B. Yudin and A. V. Lachikhin.]

In computing the values of the microphysical parameters and their errors it was assumed that the accuracy in determining the volume of the air sample passing through the photoelectric counter is ±20%. Most of this error is attributable to the error caused by the error in the cross section of the computation volume, since the velocity of air flow is known with a rather high accuracy (2-3%).

An analysis of the individual components (see Table 2) indicated that the errors caused by the randomness of spatial distribution of droplets in all cases are negligible in comparison with the errors caused by an inexact knowledge of the

Table 1

Errors in Determining Microphysical Parameters

Parameter	Value of Parameter and its Error		
	Spectrum 1	Spectrum 2	Spectrum 2
Droplet concentration, $1/cm^3$	700±140	840±170	670±130
Mean radius, μm	3.96±0.26(±0.68)*	4.64±0.30(0.04)**	5.64±0.42(0.05)**
Mean square radius, μm^2	17.9±3.5	25.8±2.7(0.4)**	33.6±5.1(0.6)**
Dispersion of spectrum, μm^2	2.7±1.6	4.2±1.1	1.8±1.1
Mean cubic radius, μm^3	93.1±17.9	170.4±35.4(4.0)**	210.1±48.0(5.2)**
Relative dispersion	0.41±0.15	0.44±0.25	0.2365±0.05(0.0025)**
Liquid-water content, g/m^3	0.28±0.08		
Radar reflectivity (B = 1) $\mu m^6/cm^3$	3000±1200		
Exponent in formula describing large-droplet part of spectrum ($N = Ar^{-m}$)	6.4±0.7		

*With allowance for possible correlations of errors r_i.
**With relative error in width of analyzer channel ±1%.

Table 2

Components of Dispersions of Some Integral Parameters

N' $1/cm^3$		$\bar{r}\ \mu m$		$\bar{r}^2\ \mu m^2$		$\bar{r}^3\ \mu m^3$	
statistics (ΔN_i)	sample volume*	statistics (ΔN_i)	Δr_i**	statistics (ΔN_i)	Δr_i**	statistics (ΔN_i)	Δr_i**
10	28600	0.000598	0.0918	0.0519	13.4	3.13	1248
--	-----	0.000319	0.175	0.0440	25.6	3.99	2302

*With an error in the section of the computation volume of ±20%.
**With an error of ±1 analyzer channel in determining particle radius and $\rho_{r_i r_k} = 0$.

relationship between the amplitude of the light pulse and the particle size (error in radius) and inexact knowledge of sample volume (in those cases when this error gives a contribution to the error in the result). In a case when the errors of individual r_i values (radii of channels) are correlated for the entire scale of sizes (uncontrollable shift of scale) the errors indicated in Table 1 must be supplemented by terms in the form

$$\sum_i \sum_k p_i p_k \, c(r_i, r_k) \Delta r_i \, \Delta r_k,$$

which in the case of the mean radius, for example, leads to an increase in the errors by more than a factor of 2. For the higher moments of the distribution the role of the correlations is still greater.

Since the values of the errors cited in Table 1 can be considered typical, they also determine the range of values in which the comparison of experimental data with the results of theoretical examinations can assist in the checking or improvement of theory.

For example, if the computed integral parameters obtained in [1] are used for comparison with the results of experiments, it can be asserted that the differences between the results of computations and experiments will also be significant for the mean radius and for the relative dispersion. However, the values of the concentration of droplets under the condition that the range of sizes in which the determination of the number of droplets in both cases is one and the same can be considered to coincide within the limits of errors.

The ν values, the exponent in the spectrum of condensation nuclei, adopted in [4] and determined from experimental data, also coincide well.

Conclusions

1. The principal sources of errors in determining the integral parameters on the basis of data from microphysical measurements are the errors in a knowledge of the relationship between the amplitude of the light pulse and droplet size, and in a case when parameters related to the concentration of droplets are determined, the error in the volume of air passing through the instrument for measuring particle size.

2. The correlation of the errors in the values of the radii leads to an increase in the errors of the results. Thus, when determining the errors the evaluation of the influence of the correlations is significant.

3. When making measurements of the size distribution of particles using multichannel amplitude analyzers the widths of the channels must be made as small as possible in order to decrease the relative error in determining radius. The necessary statistical accuracy in determining the number of particles in a stipulated size range in this case is attained in the processing procedure by means of combining several channels into a wider channel.

BIBLIOGRAPHY

1. Aleksandrov, E. L., et al., "Evaluation of the Influence of Modification of the Spectrum of Cloud Droplets on the Coagulation Process," TRUDY IEM (Transactions of the Institute of Experimental Meteorology), No 19(72), 1978.

2. Borovikov, A. M., et al., FIZIKA OBLAKOV (Cloud Physics), Leningrad, GIMIZ, 1961.

3. Levin, L. M., ISSLEDOVANIYE PO FIZIKE GRUBODISPERSNYKH AEROZOLEY (Investigation of the Physics of Coarsely Disperse Aerosols), Moscow, Izd-vo AN SSSR, 1961.

4. Linnik, Yu. V., METOD NAIMEN'SHIKH KVADRATOV I OSNOVY TEORII OBRABOTKI NABLYUDENIY (Least Squares Method and Principles of the Theory of Processing of Observations), Moscow, Fizmatgiz, 1962.

5. Smirnov, V. I., "Approximation of Empirical Size Distributions of Cloud Particles and Other Aerosol Particles," IZV. AN SSSR, FIZIKA ATMOSFERY I OKEANA (News of the USSR Academy of Sciences, Physics of the Atmosphere and Ocean), Vol IX, No 1, 1973.

6. Fedorov, V. V., TEORIYA OPTIMAL'NOGO EKSPERIMENTA (Theory of an Optimum Experiment), Moscow, Nauka, 1971.

7. Aleksandrov, E. L., et al., "Photoelectric Analyzers for Aerosol Size Distribution and Concentration Determination," Report to IX International Conference on Atmospheric Aerosols, Galway, Ireland 21-27 Sept., 1977.

8. Warner, J., "The Microstructure of Cumulus Clouds. Part I," J. ATMOS. SCI., Vol 26, No 9, 1969.

UDC 551.(577+576+507.362)

ZONES OF CONSIDERABLE PRECIPITATION IN THE CLOUD COVER FIELD DETECTED BY ARTIFICIAL METEOROLOGICAL EARTH SATELLITES

Moscow METEOROLOGIYA I GIDROLOGIYA in Russian No 9, Sep 80 pp 32-38

[Article by N. N. Fedorova, USSR Hydrometeorological Scientific Research Center, manuscript submitted 22 Feb 80]

[Text]

Abstract: Dispersion analysis is used in establishing the correlations between considerable precipitation at the earth's surface and different characteristics of cloud cover obtained by an analysis of cloud cover photographs taken from artificial meteorological earth satellites. It was possible to ascertain the most significant characteristics and their paired and triple combinations. Curves and regression equations were derived for computing the quantity of precipitation based on the use of cloud cover photographs.

This article gives an analysis of cyclonic cloud systems which developed from cyclogenetic cloud forms [2, 4, 6], frequently having the form of an undefined cloud mass, which then acquired the form of an eddy, and which during destruction of the eddy were transformed either into a cloud band or into a cloud mass of an indefinite form. We examined thirty cloud systems in the process of their development and destruction which were observed during the winter months of 1973-1977 over the territory of Europe.

As the initial information on cloud cover we used cloud cover photographs taken in the IR spectral region. The times when the cloud cover photographs were taken (morning and evening) virtually coincided with the beginning and end of a 12-hour interval during which maps of the quantity of precipitation were constructed. Since the photographs were assigned to fixed moments in time and the quantity of precipitation on the maps was related to a 12-hour interval, the position of the cloud system was interpolated to the middle of this interval and from the entire zone of precipitation we selected that part which was localized within the cloud system at a mean moment in time. It was assumed that during a 12-hour interval the cloud system moved at a uniform rate.

In this study statistical methods were used in establishing the correlations between considerable precipitation at the ground surface (more than 3 mm in 12 hours) and some characteristics determined from photographs from artificial meteorological earth satellites (MES). The following characteristics were used: 1) type of cloud system B; 2) form of clouds F; 3) cloud brightness H; quantity of clouds Π; 5) trajectory of cyclonic eddy T; 6) position of the considered sector in the cloud system P; 7) stage in development of cloud system C. We will make some comments concerning the selected characteristics.

In determining the type of cloud system B we took into account three varieties defined by the author in [5]: eddies, bands and cloud masses of an indefinite form.

In determining the form of clouds F, given in the WMO TECHNICAL NOTE [3], reference is to seven groups of clouds, of which three groups are related to the principal cloud genera (cirrus, stratus and cumulus types), whereas four are combinations of these forms.

Cloud brightness H, from which it is possible to judge the height of the upper cloud cover boundary, was taken in two gradations: bright and gray clouds.

In this study the quantity of clouds Π was determined from the degree (percentage) of coverage of the earth's surface by clouds in any particular considered square in four gradations: from 1 to 19%, from 20 to 49%, from 50 to 79%, from 80 to 100% of the area of the square.

The trajectories of cyclonic eddies T, as was adopted in [7], were divided into five groups: northerly, northwesterly, westerly, southwesterly and southerly. As was demonstrated in [7], between these groups there are differences in the relative position of the zone of considerable precipitation.

The position of the sector in the cloud system P was determined as indicated in Fig. 1. This figure shows how the cloud systems were divided into sectors and their conventional numbers are indicated. The defining of these sectors was accomplished in accordance with [7].

The stage in development of the cloud system C was determined, as indicated in [3] (a total of five stages), with the following difference. To the first stage, in addition to the cloud cap of a frontal wave mentioned in [3], we also assigned (in accordance with [2, 4, 6]), an isolated cloud cap, the cap (fan) of cirrus clouds on the northern end of a ridge of cold front clouds and the cloud cap at the occlusion point.

Next the considered cloud systems were broken down into squares with a 300-km side. For each square we determined the above-mentioned characteristics, and also found the mean quantity of precipitation. If we arbitrarily take the investigation for one such square as one case, we will examine more than 3,500 cases.

Since some of the above-mentioned characteristics cannot be expressed quantitatively, in this study we made use of dispersion analysis [1]. We sought the correlations between the amounts of precipitation and each of the seven criteria corresponding to

one of the mentioned characteristics or another. We also examined different combinations of these criteria.

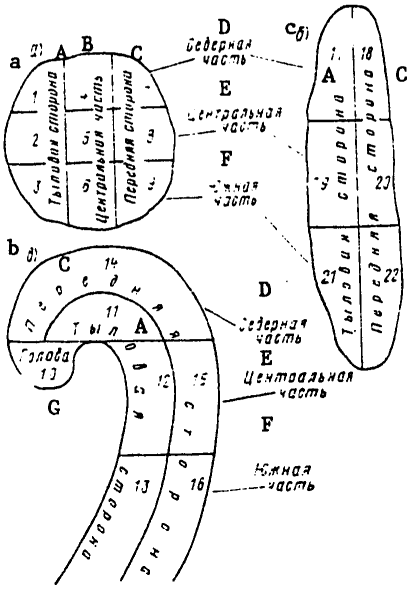

Fig. 1. Diagram of separation of cloud systems into sectors in cases of systems of an indefinite form (a), cloud bands (b) and cloud eddies (c).

KEY:

A) Rear side
B) Central part
C) Front side
D) Northern part
E) Central part
F) Southern part
G) Head

An evaluation of the difference between the dispersions of the considered parameters was made using the Fisher test

$$F = \frac{S_1^2}{S_2^2},$$

where S_1^2 and S_2^2 are unbiased evaluations of the dispersions between the criteria and within the criteria respectively:

$$S_1^2 = \frac{1}{r-1}\sum_{i=1}^{r} n_i(\overline{x}_i - \overline{x})^2;$$

$$S_2^2 = \frac{1}{n-r}\sum_{i=1}^{r}(n_i - 1)S_i^2;$$

$$S_i^2 = \frac{1}{n_i - 1} \sum_{k=1}^{n_i} (x_{ik} - \bar{x}_i)^2;$$

$$\bar{x}_i = \frac{1}{n_i} \sum_{k=1}^{n} x_{ik};$$

$$\bar{x} = \frac{1}{n} \sum_{i=1}^{r} n_i \bar{x}_i;$$

$$n = \sum_{i=1}^{r} n_i;$$

n_i is the volume of the sample in the group; r is the number of groups in the criterion; n is the total number of cases.

It is known that the Fisher criterion conforms to a F-distribution with n-r and r-1 degrees of freedom. With a significance level $\alpha = 0.01$, using known tables we found the critical values of the Fisher test F_{cr}, with which the specific F values were compared. Using the $F-F_{cr}$ and F values we judged the existence of the interrelationship between this criterion and the quantity of precipitation and the degree of its influence.

All the computations were made on an electronic computer and some of the results are given in the table. In this table, in the column entitled "Criterion," we give the corresponding characteristics, as indicated at the beginning of this article. The two or three letters in the "Criterion" column represent combinations of the the corresponding two or three characteristics.

The data in the table make it possible to draw the following conclusions. If only one of the mentioned seven characteristics is taken as a predictor (without its combination with others), the most significant is the characteristic P and the characteristics ПТ, F and H are somewhat less significant. The T criterion was the least significant.

If we take combinations of two characteristics, the most significant were the pairs of characteristics PC and PПТ, whereas the least significant were those pairs which include the T criterion. It should be noted that allowance for any second criterion in addition to the P criterion increases the reliability of computing considerable precipitation in the rear regions of the cloud systems, whereas for the frontal regions such an increase is not discovered. Allowance for any other characteristics in addition to the cloud form F does not improve the diagnosis of precipitation if we examine cirriform clouds, their combinations with stratiform clouds, and also combinations of cirriform and stratiform-cumuliform clouds. In cases of presence of clouds of remaining forms the reliability of the computations of considerable precipitation is increased if the characteristics ПТ or C are also taken into account (but not the characteristic T).

If a combination of three characteristics is taken as a predictor, the most significant, as seen from the data in the table, are combinations containing PC (that is PCП, PCF, PCT). The least significant are the characteristics FTC and FПT.

As already mentioned, in the limits of any characteristic we examined a number of varieties (from 3 to 22). Therefore, with allowance for the varieties the number of possible combinations was very great. Thus, with the two characteristics P and F the number of combintions (with allowance for the varieties) theoretically attains 154, whereas with three characteristics (P, F and T) the number of such combinations attains 770. For practical purposes, however, the number of combinations is considerably less, since some combinations of varieties are almost never encountered.

For all the characteristics and their combinations we determined the probability of falling of precipitation independently of its quantity, and also (separately) the probability of falling of considerable precipitation. We also computed the mean quantity of precipitation and its dispersion. The results of these computations made it possible to draw the following conclusions. Considerable precipitation falls primarily at the rear side of a cloud spiral, band or cloud mass of indefinite form. Most frequently it falls from bright stratiform clouds and with a combination of cirriform and cumuliform clouds. The greatest quantity of precipitation falls in the northern part of the rear side of the cloud eddy, in the central part of the rear side of a band, in the central and rear parts of a cloud mass of indefinite form. The greatest quantity of precipitation and the maximum probability of falling of considerable precipitation are characteristic for the first three stages in the development of a cloud system. The probability of considerable precipitation in one square or another measuring 300 x 300 km is maximum in a case when the square is situated in a cloud mass of indefinite form and minimum in a cloud band. This is attributable to the fact that cloud masses of an indefinite form were observed in the initial stage of development of a cyclonic cloud eddy where great areas are occupied by precipitation. Accordingly, the probability that a square will fall in a region with

Values of Fisher Tests F and F_{cr}

Criterion	F	F_{cr} $\alpha = 0.01$
B	17.4	4.6
F	37.1	2.8
T	2.7	3.3
П	46.7	3.8
P	71.1	1.9
C	28.4	3.3
H	40.2	1.9
For combinations of two characteristics		
BF	17.0	1.9
FT	9.3	1.6
FC	13.2	1.6
ПT	10.4	1.9
ПF	16.4	1.7
ПC	15.6	1.9
PT	19.3	1.4
PП	24.5	1.4
PC	25.6	1.4
PF	19.7	1.3
PH	14.5	1.2
ПH	15.7	1.4
TH	11.3	1.4
CH	12.4	1.4
BH	16.8	1.5
For combinations of three characteristics		
FПC	7.3	1.3
FПB	8.8	1.4
FПT	5.6	1.3
PFП	11.0	1.1
PFT	9.3	1.0
PFC	11.7	1.0
PПC	12.8	1.2
PПT	9.7	1.2
PTC	12.5	1.2
FTC	5.2	1.3

precipitation is greater than in cloud bands which were observed after destruction of the eddy and which had small areas of zones of precipitation. In cloud eddies, in addition to great areas of zones of precipitation there were large areas of the entire cloud system, which in comparison with a cloud mass of indefinite form decreased the probability of a square falling into a region with precipitation.

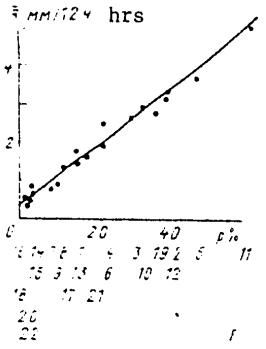

Fig. 2. Graph for determining the mean quantity of clouds $\bar{R}$ and the probability of falling of considerable precipitation p on basis of P characteristic.

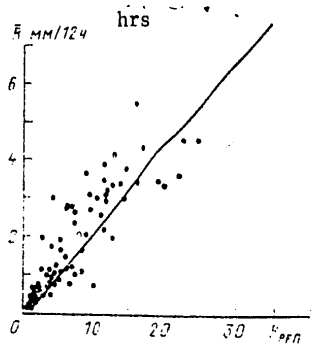

Fig. 3. Dependence between quantity of precipitation and $R_{PFП}$ criterion.

In this study we obtained data on the frequency of recurrence of clouds of different forms and brightness in different parts of cloud systems. For example, cirriform clouds are encountered most frequently in the northeastern part of a cloud mass of indefinite form and in a cloud eddy, whereas stratiform clouds are almost never observed in the southeastern part of a cloud mass of indefinite form.

Data on the mean quantity of precipitation were obtained for combinations of the two characteristics. These data made it possible to draw a number of conclusions. In particular, the greatest quantity of precipitation is observed in the head of the eddy in the case of a combination of stratiform clouds with cumuliform clouds and on the rear side of the eddy in the presence of stratiform clouds. At the head of a cloud eddy the greatest quantity of precipitation falls when there are northerly, northwesterly and westerly cyclones and the least precipitation falls when there are southwesterly cyclones. With any forms of clouds, other than a combination of cumuliform and cirriform clouds, the greatest quantity of precipitation is observed in the first three stages in the development of a cloud system and the least quantity of precipitation falls in the last two stages. However, with a combination of cirriform and cumuliform clouds there will be an opposite distribution of maximum and minimum precipitation.

In this study we also examined combinations of four criteria and defined those combinations in which the probability of the falling of considerable precipitation was in the range from 70 to 100%. It was discovered that considerable precipitation

virtually always falls in the northern rear part of a cloud eddy when there is total coverage of the sky by clouds. In this case the stage in development of the cloud system can be the second, third or fourth. In the second and third stages of development considerable precipitation falls from bright stratiform clouds and when these are combined with bright cumuliform clouds, whereas in the fourth stage -- when there is a combination of bright or gray stratiform clouds with bright cumuliform clouds.

Considerable precipitation is virtually never encountered (probability of falling not more than 10%) in the northern rear part of a cloud eddy and its head whatever may be the sky coverage with dark cumuliform clouds in the fourth stage of development of the cloud eddy. In the southern rear part of a cloud eddy considerable precipitation does not fall in the third and fourth stages of development of a cloud eddy regardless of the quantity of bright cumuliform or stratiform clouds and their combinations. In the northern frontal part of the cloud eddy considerable precipitation does not fall in the third and fourth stages of development of an eddy even from bright stratiform and cumuliform clouds and their combinations.

In the frontal central part of the cloud eddy considerable precipitation does not fall in the third and fourth stages of development of the eddy when there is complete coverage of the sky by clouds, when bright stratiform clouds and their combinations with bright cumuliform clouds are observed, and in the second stage of development when there is a combination of bright stratiform and cumuliform clouds. In the southern frontal part of the cloud eddy considerable precipitation does not fall in the third and fourth stages of development of the cloud system even with complete coverage of the sky by bright cumuliform clouds and their combinations with bright stratiform clouds.

Graphs (Fig. 2, as an example) of the dependence between the mean quantity of clouds $\overline{R}$ and the probability of the falling of considerable precipitation p were constructed for the considered criteria and combinations of two and three criteria. Below the graph we have plotted the arbitrary numerical values of the P characteristic adopted in this study. The position of the annotated values of the characteristic in the figure corresponds to the probability p on the x-axis. We also computed the correlation coefficients r_p, $\overline{R}$ between $\overline{R}$ and p and the coefficients A and B in a regression equation of the form $\overline{R} = Ap + B$. These graphs and the regression equations can be used in precomputing the mean quantity of precipitation in squares with sides 300 x 300 km and the probability of falling of considerable precipitation on the basis of photographs from meteorological satellites.

Now we will discuss still another aspect of this investigation. It was found above that a relatively good correlation exists between considerable precipitation and the characteristics P, Π and F. This made it possible to assume that the mean quantity of precipitation $\overline{R}$ in a square measuring 300 x 300 km can be computed using the formula

$$\overline{R} = aR_{P\Pi F}; \quad R_{P\Pi F} = 0{,}001 \prod N_i$$

where i is one of the characteristics P, Π or F; N_i is an arbitrary numerical value of the characteristic; $N_i = 5\overline{R}_i$; $\overline{R}_i$ is the mean quantity of precipitation for a given characteristic.

The coefficients 0.001 and 5 present in these formulas were determined empirically.

Data on the actual quantity of precipitation were used in computing the $\overline{R}$ value and the just-cited formulas were used in computing $R_{P\Pi F}$. It was found that there is a significant correlation between $\overline{R}$ and $R_{P\Pi F}$ (correlation coefficient 0.71). The corresponding regression equation has the form

$$\overline{R} = 0.22\ R_{P\Pi F}.$$

The graph of this correlation is shown as Fig. 3.

The graphs and formulas cited above can be used in a diagnosis of precipitation. Further improvement in the method for predicting a cloud system will make it possible to use these graphs in precomputing precipitation.

BIBLIOGRAPHY

1. Van der Varden, B. L., MATEMATICHESKAYA STATISTIKA (Mathematical Statistics), Moscow, IL, 1960.

2. Zhalyu, R., Popova, T. P., "Use of Cloud Cover Photographs in Predicting Cyclogenesis," METEOROLOGIYA I GIDROLOGIYA (Meteorology and Hydrology), No 4, 1974.

3. ISPOL'ZOVANIYE IZOBRAZHENIY SO SPUTNIKOV V ANALIZE I PROGNOZE POGODY (Use of Images from Satellites in the Analysis and Prediction of Weather), TEKHNICHESKAYA ZAPISKA VMO (WMO Technical Note), No 124, Leningrad, 1974.

4. Neronova, G. Yu., "Fanlike Structure of Cloud Cover as an Indicator of Cyclogenesis," TRUDY GosNITsIPRa (Transactions of the State Scientific Research Center for the Study of Natural Resources), No 1, 1976.

5. Popova, T. P., Fedorova, N. N., "Use of Photographs of Cloud Cover from Artificial Earth Satellites for the Analysis of Precipitation," TRUDY GIDROMETTSENTRA SSSR (Transactions of the USSR Hydrometeorological Center), No 165, 1975.

6. SINOPTICHESKAYA ANALIZ SNIMKOV OBLACHNOGO POKROVA, POLUCHAYEMYKH S MSZ: POSOBIYE DLYA SINOPTIKOV (Synoptic Analysis of Cloud Cover Photographs Obtained from Meteorological Satellites: Handbook for Weathermen), Leningrad, Gidrometeoizdat, 1976.

7. Fedorova, N. N., "Precipitation Zone in the Cloud Cover and Wind Field," TRUDY GosNITsIPRa, No 1, 1976.

UDC 551.(509.314+524)

PROBABILISTIC MODEL OF AIR TEMPERATURE TIME SERIES

Moscow METEOROLOGIYA I GIDROLOGIYA in Russian No 9, Sep 80 pp 39-47

[Article by Professor A. S. Marchenko and L. A. Minakova, Computation Center Siberian Department USSR Academy of Sciences, manuscript submitted 18 Feb 80]

[Text]

Abstract: The authors have formulated a model of connected air temperature time series in the approximation of one-dimensional probability distributions by a mixture of two normal distributions. It is shown that a family of distributions of this type contains a distribution with any prestipulated moments of the first three orders. A method for evaluating the parameters of one-dimensional and joint distributions is proposed.

In solving some practical problems it is necessary to use an electronic computer for modeling a series of values $\xi_1, \xi_2, \ldots, \xi_n$ of a meteorological element ξ with the same probabilistic properties as for a real process. These are primarily problems which cannot be solved by the statistical processing of observational data since observations with the necessary frequency or duration in many cases are lacking (for example, computations of different characteristics of "surges" of meteorological elements [2, 5]). Another important field of application is a study of the systematic and random errors in the parameters of sample probability distributions computed on the basis of a limited number of observations (for example, see [7]). Statistical modeling of series of a random process is an effective and universal means for solving this sort of problems, in contrast to analytical methods, making it possible to find only very simple characteristics when there are rigorous limitations on the probabilistic structure of the process.

In this article we propose a probabilistic model of a series of air temperature values. Numerous investigations of one-dimensional probability distributions of this element for different seasons, hours of the day and different geographical locations show that usually they differ appreciably from a normal distribution [1, 4, 8]. In winter at stations with frequent thaws it is even possible to observe bimodal distributions. The introduction of corrections for asymmetry and excess of a distribution using Gram-Charlier series frequently gives virtually satisfactory results [1, 8], but in mathematical respects it is incorrect because

these series (with a finite number of terms) are not always the probability density: with some x values the approximating function f(x), depending on the specific values of the asymmetry and excess coefficients, can be negative. A more satisfactory choice is the expansion of the random parameter itself, not the probability density, into a Fourier series in a suitable orthonormalized base. For example, for ξ with values in the range $(-\infty, \infty)$ it can be assumed that

$$\xi = a_0 H_0(\eta) + a_1 H_1(\eta) + a_2 H_2(\eta) + \ldots,$$

where η is a normal parameter, $\{H_k(\eta)\}$ is a system of orthonormalized Hermite polynomials, $\{a_k\}$ are constants selected from the condition of an equality of several lower-order moments of the actual and approximating distributions.

There is still another family of approximating distributions which differ fundamentally from those considered and to a certain degree take into account the nature of the phenomenon. These are mixtures of distributions. The formation of a probability distribution $p_\xi(x)$ of a meteorological element ξ is never an isolated process, but occurs under the influence of the totality of influencing factors $\varphi = (\varphi_1, \varphi_2, \ldots)$ of a local or global character, reflecting, for example, the synoptic conditions, etc. The set Ω of all possible values of the φ vector is broken down into nonintersecting subsets $\Omega_1, \Omega_2, \ldots, \Omega_k$, such that with $\varphi \in \Omega_i$ the ξ distribution is most uniform, but differs to the maximum degree from the distribution with $\varphi \in \Omega_j \neq i$. Then

$$p_\xi(x) = p_\xi(x, \varphi \in \Omega) = \Theta_1 p_1(x) + \Theta_2 p_2(x) + \ldots + \Theta_k p_k(x), \tag{1}$$

where

$$\Theta_i = P\{\varphi \in \Omega_i\}, \quad \sum_{i=1}^{k} \Theta_i = 1, \quad p_i(x) = p_\xi(x \mid \varphi \in \Omega_i),$$

Formula (1) represents $p_\xi(x)$ in the form of a mixture of several distributions. This idea has long been known to climatologists, but judging from available publications, has not been put into practical use, evidently due to difficulties in choosing the influencing factors and the complexity in breaking Ω down into suitable classes.

In the probabilistic model which we propose the air temperature distribution is approximated by a mixture of two normal distributions in the form

$$p_\xi(x) = \frac{\Theta}{\sqrt{2\pi}\,\sigma_1} e^{-\frac{(x-\mu_1)^2}{2\sigma_1^2}} + \frac{\Theta'}{\sqrt{2\pi}\,\sigma_2} e^{-\frac{(x-\mu_2)^2}{2\sigma_2^2}}, \tag{2}$$

$$0 \leq \Theta \leq 1, \quad \Theta + \Theta' = 1.$$

Thus, if $\xi^{(1)}$ and $\xi^{(2)}$ are normal values with the parameters μ_1, σ_1^2 and μ_2, σ_2^2 respectively and S is an event appearing with the probability $\Theta = P\{S\}$ (the inverse event $\bar{S}$ occurs with the probability $\Theta' = 1 - \Theta$), the distribution (2) is generated by the mechanism

$$\xi = \omega \xi^{(1)} + (1 - \omega)\xi^{(2)}. \tag{3}$$

Here ω is an indicator of the event S. Since $\omega(1 - \omega) \equiv 0$, the existence of a dependence between $\xi^{(1)}$ and $\xi^{(2)}$ exerts no influence on the ξ distribution. This important circumstance makes it possible in (3) to limit ourselves to one normal η value with a zero mean value and a unique dispersion, assuming

$$\xi = \omega(\mu_1 + \sigma_1\eta) + (1-\omega)(\mu_2 + \sigma_2\eta). \tag{3'}$$

The five parameters of the mixed distribution should be selected in such a way that in some sense it corresponds best to the observed distribution. As indicated above, one way to solve this problem is a study of the factors forming the probability distributions and the breakdown of the set of ξ observations into two groups on the assumption that within each group they have a normal distribution. The second approach set forth in this article is a choice of the parameters from the condition that the lower-order moments of the approximating distribution coincide with those actually observed, and in addition, that the functional characterizing the difference between the approximating and actual distribution curves has a minimum value. This approach, although it seems too formal, is not without interest and not only because at the present time we are unable to make a reliable selection of the influencing factors and divide the set of their possible values into suitable classes. It is most important that the algorithm described below uses the totality of ξ observations, whereas with its breakdown into two groups one of them in the case $\theta \approx 0$ (or $\theta \approx 1$) is extremely small and unsuitable for reliable determination of the parameters of the mixture component.

Assume that μ_ξ, σ_ξ^2, A_ξ are the mean value, dispersion and asymmetry coefficient for the parameter ξ with the distribution (2), and m, s^2 and A are the stipulated (for example, computed from the observations) values of these characteristics. We will show that by careful choice of the density parameters (2) it is always possible to ensure the equalities $\mu_\xi = m$, $\sigma_\xi^2 = s^2$, $A_\xi = A$, whatever may be the m, s^2 and A values. In other words, the family of distributions (2) contains distributions with any prestipulated mean value, dispersion and asymmetry.

Using (2) we find

$$\mu_\xi = \int x p_\xi(x)\, dx = \theta\mu_1 + \theta'\mu_2,$$

$$\sigma_\xi^2 = \int (x-\mu_\xi)^2 p_\xi(x)\, dx = \theta[\sigma_1^2 + (\mu_1-\mu_\xi)^2] + \theta'[\sigma_2^2 + (\mu_2-\mu_\xi)^2],$$

$$A_\xi = \int \left(\frac{x-\mu_\xi}{\sigma_\xi}\right)^3 p_\xi(x)\, dx = \theta\,\frac{3\sigma_1^2(\mu_1-\mu_\xi) + (\mu_1-\mu_\xi)^3}{\sigma_\xi^3} +$$

$$+ \theta'\,\frac{3\sigma_2^2(\mu_2-\mu_\xi) + (\mu_2-\mu_\xi)^3}{\sigma_\xi^3}.$$

Without impairing universality, it can be assumed that $\mu_2 \geq \mu_1$. We will assume that

$$\frac{\mu_2-\mu_1}{s} = a, \quad \frac{\sigma_2^2-\sigma_1^2}{s^2} = c, \quad a \geq 0. \tag{4}$$

Then from the condition $\mu_\xi = m$ we obtain

$$\mu_1 = m - \theta' as, \quad \mu_2 = m + \theta as. \tag{5}$$

The equation $\sigma_\xi^2 = s^2$ is transformed to the form $z_1^2 = \theta z_1^2 + \theta' z_2^2 + s^2 \theta\theta' a^2 = s^2$

and gives

$$z_1^2 = s^2 (1 - \theta\theta' a^2 - \theta' c), \quad z_2^2 = s^2 (1 - \theta\theta' a^2 + \theta c). \tag{6}$$

Since the dispersion must be a positive value, the parameters a and c must assume values in the intervals

$$0 \leqslant a < \frac{1}{\sqrt{\theta\theta'}}, \quad -\frac{1 - \theta\theta' a^2}{\theta} < c < \frac{1 - \theta\theta' a^2}{\theta'}. \tag{7}$$

Taking into account that $\sigma_\xi^2 = s^2$, the equation $A_\xi = A$ is written in the form

$$A_\xi = 3\theta\theta' ac + \theta\theta' (\theta - \theta') a^3 = A. \tag{8}$$

We will show that with any A there are such values of the parameter θ and the parameters a and c from the intervals (7) with which the equality (8) is satisfied.

First we will examine the case A = 0. In this case we should have either $\theta\theta' = 0$ with arbitrary a and c values from the intervals $(0, \infty)$ and $(-\infty, \infty)$ respectively or a = 0 with arbitrary θ and c from the intervals (0, 1) and $(-1/\theta, 1/\theta')$. There are no other possibilities for reducing A_ξ to zero which are compatible with the limitations (7). We note that with a = 0 and $\theta\theta' \neq 0$ the approximating density, having a zero asymmetry coefficient, will be anormal with an excess index $E_\xi = 3\theta\theta'$ sec^2.

Assume now that $A \neq 0$. Since in this case neither a nor $\theta\theta'$ are equal to zero, equation (8) can be solved formally relative to c:

$$c = \frac{A - \theta\theta' (\theta - \theta') a^3}{3\theta\theta' a}. \tag{9}$$

The equality $A_\xi = A$ is thereby ensured. However, this solution makes sense only with such a and θ values with which the conditions (7) are satisfied. Since the case $\theta\theta' \neq 0$ is considered, it is convenient to convert from a and c to the normalized values z and w using the formulas

$$a = \frac{z}{\sqrt{\theta\theta'}}, \quad c = \frac{w - \theta'}{\theta\theta'} (1 - z^2). \tag{10}$$

Then in place of (5) and (6) we will have

$$\mu_1 = m - \sqrt{\frac{\theta'}{\theta}}\, sz, \quad \mu_2 = m + \sqrt{\frac{\theta}{\theta'}}\, sz, \tag{5'}$$

$$\sigma_1^2 = \frac{(1 - z^2)(1 - w)}{\theta} s^2, \quad \sigma_2^2 = \frac{(1 - z^2) w}{\theta'} s^2; \tag{6'}$$

in this case z and w must assume values in the intervals

$$0 < z < 1, \quad 0 < w < 1. \tag{11}$$

Expression (9) is transformed to the form

$$w = \frac{1 \pm \sqrt{\theta\theta' A - (\theta - \theta')\, z^2 - 3\,\theta' z\,(1 - z^2)}}{3\,z\,(1 - z^2)} = f_A(\theta;\ z). \tag{12}$$

Accordingly, the problem is reduced to proof that with arbitrary $A \neq 0$ the set of z and θ values with which $0 < w < 1$ is not empty. With each fixed z from a unit interval the function $f_A(\theta;\ z)$ assumes values

$$1 + \frac{z^2}{3(1 - z^2)} > 1$$

in the neighborhood of the point $\theta = 0$,

$$\theta = 0, \quad -\frac{z^2}{3(1 - z^2)} < 0$$

in the neighborhood of the point $\theta = 1$ and passes through zero only once at the point

$$\theta_0 = \theta_0(z;\ A) = \frac{t_0^2}{1 - t_0^2}, \quad t_0 = \frac{A}{2z^3} + \sqrt{\left(\frac{A}{2z^3}\right)^2 + \frac{3(1 - z^2)}{z^2}} + 1. \tag{13}$$

With $A > 0$ in the interval (0, 1/2) it first increases and attains a positive maximum, after which it monotonically approaches the negative minimum $-z^2/3(1 - z^2)$. With $A < 0$, on the contrary, it first decreases until it attains a negative minimum within the interval (1/2, 1), then increases to the value $-z^2/3(1 - z^2)$. Thus, the inequality $0 < w < 1$ is satisfied with any z and θ from the intervals

$$0 < z < 1, \quad \theta_1 < \theta < \theta_0. \tag{14}$$

where $\theta_1 = \theta_1(z;\ A)$ is the unique root of the equation $f_A(\theta;\ z) = 1$, which is equal to

$$\theta_1 = \frac{1}{1 + t_1^2}, \quad t_1 = -\frac{A}{2z^3} + \sqrt{\left(\frac{A}{2z^3}\right)^2 + \frac{3(1 - z^2)}{z^2}} + 1. \tag{15}$$

[*The roots of the equations $f_A(\theta;\ z) = 0$, $f_A(\theta;\ z) = 1$ are found without difficulty by their reduction to quadratic equations relative to $\sqrt{\theta / \theta'}$.]

By careful selection of the z and θ parameters within the intervals $0 < z < 1$, $\theta_1 < \theta < \theta_0$ it is possible to satisfy additional conditions. A graphic idea concerning the structure of the set of admissible z and θ values is given in Fig. 1. Since these parameters are interrelated, the tie-in of any functional of the form

$$F(\theta,\ z) = M\varphi(\xi)$$

to a stipulated number F_0 in a general case is evidently impossible. For example, it is impossible to bring about a situation when the excess of the approximating distribution always coincides with the actual values (in this case it must be assumed that $\sigma^4 \varphi(\xi) = (\xi - \mu_\xi)^4 - 3\sigma_\xi^4$); on the other hand, it is scarcely desirable to strive to achieve this because moments of an order above the third are computed on the basis of observational data with large systematic and random errors. Finally, the choice of z and θ can be accomplished by minimizing the appropriate functional $F(\theta,\ z)$, characterizing the discrepancy between the approximating and actual distributions, for example,

$$F(\theta, z) = \sum_{i=1}^{k} \frac{(p_i^* - p_i)^2}{p_i}, \quad p_i > 0, \; i = 1, 2, \ldots, k, \tag{16}$$

where $p_i = P\{\xi \in \Delta_i\}$ is the computed probability that ξ will fall in the interval Δ_i, P_i^* is the actual probability, k is the number of all the intervals.

As an illustration of the described method we will examine an approximation of the distribution of probabilities of the air temperature values registered at scheduled times at the stations Kiev and Dzhusaly in January and July. The numerical characteristics of the sample distributions for two scheduled observation times, computed using observational data for 1936-1964, are cited in Table 1.

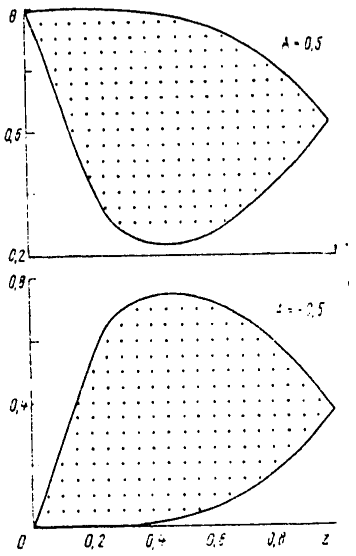

Fig. 1. Characteristic appearance of set of admissible values of the θ and z parameters in dependence on the asymmetry coefficient.

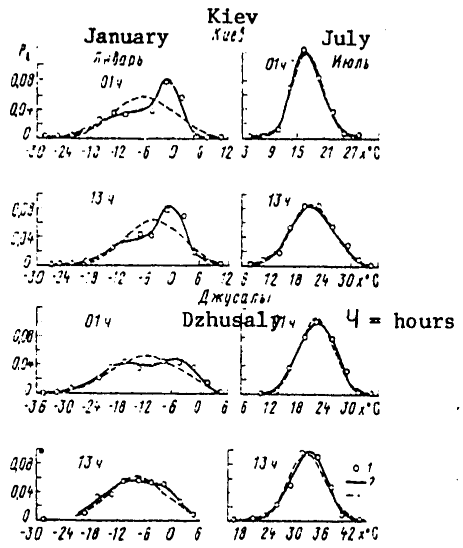

Fig. 2. Approximation of actual probability distribution of air temperature (1) by mixture of normal distributions (2) and normal distribution (3) at Kiev and Dzhusaly stations.

In Fig. 2 the actual probability density is compared with the approximating density (2) in which the optimum values of the z and θ parameters are found by minimizing the functional (16); the corresponding values of the parameters θ, μ_1, σ_1, μ_2, σ_2 and the excess coefficient E_ξ of the approximating distribution are given in Table 2. The dashed curve in Fig. 2 also shows the normal probability density, computed using the data in Table 1. It can be seen that a mixture of two normal distributions makes it possible to describe the actual distributions

of air temperature with a very good approximation.

The choice of a suitable one-dimensional density for approximation of the distribution of probabilities of the ξ value is only a relatively simple part of the problem of constructing a probabilistic model of a series of its values ξ_1, ξ_2, ..., ξ_n. This series is considered stipulated if the joint probability density is determined for any subset of its elements. In our case a necessary solution is found, in principle, without difficulty since it is assumed that the nature of the distribution of the ξ value is governed by the mechanism (3'). Assume that η_1, η_2,..., η_n is a series of normal parameters with zero mean values, unique dispersions and a correlation function $\alpha_{ij} = M\eta_i\eta_j$, and ω_1, ω_2,..., ω_n is a series of indicators with a known probability function $P\{\omega_1 = x_1, \omega_2 = x_2, \ldots, \omega_n = x_n\}$, $x_i = \overline{0, 1}$. Then, assuming

$$\xi_i = \omega_i(\mu_{1i} + \sigma_{1i}\eta_i) + (1-\omega_i)(\mu_{2i} + \sigma_{2i}\eta_i), \tag{17}$$

we obtain a series (generally speaking, nonstationary) ξ_1, ξ_2,..., ξ_n with one-dimensional marginal distributions of the type (2) and with a joint distribution which is unambiguously determined by the distributions of the series $\{\eta_i\}$ and $\{\omega_i\}$. In the statistical modeling of artificial time series this joint distribution is not required in explicit form and we will not write it here, especially since it has an unwieldy structure. We will only indicate the joint density for any two elements ξ_i and ξ_j:

$$\begin{aligned} p_{\xi_i,\xi_j}(x_i, x_j) = \theta_{ij} N(x_i, \mu_{1i}, \sigma_{1i}^2; x_j, \mu_{1j}, \sigma_{1j}^2; \alpha_{ij}) + \\ + (\theta_i - \theta_{ij}) N(x_i, \mu_{1i}, \sigma_{1i}^2; x_j, \mu_{2j}, \sigma_{2j}^2, \alpha_{ij}) + \\ + (\theta_j - \theta_{ij}) N(x_i, \mu_{2i}, \sigma_{2i}^2; x_j, \mu_{1j}, \sigma_{1j}^2; \alpha_{ij}) + \\ + \theta'_{ij} N(x_i, \mu_{2i}, \sigma_{2i}^2; x_j, \mu_{2j}, \sigma_{2j}^2; \alpha_{ij}). \end{aligned} \tag{18}$$

Here N(...) is the two-dimensional normal density with the numerical characteristics indicated in the braces:

$$\begin{aligned} \theta_i = M\omega_i = P\{\omega_i = 1\}, \quad \theta_{ij} = M\omega_i\omega_j = P\{\omega_i = 1, \omega_j = 1\}, \\ \theta'_{ij} = M(1-\omega_i)(1-\omega_j) = 1 - \theta_i - \theta_j + \theta_{ij}. \end{aligned} \tag{19}$$

When $i \neq j$ the ξ_i and ξ_j values are independent only when $\alpha_{ij} = 0$, $\theta_{ij} = \theta_i\theta_j$.

It follows from (18) that

$$\begin{aligned} \rho_{ij} = \frac{\operatorname{cov}(\xi_i, \xi_j)}{s_i s_j} = (f_i f_j + p_i p_j \beta_{ij})\alpha_{ij} + g_i g_j \beta_{ij}, \\ f_i = \frac{\mu_{1i} - \theta'_i \sigma_{2i}}{s_i}, \quad p_i = \frac{\sigma_{2i} - \sigma_{1i}}{s_i}\sqrt{\theta_i\theta'_i}, \quad g_i = \frac{\mu_{2i} - \mu_{1i}}{s_i}\sqrt{\theta_i\theta'_i}; \end{aligned} \tag{20}$$

in this case

$$\beta_{ij} = \frac{\theta_{ij} - \theta_i\theta_j}{\sqrt{\theta_i\theta'_i}\sqrt{\theta_j\theta'_j}} \tag{21}$$

is the correlation coefficient between the indicators ω_i and ω_j. It is clear that the reduction of the correlation coefficient ρ_{ij} to zero is no evidence of a nondependence of ξ_i and ξ_j since it can occur when $\alpha_{ij} \neq 0$ and $\theta_{ij} \neq \theta_i \theta_j$.

Table 1

Numerical Characteristics of Sample Air Temperature Distributions

Month, time	Kiev				Dzhusaly			
	m °C	s °C	A	E	m °C	s °C	A	E
January 01	−6.21	6,66	−0.675	−0.286	−11,5	6,59	−0,243	−0,738
13 hours	−4.52	6.08	−0,696	−0.047	−7,87	6,25	−0,176	−0,439
July 01	17.2	3,15	0.216	−0,106	22,1	3,57	−0,179	−0,290
13 hours	24.2	4,40	0,066	−0,247	32,2	4,16	−0,411	0.403

Table 2

Optimum Values of Parameters of Approximating Distribution

Parameter	Kiev				Dzhusaly			
	January		July		January		July	
	01	13	01	13	01	13	01	13
θ	0,56	0.55	0,14	0,82	0,64	0.88	0.76	0,22
μ_1 °C	−10,2	−6,17	15,2	23,2	−15,5	−8,80	21,1	26,9
σ_1 °C	6,13	5,79	1,12	0,87	6,15	6,06	3,28	4,07
μ_2 °C	−0,98	−0,11	17,5	29,3	−4,23	−1,13	25,5	33,2
σ_2 °C	2,17	2,34	3,24	3,01	3,45	2,07	2,01	3,45
A_i	−0,675	−0,696	0,216	0,066	−0,243	−0,176	−0,179	−0,411
E_i	−0,305	−0,129	0,051	−0,224	−0,644	−0,297	−0,366	0,558

The specific numerical values of the parameters $\mu_{1\,i}$, $\mu_{2\,i}$, $\sigma_{1\,i}$, $\sigma_{2\,i}$, θ_i are substituted into formula (20) after they have been found from the condition of optimum approximation of the one-dimensional probability distributions. With respect to the correlations α_{ij} and β_{ij}, they are selected in such a way that the correlation coefficients ρ_{ij} of the model process coincide with the correlations r_{ij} of the real process or are close to it (the matrix (ρ_{ij}) in this case should be positively determined).

We will clarify in greater detail how this can be done in the example of a stationary process. In order to obtain a stationary series $\xi_1, \xi_2, \ldots, \xi_n$ we will assume that

$$\mu_{1\,i} = \mu_1, \quad \mu_{2\,i} = \mu_2, \quad \sigma_{1\,i} = \sigma_1, \quad \sigma_{2\,i} = \sigma_2, \quad \theta_i = \theta,$$
$$\alpha_{ii-h} = \alpha_h, \quad \beta_{ii+h} = \beta_h. \tag{22}$$

In this case formula (20) assumes the form

$$\rho_h = \rho_{ii+h} = (f^2 + p^2\beta_h)\,\alpha_h + g^2\beta_h;$$
$$f^2 = \frac{(\theta\sigma_1 - \theta'\sigma_2)^2}{s^2}, \quad p^2 = \frac{(\sigma_2 - \sigma_1)^2}{s^2}\,\theta\theta', \quad g^2 = \frac{(\mu_2 - \mu_1)^2}{s^2}\,\theta\theta', \tag{23}$$
$$f^2 + p^2 + g^2 = 1.$$

By careful choice of the appropriate functions α_h and β_h it is always possible to obtain an adequately good approximation of the actual correlation function r_h, computed on the basis of observations. As a rule, it is even possible to ensure a total coincidence of ρ_h and r_h for all h. In actuality, if for the purpose of simplifying the model it is assumed that $\alpha_h = \beta_h = \gamma_h$, then the following quadratic equation is derived

$$p^2\gamma_h^2 + (f^2 + g^2)\,\gamma_h = p^2\gamma_h^2 + (1 - p^2)\,\gamma_h = r_h,$$

whose solution

$$\gamma_h = -\frac{1 - p^2}{2p^2} + \sqrt{\left(\frac{1 - p^2}{2p^2}\right)^2 + \frac{r_h}{p^2}} \tag{24}$$

is a correlation function with any r_h satisfying the condition

$$-p^2\left(\frac{1 - p^2}{2p^2}\right)^2 \leq r_h \leq 1 \tag{25}$$

(if $p^2 = 0$, then $\gamma_h = r_h$). The equality $\rho_h = r_h$ for individual h cannot be ensured except in those relatively rare cases when the actual correlation coefficients are not only negative, but also extremely great in absolute value. In the case of the correlation functions for air temperature time series such a confluence of circumstances should be rare, because, as indicated by available data [3, 4, 6], the r_h values are non-negative for all h with which they are in general statistically significant. However, we note that it is infeasible to achieve an agreement of ρ_h and r_h with all h because the sample correlation function r_h contains systematic and random errors and therefore does not warrant full trust, especially in the case of large h. It is more reasonable to regard ρ_h as a function, which, generally speaking, does not coincide with r_h but in a certain sense approximates it well and at the same time smoothes its characteristic irregularities. The choice of suitable approximating functions is dependent not only on the behavior of r_h, but also on the nature of the specific problem for the sake of whose solution the random process is modeled.

The results of practical modeling of air temperature time series applicable to "surge" problems and the statistical properties of sample evaluations for the parameters of a distribution of the type (2), including evaluations obtained by the described method, merit separate consideration.

The authors express appreciation to A. G. Semochkin for providing the actual materials for the illustrations.

BIBLIOGRAPHY

1. Bryukhan', F. F., "Approximation of the Distributions of Meteorological Elements by a Gram-Charlier Expansion," TRUDY VNIIGMI-MTsD (Transactions of the All-Union Scientific Research Institute of Hydrometeorological Information-World Data Center), No 56, 1978.

2. Kagan, R. L., Kanashkin, V. K., Fedorchenko, Ye. I., "Computation of the Characteristics of Time Series by the Statistical Modeling Method," TRUDY GGO (Transactions of the Main Geophysical Observatory), No 286, 1972.

3. Kagan, R. L., Fedorchenko, Ye. I., "Computation of the Statistical Characteristics of 'Surges' of a Random Function," TRUDY GGO, No 268, 1970.

4. Kiseleva, T. L., Chudnovskiy, A. F., "Statistical Investigation of the Diurnal Variation of Air Temperature," BYULLETEN' NAUCHNO-TEKHNICHESKOY INFORMATSII PO AGRONOMICHESKOY FIZIKE (Bulletin of Scientific and Technical Information on Agronomic Physics), No 11, 1968.

5. Marchenko, A. S., Romanenko, T. P., "Modeling of Gamma Series and Their Use for Study of Wind Velocity Surges," METEOROLOGIYA I GIDROLOGIYA (Meteorology and Hydrology), No 7, 1975.

6. Marchenko, A. S., Pomozova, L. I., Chubenko, M. I., "Time Statistical Structure of Meteorological Processes," TRUDY NIIAK (Transactions of the Scientific Research Institute of Aeroclimatology), No 54(4), 1968.

7. Rozhdestvenskiy, A. V., OTSENKA TOCHNOSTI KRIVYKH RASPREDELENIYA GIDROLOGICHESKIKH KHARAKTERISTIK (Evaluation of Accuracy of Distribution Curves of Hydrological Characteristics), Leningrad, Gidrometeoizdat, 1977.

8. Tikhomirova, L. V., "Experience in Investigation of the Statistical Laws of Air Temperature Distribution at Individual Hours of the Day," TRUDY NIIAK, No 51, 1969.

UDC 551.(510.72+515.3)

CONTAMINATION OF THE NEAR-SURFACE ATMOSPHERIC LAYER BY Cs^{137}

Moscow METEOROLOGIYA I GIDROLOGIYA in Russian No 9, Sep 80 pp 48-53

[Article by Candidate of Physical and Mathematical Sciences K. P. Makhon'ko, Institute of Experimental Meteorology, submitted for publication 4 Mar 80]

[Text]

Abstract: A study was made of the concentration of radioactive dust in air raised by the wind from the soil surface, which is determined through the concentration of radioactivity in the surface soil layer and the weight concentration of the dust raised into the air. The profile of the concentration of isotope in the soil and the percentage of tilled land in the studied region are taken into account. The author gives the temporal change in the mean annual values of the contribution of the "wind component" of the concentration of Cs^{137} in the air to contamination of the near-surface layer of the atmosphere by Cs^{137} of global origin during the period 1963-1978 for the zone of semideserts, zone of tilled lands and as an average for the USSR. The seasonal variation of this parameter is described.

The long-lived isotope Cs^{137} enters the earth's atmosphere during tests of nuclear weapons [3] and falling onto the underlying surface, with the passage of time is accumulated in the soil. Under the influence of the wind the soil dust, containing Cs^{137}, is capable of again rising into the atmosphere, creating additional, secondary contamination of air by the radioactive impurity [4].

We will attempt to estimate the contribution of Cs^{137} caused by its wind capture from the ground surface to the total contamination of the near-surface layer of the atmosphere by Cs^{137} of global origin.

The concentration q_α of radioactive dust in the air raised by the wind from the soil surface is obviously determined easily if the concentration of radioactivity in the surface dust-contaminated soil layer n and the weight concentration C of the dust raised into the air are known.

$$q_{\pi} = \frac{n}{\rho} C. \tag{1}$$

where ρ is soil density.

In order to determine the n value it is possible to employ the data in [1] on the density of contamination of soils in the territory of the USSR with Cs^{137}. [In [1] the density of contamination of soils in the USSR with Cs^{137} was erroneously indicated in μKi/km^2 instead of the proper mKi/km^2.] Here it must be remembered that the Cs^{137} concentration in the surface soil layer can be different in dependence on the vertical distribution of the isotope in the soil profile. In cultivated soils Cs^{137}, falling from the atmosphere onto the ground surface, is regularly mixed in the entire cultivated layer with the depth H. Accordingly, the Cs^{137} concentration in the surface layer n_{surf} will be the same as in the entire soil layer from the surface to the depth H and it can be represented in the form

$$n_{surf} = A/H, \tag{2}$$

where A is the density of soil contamination by Cs^{137} or the isotope reserve in the soil. In naturally bedded soils near the surface there will be a vertical distribution of the isotope concentrations in the soil profile whose character is determined by the rate of vertical migration of the isotope in the soil and changes in the fallout of Cs^{137} from the atmosphere with time [5]. In a general case the concentration of the isotope in the soil n(x) at the depth x at the time t is described by the formula [6]

$$n(x) = \frac{1}{v\Gamma(\nu)}\left(\frac{x}{v_D}\right)^{\nu}\int_0^t \frac{P(\tau)}{(t-\tau)^{\nu+1}} \exp\left[-\frac{x}{v_D(t-\tau)} - \lambda(t-\tau)\right] d\tau, \tag{3}$$

where P(t) is the atmospheric fallout of an isotope with a radioactive decay constant λ, v and v_D are the rates of directed and diffusional migration of the isotope $\nu = v/v_D$, $\Gamma(\nu)$ is the gamma function. The concentration of the isotope at the soil surface n(0) is found by assuming in (3) that $x \to 0$.

Under real conditions part of the considered region can be occupied by plowed fields and part by soils in their natural bedding. In general, both plowed and unplowed sectors of lands will participate in dust formation in the entire region. If p is the fraction of the area of the region occupied by cultivated lands the average Cs^{137} concentration in the surface soil layer for the entire region as a whole can be estimated using the obvious formula

[π = surf]

$$\bar{n} = n_{\pi}p + n(0)\cdot(1-p) = n_{\pi}[p + \varepsilon(1-p)], \tag{4}$$

where the notation $\varepsilon = n(0)/n_{surf}$ has been introduced.

Thus, the concentration of the isotope in the air over a region consisting of plowed and unplowed lands caused by wind capture of dust from the underlying surface can be found if the n in (1) is replaced by $\bar{n}$, with (2) and (4) taken into account, and using the mean soil density value ρ:

$$q_{\pi} = \frac{AC}{H\rho}[p + \varepsilon(1-p)]. \tag{5}$$

The parameters entering into (5), strictly speaking, are dependent on time. We will attempt to restore the pattern of change of the q_α parameter over the territory of the USSR with the passage of time. For this we will consider how the individual parameters in (5) change with time. We will consider only the mean annual values of the parameters. Then the atmospheric dust content C in the first approximation can be considered constant; the fraction of cultivated lands p also has remained virtually unchanged during the last 20 years; soil density ρ can also evidently be considered constant. Thus, there is a time dependence of the density of soil contamination A, which can be computed from the soil accumulation of radioactive fallout from the atmosphere [7], and the parameter ε — the ratio of the surface concentrations of the isotope in naturally bedded soils and in cultivated soils.

The ε value is dependent on the rate of entry of the isotope from the atmosphere onto the soil surface P(t), which changes with time. Using (3) and assuming $\nu = 0$, as a first approximation it is possible to derive the following simple formula for computing ε:

$$\varepsilon = \frac{H}{x}\left[1 - \frac{\int_0^t P(\tau)\exp\left[-\frac{x}{v_D(t-\tau)} - \lambda(t-\tau)\right]d\tau}{\int_0^t P(\tau)\exp\left[-\lambda(t-\tau)\right]d\tau}\right] \qquad (6)$$

Here as the concentration of the isotope in the surface soil layer we use the concentration in the layer 0-x, since in actual practice it is impossible to measure the concentration in a layer of zero thickness and it is assumed that most of the isotope is contained in the layer 0-H. It follows from (6) that for the different geographical regions in which the fallout values P are proportional to one another ε retains one and the same value with identical migration parameters and is dependent only on time. This is attributable to the fact that with time the isotope falling from the atmosphere onto the soil surface gradually migrates in depth, which leads to a decrease of ε.

In Fig. 1 the ε values were computed with formula (6) for $\lambda = 2.3 \cdot 10^{-2}$ yr^{-1}, x = 0.5 cm and typical values of the parameters v_D = 0.5 cm/year, H = 20 cm; the quantity of annual fallout of Cs^{137} from the atmosphere P(t) for the territory of the USSR was taken from [7] in corrected form with the use of [14, 15]. The year 1954, when the intensive entry of Cs^{137} into the atmosphere began due to tests of thermonuclear weapons, was used as the origin of reading t = 0. In this same figure the dots represent the experimental ε values which we computed using the data in [2, 9-13, 16-18] on the vertical profiles of the concentration of Cs^{137} in soils; the vertical lines represent the mean square scatter of data from individual measurements. It is easy to see that there is a satisfactory agreement between the computed curve and the experimental ε values. This makes it possible to use the computed ε values for determining the temporal variation of the Cs^{137} concentration in the atmosphere caused by wind capture from the soil surface. We will refer to this concentration as the wind component.

In order to compute the wind component of the concentration on the basis of formula (5) it is necessary to know the weight concentration of the mineral component of atmospheric dust because the Cs^{137} content in the soil in actual practice is always measured after reduction of the soil sample to ash, when only the mineral part of it remains. Accordingly, we undertook special measurements of the

concentration of mineral dust in the surface layer of the atmosphere in the territory of the Soviet Union. The dust samples were taken at meteorological stations using filtering apparatus and were reduced to ash at a temperature of 450°C, as soil samples are usually reduced to ash.

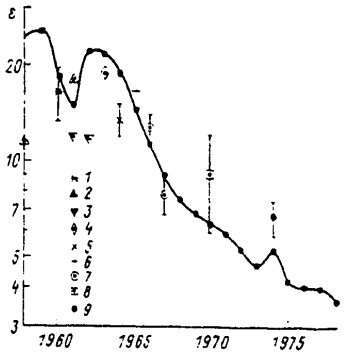

Fig. 1. Temporal change in ε parameter (computations using formula (6)). The dots on the graph represent computations of ε on the basis of experimental data [18] -- 1, [16] -- 2, [17] -- 3, [2] -- 4, [9] -- 5, [13] -- 6, [12] -- 7, [11] -- 8, [10] — 9.

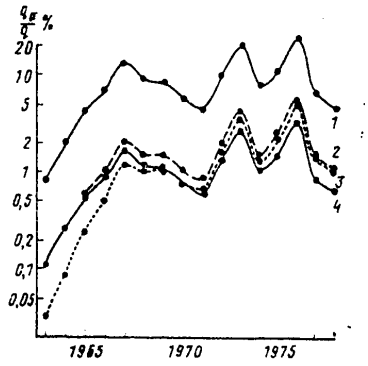

Fig. 2. Temporal change in the fraction of the wind component of the concentration of Cs^{137} in the surface layer of the atmosphere. 1) in zone of semidesert of Kazakhstan and Central Asia, 2) in the Ukraine, 3) in cultivated fields of Kazakhstan, 4) average for the USSR

In the computations of the dust concentration averaged over the area we excluded from consideration the aureoles of increased concentrations around industrial centers caused by technogenic contamination of the atmosphere. The mean concentration was determined as the mean weighted concentration for the area. As a control we also determined the background dust concentration, which was found from the left maximum of the distribution function of quantitative concentrations. There was a good agreement between these two concentrations. For example, for the entire territory of the USSR the mean weighted dust concentration for 1978 was $13\mu g/m^3$, whereas the modal concentration was $15\mu g/m^3$. This indicates a high reliability of exclusion of the technogenic sources of contamination from the averaging.

The wind component of the concentration of Cs^{137} in the atmosphere is always observed against a background of global concentrations of this isotope and therefore we will be interested in the ratio of these concentrations q_α/q. Figure 2 shows the curves of change in the q_α/q values with time, computed using (5), for the semidesert zone, for regions of plowed lands, and as a comparison, as an average for the USSR. The reserve of the isotope in the soil A was determined from the accumulation of its fallout from the atmosphere [7]; data on the concentration of global Cs^{137} q were taken from [3]; data on the fraction of cultivated lands p were taken from [8]; H = 20 cm, ρ = 1 g/cm^3.

Figure 2 shows that the fraction of the wind component of the concentration of Cs^{137} as an average for the country for the period 1963-1978 varied in a wide range and attained maximum values in 1967, 1973 and 1976, that is, in the years when there were minimum concentrations of global Cs^{137}. Thus, the highest value $q_\alpha/q = 3.3\%$ was observed in 1976 when the concentration of global Cs^{137} was $q = 0.44 \cdot 10^{-15}$ Ki/m^3. The highest values $q_\alpha = 6.4 \cdot 10^{-17}$ Ki/m^3 were observed in 1963 and 1964, when there were maximum fallouts of Cs^{137} from the atmosphere and the soil surface was greatly contaminated. During this period the concentrations of global Cs^{137} were also maximum and in 1963 attained $q = 60 \cdot 10^{-15}$ Ki/m^3; accordingly, in this year the fraction of the wind component, despite the high q_α value, was insignificant and amounted to only 0.1%, that is, 30 times less than in 1976.

We will estimate the extremal values of the fraction of the wind component of the concentration of Cs^{137} in the territory of the USSR. The minimum q_α/q values will evidently be observed over swampy expanses of the tundra and for us they are of no interest. Relatively low q_α/q values should be observed over great expanses of cultivated lands due to the low concentration of Cs^{137} in the soil surface layer. Figure 2 shows our computed curve of the change in the fraction of the wind component of the concentration of Cs^{137} over extensive expanses of cultivated lands occupied by grain crops in Northern Kazakhstan (zone of the former virgin lands). In this zone $p = 1$, $C = 65\,\mu g/m^3$ (1978); the concentration q of global Cs^{137} exceeds the average for the USSR by a factor of 1.21 [3], and the reserve A of this isotope in the soil, according to the measurements in [1], is greater by a factor of 1.26 than the average for the USSR, computed in [7]. Figure 2 shows the q_α/q curve for the Ukraine, where the fraction of cultivated lands is great ($p = 0.81$ [8]), $C = 30\,\mu g/m^3$ (1978), the concentration of global Cs^{137} is greater by a factor of 0.82 than the average for the USSR [3], and the relationship between the reserve A of Cs^{137} in the soil and the average value for the USSR is the same as for Northern Kazakhstan [1, 7].

The maximum q_α/q values must be expected in the semidesert zone of Kazakhstan and Central Asia. In this zone $p = 0$, $C = 120\,\mu g/m^3$ (1978); the concentration q of global Cs^{137} is 1.5 times greater than the average for the USSR and the reserve A of Cs^{137} in the soil is the same as the average for the USSR [1, 7]. The q_α/q curve as a function of time, computed using (5) with these values of the parameters, is shown in Fig. 2.

A comparison of the enumerated curves shows that despite the highly differing values of the parameters, the general shape of the curves, shown at a logarithmic scale, coincides well. The maximum q_α/q values were everywhere observed in 1976 and for the cultivated expanses of Kazakhstan were 5.1%, for the Ukraine -- 5.4%, for the semidesert zone -- 24.4%; the average value for the USSR, as already noted above, was 3.3%.

Thus, taking into account the errors in measuring q it can be said that the effect of wind capture of radioactive dust from the underlying surface has practical importance only for the semidesert zone. In the desert zone there are also high values of the dust concentration C and rather high values of the Cs^{137} reserve in the soil ($A = 59$ mKi/km^2 [1]), but as a result of deflation of the soil surface layer by the wind it is difficult to judge the vertical profile of the isotope in the

soil and the Cs^{137} concentration in the surface layer. This problem has not been studied at all experimentally.

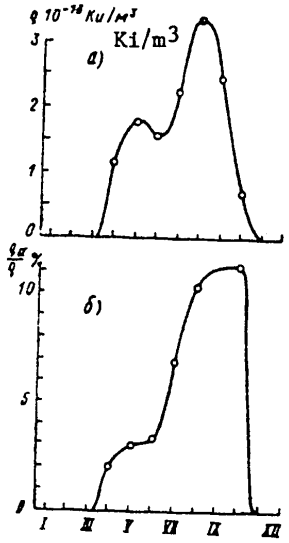

Fig. 3. Annual variation for the semidesert zone in 1978. a) wind component of Cs^{137} concentration in the surface layer of the atmosphere, b) contribution of wind component to contamination of the surface layer of the atmosphere with Cs^{137}.

During dust storms, when the soil surface layer is completely deflated, the effect of secondary radioactive contamination will be especially great, although brief. This problem did not fall within the scope of our study.

It is of interest to examine the annual variation of the wind component of the concentration of radioactive products in the near-surface layer of the atmosphere. As an example, Fig. 3a gives the annual variation of q_α for Cs^{137} in the zone of semideserts in the USSR, computed for 1978. The maximum q_α concentrations are observed late in the summer and the minimum values in winter, when the soil surface is frequently covered with snow and dust formation is difficult. Figure 3b shows the annual variation of the ratio q_α / q for this same region. The figure shows that the maximum contribution of the wind component to contamination of the atmosphere by Cs^{137} is not observed in summer, but in autumn, which is attributable to the influence of the annual variation of q -- the global concentrations of Cs^{137}, which have a maximum at the end of spring and a minimum in autumn.

In conclusion it should be noted that the mean concentration of the isotope q_α for some region, it goes without saying, only in the first approximation, can be considered simply as proportional to the mean weighted concentration $\bar{n}$ for cultivated

and uncultivated sectors in accordance with the fractions of the areas of such soils. The pulverization of the soil is also dependent on its moisture content, the density of the plant cover and similar factors which must be taken into account in the weight factors for each physiographic region separately. However, the lack of such information in the published literature and the obvious difficulties in organizing such large-scale measurements force us to limit ourselves to the simplified approach to the influence mentioned above. The absolute levels q_{α} must be regarded as only estimates whereas their temporal change is more reliable.

BIBLIOGRAPHY

1. Boltneva, L. I., et al., "Global Contamination With Cesium-137 and Strontium-90 and Doses of External Irradiation in the Territory of the USSR," ATOMNAYA ENERGIYA (Atomic Energy), Vol 42, No 5, 1977.

2. Brendakov, V. F., et al., "Vertical Distribution of Fission Products in Some Types of Soils in the USSR," ATOMNAYA ENERGIYA, Vol 25, No 4, 1968.

3. Makhon'ko, K. P., et al., "Patterns of Behavior of Radioactive Aerosols in the Surface Layer of the Atmosphere," METEOROLOGIYA I GIDROLOGIYA (Meteorology and Hydrology), No 10, 1979.

4. Makhon'ko, K. P., "Secondary Entry of Dust Settling on the Ground into the Atmosphere," IZV. AN SSSR, FIZIKA ATMOSFERY I OKEANA (News of the USSR Academy of Sciences, Physics of the Atmosphere and Ocean), Vol 15, No 5, 1979.

5. Makhon'ko, K. P., "Type of Profiles of the Concentration of Fission Products in the Soil for Global and Local Fallout," TRUDY AFI (Transactions of the Agrophysical Institute), No 18, 1969.

6. Makhon'ko, K. P., "Prognostic Computation of Vertical Profiles of the Concentration of Radioisotopes in Soils," TRUDY IPG (Transactions of the Institute of Applied Geophysics), No 8, 1967.

7. Makhon'ko, K. P., et al., "Soil Accumulation of Strontium-90, Cesium-137, Cerium-144 and Zirconium With Niobium-95 as an Average for the USSR," TRUDY IEM (Transactions of the Institute of Experimental Meteorology), No 6(64), 1977.

8. NARODNOYE KHOZYAYSTVO SSSR V 1978. STATISTICHESKIY YEZHEGODNIK (National Economy of the USSR in 1978. Statistical Yearbook), Moscow, Statistika, 1979.

9. Rosyanov, S. P., et al., RASPREDELENIYA STRONTSIYA-90 I TSEZIYA-137 PO PROFILYU POCHV V PRIRODNYKH USLOVIYAKH V 1964 (Distributions of Strontium-90 and Cesium-137 in the Soil Profile Under Natural Conditions in 1964), Moscow, Atomizdat, 1967.

10. Silant'yev, A. N., Shkuratova, I. G., Khatskevich, R. N., "Cesium-137 and Strontium-90 in the Soils of the Central Regions of the European USSR," TRUDY IEM, No 7(76), 1977.

11. Tyuryukanova, E. B., RADIOGEOKHIMIYA POCHV POLESIY RUSSKOY RAVNINY (NA PRIMERE MESHCHERSKOY NIZMENNOSTI) (Radiogeochemistry of Forest Soils on the Russian Plain (In the Example of the Meshcherskaya Lowland)), Moscow, Nauka, 1974.

12. Fedorov, G. A., et al., KHARAKTER RASPREDELENIYA TSEZIYA-137 PO GLUBINE POCHVY V NEKOTORYKH RAYONAKH SOVETSKOGO SOYUZA V 1966-1967 (Nature of the Distribution of Cesium-137 in the Depth of the Soil in Some Regions of the Soviet Union in 1966-1967), Moscow, Atomizdat, 1968.

13. Alexander, L. T., DEPTH OF PENETRATION OF THE RADIOISOTOPES STRONTIUM-90 AND CESIUM-137, HASL-183, 1967.

14. Cambray, R. S., et al., RADIOACTIVE FALLOUT IN AIR AND RAIN. RESULTS TO THE MIDDLE OF 1974, AERE-R 7832, 1974.

15. ENVIRONMENTAL QUARTERLY, EML-335, Appendix, 1978.

16. Trojan, O. A. D., McNeill, K. Q., "Radioactive Contamination of Soil," CANAD. J. PHYS., Vol 40, No 3, 1962.

17. Telfair, D., Luetzelschwab, J., "Penetration of Fallout Fission Products into an Indiana Soil," SCIENCE, Vol 138, No 3542, 1963.

18. Walton, A., "The Distribution in Soils of Radioactivity from Weapon's Tests," JGR, Vol 68, No 5, 1963.

UDC 551.515.2

ON THE DYNAMIC BOUNDARY LAYER OF A WELL-DEVELOPED HURRICANE

Moscow METEOROLOGIYA I GIDROLOGIYA in Russian No 9, Sep 80 pp 54-61

[Article by Candidate of Physical and Mathematical Sciences V. Ye. Zakharov and V. A. Semenov, Institute of Experimental Meteorology, submitted for publication 4 Mar 80]

[Text]

Abstract: A study was made of the problem of a turbulent boundary layer of a stationary well-developed hurricane with a stipulated distribution of tangential velocity. The system of equations of dynamics was closed by the equation for turbulent energy. The mixing path was profiled vertically and in radius applicable to the problem. The formulated system of equations was solved by a numerical method based on use of the momentum theorem. The results correspond to well-known experimental data. The influence of different types of approximations in the equations of dynamics on the results is demonstrated.

In the investigation of a tropical hurricane it is customary to discriminate and separately study its regions differing in their thermohydrodynamic characteristics and the role which each of these regions plays in the process of development and existence of the phenomenon as a whole. Such a method is useful because at the present time it is impossible to formulate a model of a hurricane which would include movements of many scales and their interaction without a parameterized description of some of them. But a successful parameterization can be formulated only on the basis of sufficiently clear theoretical concepts concerning the corresponding processes.

The boundary layer (BL) is the part of a hurricane which is of independent theoretical interest. In the BL the air particles adjacent to the ocean lose their tangential velocity and in conformity to the pressure field move toward the axis of the hurricane with some radial velocity, exchanging heat and moisture with the ocean. The radial velocity causes the appearance of frictional forces which compensate the decrease in centrifugal force, which sooner or later leads to cessation

of translational movement. But air cannot be accumulated in the internal region of a hurricane and acquires a vertical velocity which enables it to rise to the condensation level, which finally leads to the formation of cumulonimbus clouds in the convective zone of the hurricane. The released heat of condensation facilitates an increase in the pressure gradient and accordingly an intensification of meridional circulation. As a result of operation of Coriolis force and centrifugal force some of the energy of this circulation is transformed into the energy of tangential circulation. In order for the hurricane to intensify this inflow must be greater than the losses in friction. This brief exposition of the principal aspects of self-sustaining movement in a hurricane shows that the problem of describing the BL is closely related to the problem of describing the energy supply of a hurricane.

A rather great many studies have been devoted to a theoretical study of the BL. We will mention the principal stages in these investigations. In [7, 12] the BL of a symmetric hurricane was described by the equations of dynamics in the Prandtl approximation in a cylindrical coordinate system with an a priori stipulated turbulence coefficient (k). In [1] the mentioned equations were supplemented by the equation of turbulent fluctuations [3] with the use of the semi-empirical Monin-Obukhov approach [4]. The results obtained in [1] and their comparison with data from an in situ experiment (and the data of a numerical experiment with constant k) indicated the preferability of the description of the BL proposed in [1].

The authors of [6] developed a two-layer model of the BL. The lower layer is described on the basis of the Monin-Obukhov similarity theory. The equation of turbulent fluctuations is used in the upper layer for obtaining k.

In this study an attempt is made to refine the BL model used in [1] by a better profiling of the mixing path (l) both vertically and along the radius, relying on the results obtained in [2]. The numerical experiments were made with a model.

Formulation of Problem and Fundamental Equations

Now we will examine an axially symmetric well-developed hurricane during the period of quasistationarity. Then above the boundary layer it is possible to stipulate the profile of tangential velocity (V) on the basis of in situ observations [9, 12]. We will study a boundary layer forming as a result of the interaction of stipulated movement with the underlying surface. It is assumed that the boundary layer is well mixed and neutrally stratified. Above the BL, as follows from the in situ observations, the radial velocity is much less than the tangential velocity [8, 9]. Therefore, there the gradient balance equation (cylindrical coordinate system) is approximately correct

$$\frac{V^2(r)}{r} + fV(r) = \frac{1}{\rho}\frac{\partial P}{\partial r}, \qquad (1)$$

where r is the radius, f is the Coriolis parameter, ρ is density, P is pressure.

Using the Prandtl approximation, the BL equations of dynamics can be written in the form

$$\frac{1}{r}\frac{\partial (ru^2)}{\partial r} + \frac{\partial (uw)}{\partial z} + \frac{V^2 - v^2}{r} + f(V - v) = \frac{\partial}{\partial z} k \frac{\partial u}{\partial z}, \tag{2}$$

$$\frac{1}{r}\frac{\partial (ruv)}{\partial r} + \frac{\partial (vw)}{\partial z} + \frac{uv}{r} + fu = \frac{\partial}{\partial z} k \frac{\partial v}{\partial z}, \tag{3}$$

$$\frac{1}{r}\frac{\partial (ru)}{\partial r} + \frac{\partial w}{\partial z} = 0. \tag{4}$$

Here u, v, w are the radial, tangential and vertical velocity components in the BL, z is the vertical coordinate.

We note that with an adequate reliability it can be assumed that the Prandtl approximation is satisfied only to the zone of maximum winds. The possibility of using it thereafter is for the time being a debatable problem [10].

We will assume that

$$k = l\sqrt{b}, \tag{5}$$

where b is the energy of turbulent fluctuations. We will discuss the determination of l in greater detail when discussing the method for solving the problem.

On the assumption that the transfer of energy caused by operation of pressure forces is small in comparison with the transfer of velocity fluctuations, that the transfer of energy due to viscosity is small and that the stratification of temperature is neutral, the energy equation for the formulated problem can be written in the form [1, 4]

$$u\frac{\partial b}{\partial r} + w\frac{\partial b}{\partial z} - a_b \frac{\partial}{\partial z} k \frac{\partial b}{\partial z} = -c\frac{b^{3/2}}{l} + k\left[\left(\frac{\partial u}{\partial z}\right)^2 + \left(\frac{\partial v}{\partial z}\right)^2\right]. \tag{6}$$

The constants a_b, c were selected equal to 0.73 and 0.46 respectively [4].

The system of equations (2)-(6) is closed. It remained to form the boundary-value conditions. The vertical boundary conditions are:

$$\begin{aligned} &u \to 0, \quad v \to V, \quad b \to 0 && \text{with } z \to \infty; \\ &u = 0, \quad v = 0; \ \frac{\partial b}{\partial z} = 0 && \text{with } z = 0. \end{aligned} \tag{7}$$

The following must be taken into account in order to formulate the additional conditions along the radius. For sufficiently large r the equations (2), (3), (6) are simplified by discarding the terms containing the derivative of r or the factor 1/r, and terms of the same order of magnitude with them:

$$f(V_n - v_n) = \frac{\partial}{\partial z} k_n \frac{\partial u_n}{\partial z}, \tag{8}$$

[π = per]

$$fu_n = \frac{\partial}{\partial z} k_n \frac{\partial v_n}{\partial z}, \tag{9}$$

$$-a_b \frac{\partial}{\partial z} k_n \frac{\partial b_n}{\partial z} = -c\frac{b_n^{3/2}}{l} + k_n\left[\left(\frac{\partial u_n}{\partial z}\right)^2 + \left(\frac{\partial v_n}{\partial z}\right)^2\right]. \tag{10}$$

The subscript "per" [π] relates to the periphery, where the boundary layer, as follows from (8)-(10), becomes an Ekman boundary layer.

The solution of the system of equations (5), (8)-(10) with boundary conditions of the type (7) also makes it possible to obtain the condition at the outer boundary of the BL of the hurricane.

Solution Method

Assume that r_{per} corresponds to the radius for which the equations (8)-(10) are approximately correct (r_{per} was determined in solving the problem in a numerical experiment). The variables are made dimensionless in the following way:

[π = per]
$$\overline{u} = u/V_n,\ \overline{v} = v/V_n,\ \overline{V} = V/V_n,\ \overline{w} = w/V_n,\ \overline{z} = \frac{zf}{V_n},$$

$$\overline{r} = \frac{rf}{V_n},\ \overline{b} = b/V_n^2,\ \overline{k} = \frac{kf}{V_n^2},\ \overline{l} = lf/V_n.$$

Below for the parameters with a line we use the old notations, provided this does not lead to perplexities. In integrating the derived equations we used an approximate method based on use of the theorem of momenta. The idea of the method is that the velocity and vertical turbulent energy profiles are assumed to change similarly with a change in radius. With such an approach the similarity parameters and coefficients, dependent only on the radius, are unknown. Accordingly, the problem is reduced to a system of ordinary differential equations.

The sought-for parameters are represented in the following form:

[π = per]
$$\begin{aligned} u(r, \eta) &= V(r)\, U(r)\, u_n(\eta), \\ v(r, \eta) &= V(r)\, v_n(\eta), \\ b(r, \eta) &= V^2(r)\, B(r)\, b_n(\eta), \end{aligned} \tag{11}$$

where $\eta = z/\delta(r)$, and $\delta(r)$ is the dimensionless vertical scale of the boundary layer, equal to the ratio of the thickness of a layer with a given r to the thickness of the layer on the hurricane periphery. The parameters $u_{per}(\eta)$, $v_{per}(\eta)$, $b_{per}(\eta)$ are solutions of the problem formulated above for the hurricane periphery.

Now we can discuss the choice of the functional dependence for the mixing path $\overline{l}$. An integral representation was proposed in [2] for the turbulence coefficient. Its use within the framework of a traditional description of a homogeneous BL (8)-(10) made it possible to compute the wind profiles which rather successfully duplicate the profiles obtained experimentally. Since the accuracy of the method for solving the system of nonlinear BL equations proposed here (2)-(7) is dependent on the accuracy with which the u_{per}, v_{per}, b_{per} profiles were obtained for the hurricane periphery, it was desirable to use an integral representation for k. However, in this case this was technically a rather unwieldy procedure. Accordingly, for determining k it was nevertheless decided to use expression (5), and for $\overline{l}$ the Blackadar representation [5]

[π = per]
$$\overline{l} = \frac{c^{1/4}\,\varkappa\,(z + 1/\mathrm{Ro})}{1 + \frac{\varkappa}{V \cdot 0{,}00027}\left(z + \frac{1}{\mathrm{Ro}}\right)},\quad \mathrm{Ro} = \frac{V_n}{z_0 f}, \tag{12}$$

since it was demonstrated in [2] that in this case the differences between the computed and observed wind profiles evidently fall in the range of accuracy of an in situ experiment. We note that expression (12) was used in a modified form

$$\overline{l} = \frac{c^{1/4}\varkappa\left(z+\frac{1}{\mathrm{Ro}}\right)}{1+\frac{(1+Vr)^{3/4}}{0{,}018\,V^{3/4}}\,\mathrm{Ro}^{1/4}\left(z-\frac{1}{\mathrm{Ro}}\right)}. \tag{13}$$

It was taken into account in (13) that a study was made in a rotating fluid and the expression derived in [2] was used for the limiting value of the turbulence scale

$$l_{\max} = \varkappa z_0 (\mathrm{Ro})^{3/4} \cdot 0{,}018.$$

For the effective integration of the energy equation (6) we somewhat transform it, writing it in the form

$$\beta\left(u\frac{\partial b}{\partial r}+w\frac{\partial b}{\partial r}-a_b\frac{\partial}{\partial z}\,k\,\frac{\partial b}{\partial z}\right)=c\,\frac{b^{3/2}}{l}+ \\ +\sqrt{b}\left[\left(\frac{\partial u}{\partial z}\right)^2+\left(\frac{\partial v}{\partial z}\right)^2\right]. \tag{14}$$

Here in

$$\beta=\left(\frac{1-Vr}{V}\right)^{3/4}\frac{\mathrm{Ro}^{1/4}}{c^{1/4}\varkappa\cdot 0{,}018}$$

we have replaced the parameter

$$\frac{1}{l}=\frac{1}{c^{1/4}\varkappa\,(z+1\,\mathrm{Ro})}+\beta, \tag{15}$$

which evidently does not exert a strong influence on the solution of equation (14). In actuality, the first term on the right-hand side of expression (15) has importance only for scales $z<100$-150 km; but it is well known that diffusion is not important at the underlying surface and the convective terms are small in this problem [1], especially at low altitudes.

We substitute (11) into equations (2)-(4), (14). Integrating the result along z from 0 to ∞, after some transformations we have:

$$\frac{dU}{dr}=\frac{U}{V}\,\frac{I_5\left(1-\frac{dV}{dr}\right)}{I_4-I_5}+\frac{U}{r}\,\frac{I_4}{I_4-I_5}-\frac{1}{UI_1}\left(\frac{I_2}{r}+\frac{I_3}{V}\right)+ \\ +\left(\frac{\tau_u}{I_1}-\frac{U\tau_v}{I_4-I_5}\right)\frac{1}{V^2U\delta}, \tag{16}$$

$$\frac{d\delta}{dr}=-\delta\left[\frac{2I_5+I_4\frac{dV}{dr}}{V(I_4-I_5)}+\frac{3(I_4-I_5)}{(I_4-I_5)r}-\frac{1}{U^2I_1}\left(\frac{I_2}{r}+\frac{I_3}{V}\right)\right]- \\ -\left(\frac{\tau_u}{I_1}-\frac{2U\tau_v}{I_4-I_5}\right)\frac{1}{U^2V^2}, \tag{17}$$

$$\beta \frac{dB}{dr} = -\beta B\left(\frac{1}{r} + \frac{1}{U}\frac{dU}{dr} + \frac{3}{V}\frac{dV}{dr} + \frac{1}{\delta}\frac{d\delta}{dr}\right) +$$

$$+ \frac{B^{1/2}}{I_6 U \delta^2}(U^2 I_8 + I_9) - \frac{c^{1/2} B^{3/2}}{\varkappa^2 I_6 U \delta^2}(I_7 + c^{1/4}\varkappa 2\delta\beta I_{10} + \quad (18)$$

$$+ c^{1/2}\varkappa^2\delta^3\beta^2 I_{11}), \quad (19)$$

where $$w_\infty = -\frac{1}{r}\frac{d(rUV\delta)}{dr} I_5,$$

$$I_1 = \int_0^\infty u_n^2\, d\eta, \quad I_2 = \int_0^\infty (1 - v_n^2)\, d\eta, \quad I_3 = \int_0^\infty (1 - v_n)\, d\eta,$$

$$I_4 = \int_0^\infty u_n v_n\, d\eta, \quad I_5 = \int_0^\infty u_n\, d\eta, \quad I_6 = \int_0^\infty b_n u_n\, d\eta.$$

$$I_7 = \int_0^\infty \frac{b_n^{3/2}}{(\eta + \chi)^2}\, d\eta, \quad I_8 = \int_0^\infty \sqrt{b_n}\left(\frac{du_n}{d\eta}\right)^2 d\eta, \quad I_9 = \int_0^\infty \sqrt{b_n}\left(\frac{dv}{d\eta}\right)^2 d\eta,$$

$$I_{10} = \int_0^\infty \frac{b_n^{3/2}}{\eta - \chi}\, d\eta, \quad I_{11} = \int_0^\infty b_n^{3/2}\, d\eta, \quad \varkappa = \frac{1}{\mathrm{Ro}\,\delta};$$

$$\tau_u = \frac{B^{1/2} V^2 U}{\delta}\varphi(r) I_3, \qquad \tau_v = \frac{B^{1/2} V^2}{\delta}\varphi(r) I_5,$$

$$\varphi(r) = \frac{1}{1 + c^{1/4}\varkappa\beta\, 1/\mathrm{Ro}}.$$

In accordance with (11), to the equations (16)-(19) it is necessary to add the initial conditions

$$\delta(r_n) = U(r_n) = B(r_n) = 1. \quad (20)$$

[π = per]

Thus, using equations (8)-(10), (5), (13) and boundary-value conditions of the type (7) we find u_{per}, v_{per}, b_{per}. These equations were integrated by the matrix fitting method with iterations for k in a nonuniform grid. Then the Runge-Kutta method was used in solving the system of equations (16)-(19) with the initial conditions. Then, using expressions (11), we found the solution of the problem (2)-(7), (13).

Discussion of Results and Conclusions

When carrying out numerical experiments the roughness height was selected constant (z_0 = 0.1 m), f = $5 \cdot 10^{-5}$ sec^{-1}, and for determining the V(r) profile we used equation (1) and an analytical expression for pressure at the ocean level from [12]

$$P(r) = P_c + (P_g - P_c)\, e^{\mu(b - R/r)}. \quad (21)$$

Here P_c is pressure with r = 0, P_g is pressure at the periphery, b = R/r_{surf}, μ is a constant obtained from the condition dV(R)/dr = 0. Two V(r) profiles were selected:

1) R = 40 km, $P_g - P_c$ = 60 mb; V(R) = 42.76 m/sec; $V(r_{per})$ = 3.726 m/sec;
2) R = 240 km, $P_g - P_c$ = 60 mb; V(R) = 40 m/sec; $V(r_{per})$ = 7 m/sec.

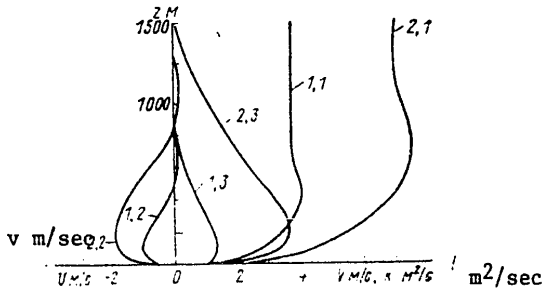

Fig. 1. Profiles of velocities and coefficient of turbulent viscosity on hurricane periphery. The first figure in the notation of the curve corresponds to the V(r) type. The second figure denotes the following: 1) tangential velocity, 2) radial velocity, 3) coefficient of turbulent viscosity.

The first profile (typical mean for well-developed hurricanes) is necessary in order to be able to compare the derived dynamic characteristics of the BL with the averaged data from an in situ experiment [11] and the results from [1]. The second profile is drawn out along r and therefore it is convenient for obtaining results near the center of the hurricane without a substantial decrease in the interval when carrying out integration by the Runge-Kutta method. Figure 1 gives the v, u, k profiles on the hurricane periphery. According to the comparison with the results in [1] there was a qualitative change only in k(z). In this case the BL on the periphery became approximately half as thick and the k(z) maximum decreased from 23 to 1.3 m^2/sec.

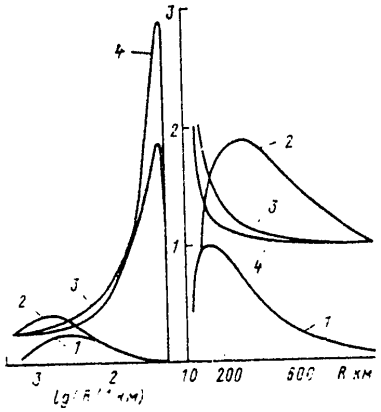

Fig. 2. Some characteristics of boundary layer of hurricane. To the right of the axis are the data corresponding to the first type of V(r), at the left -- the second type. At the left all the values have been reduced by a factor of 4. 1) curves of the maximum k values along z, reduced to dimensionless form for the absolute maximum k value: at right -- 17.8 m^2/sec, at left -- 34.4 m^2/sec; 2) δ ; 3) U, 4) B (see text).

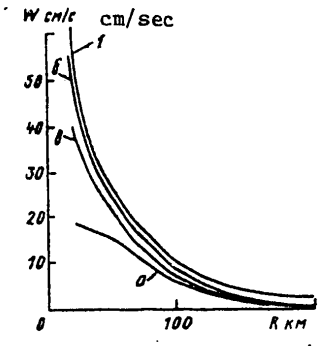

Fig. 3. Vertical velocity at top of boundary layer. 1) formulated problem. The letters correspond to the type of approximation (see text) in the formulated problem.

The data in Fig. 2, in combination with formulas (1), (11), (21) and the information in Fig. 1, make it possible to determine the dimensional values of radial velocity, thickness of the boundary layer, total frictional stress at the surface and angle of wind rotation. The analysis indicates that these computed characteristics of the BL agree well qualitatively and quantitatively with data from averaged experiments in [11].

The $\delta(r)$, U(r) curves on the right side of Fig. 2 with $r > 300$ km for all practical purposes duplicate the shape of the corresponding curves, computed in [1]. However, with $r < 300$ km $\delta(r)$ changes qualitatively in a different way and U(r) increases more rapidly. It is interesting that as a result (see expression (19)) w_∞ in Fig. 3 differs in value insignificantly from the value obtained in [1] (about 10%). The difference in the rate of increase with a change in r and the values of the k maximum is substantial. Whereas in [1] it assumed values from 23 m^2/sec on the periphery to 600 m^2/sec with r = 120 km, in this study these values are 1.3 m^2/sec and 17.8 m^2/sec respectively. This decrease in viscosity also led to a decrease in the thickness of the boundary layer with $r \to 0$ ($r < 300$ km). Evidently, it is already possible to be oriented on the values obtained here for k in the parameterization of the influence of the hurricane BL. The left part of Fig. 2 indicates the possibility of a change in the sign of radial velocity which corresponds to the observational data. Unfortunately, the writing of the equations (16)-(18) adopted here in the numerical integration did not make it possible to pass through the point where U = 0. But the cited data evidently indicate that the change in sign of radial velocity (and vertical velocity) can be obtained within the framework of the formulated problem. This means that the "eye" of the hurricane probably has a purely dynamic origin.

Vertical velocity at the top of the BL is an important characteristic since precisely vertical velocity brings about an energy interaction between the BL and the free atmosphere of the hurricane. Therefore, the quality of parameterization of

the BL must determine the degree of reliability in determining w_∞ . Since in the parameterization of the BL and the modeling of evolution of a hurricane the equations of motion are frequently simplified by one method or another, here an attempt was made at giving an evaluation of these approximations. Therefore, we studied the characteristics of the boundary layer with different formulations of the problem: a) in equation (2) the convective terms were discarded; b) the same, but in equation (3); c) same, but simultaneously in equations (2) and (3). The corresponding w_∞ are given in Fig. 3.

We note at once that in all cases in the neighborhood $r \cong 300$ km the vertical velocities become small (about 0.1-0.3 cm/sec) and negative.

It follows from Fig. 3 that the roughest approximation is the discarding of convective terms in the equation for radial velocity. This is not surprising because they determine the depth of penetration to the center of an air particle moving from the periphery of the hurricane. It is easy to see some compensation of the approximation errors in case (b). This fact is still more clearly traced in the $\delta(r)$, $u(r)$, $B(r)$ not cited here. In the case of the approximation (b) the errors in determining all the variables near the center attain approximately 20-25%. It appears that none of these approximations is acceptable. Especially if an attempt is made to model the evolution of a specific hurricane.

We note that as in [1] it was found that the convective terms in equation (6) exert a negligible influence on the distribution of turbulent energy.

In conclusion it must be emphasized that the proposed method for solving the BL equations makes no pretense at a rigorous determination of the local characteristics in the boundary layer of the hurricane. But experience in use of the theorem of momenta in classical hydrodynamics makes it possible to hope that the integral values (vertical velocity at the upper boundary of the BL, height of the BL, frictional stress, etc.) have been determined quite well.

However, a final conclusion can be drawn only after comparison with corresponding new specific (and not averaged, as in [11]) data for in situ observations or with the results of solution of the system of BL equations by a more precise method.

BIBLIOGRAPHY

1. Zakharov, V. Ye., Sapronov, Yu. T., "Description of the Boundary Layer of a Well-Developed Hurricane Using an Equation for Turbulent Energy," TRUDY IEM (Transactions of the Institute of Experimental Meteorology), No 9(52), 1975.

2. Zakharov, V. Ye., Semenov, V. A., "On the Nonlocal Representation of the Turbulent Viscosity Coefficient," TRUDY IEM, No 22(87), 1979.

3. Kolmogorov, A. N., "Equation of Turbulent Motion of an Incompressible Fluid," IZV. AN SSSR, SERIYA FIZICH. (News of the USSR Academy of Sciences, Physical Series), Vol 6, No 1-2, 1942.

4. Monin, A. S., Yaglom, A. M., STATISTICHESKAYA GIDROMEKHANIKA (Statistical Hydromechanics), Part I, Moscow, Nauka, 1965.

5. Blackadar, A. K., "The Vertical Distribution of Mass and Turbulent Exchange in a Neutral Atmosphere," JGR, Vol 67, 1962.

6. Bode, L., Smith, R. K., A PARAMETERIZATION OF THE BOUNDARY LAYER METEOROLOGY, Vol 8, 1975

7. Carrier, G. F., Hammond, A. L., George, O. D., "A Model of the Natural Hurricane," J. FLUID MECH., Vol 47, Part 1, 1971.

8. Dunn, G. E., Miller, B. I., ATLANTIC HURRICANES, Louisiana State Univ. Press, Baton Rouge, Louisiana, Vol 12, 1960.

9. Gray, W. M., Shea, D. J., "Hurricane Inner Core Region," J. ATMOS. SCI., Vol 30, No 8, 1973.

10. Maxworthy, T., "On the Structure of Concentrated Columnar Vortices," ASTRONAUTICA ACTA, Vol 17, 1972.

11. Palmen, E., Riehl, H., "Budget of Angular Momentum and Energy in Tropical Cyclones," J. METEOROL., Vol 14, No 2, 1957.

12. Smith, R. K., "The Surface Boundary Layer of a Hurricane," TELLUS, Vol 20, No 3, 1968.

UDC 551.(465.7+515.2)

REACTION OF THE UPPER LAYER OF THE OCEAN TO A MOVING TYPHOON

Moscow METEOROLOGIYA I GIDROLOGIYA in Russian No 9, Sep 80 pp 62-70

[Article by G. G. Sutyrin, Institute of Oceanology USSR Academy of Sciences, submitted for publication 29 Jan 80]

[Text]

Abstract: A study was made of the reaction of the upper layer of the ocean to a system of wind stresses and heat fluxes characteristic for a moving typhoon. The author uses an integral model of the upper layer of the ocean consisting of a quasi-homogeneous layer and a density jump layer of finite thickness. The vertical transfer by turbulent pulsations is parameterized with allowance for the balance of kinetic energy of turbulence in the mixed layer. The role of different physical mechanisms in the formation of the typhoon track is analyzed. The results of the computations are compared with observational data in the track of typhoon Tess (1975).

In tropical cyclones (typhoons, hurricanes) the wind attains an enormous force and the exchange of momentum, heat and moisture between the ocean and the atmosphere increases sharply, which leads to a sharply expressed change in the structure of physical fields in the ocean. These changes are most conspicuous in the upper layer of the ocean -- the turbulent stratified boundary layer at the water - air discontinuity.

Using an idealized distribution of wind stress and a linear two-layer model of the ocean, Geisler [17] demonstrated that a moving hurricane excites inertial oscillations whose energy is scattered by gravitational waves. A geostrophically balanced crest is formed behind the hurricane on the internal density discontinuity. The amplitude of such a crest and the velocity of the geostrophic flow associated with it increase with a decrease in the velocity of movement of the hurricane. In this model the density of the upper layer of the ocean remains constant.

Fedorov [12] made an analysis of the types of curves representing the depth distribution of temperature anomalies and constructed an idealized scheme of the vertical circulation of waters caused by the passage of a typhoon. That study emphasizes the important role of convective mixing of waters in the upper homogeneous layer with the colder waters of the upper part of the thermocline, which leads to a considerable increase in the thickness of the homogeneous layer and a temperature increase at the intermediate horizons.

A brief review of the investigations devoted to modeling of the dynamics of the upper layer of the ocean under the influence of tropical cyclones, included in the collection of articles [2], gives the results of computations by Elsberry and Krigsby of the reaction of a two-layer model of the ocean, with allowance for convective-wind mixing between the layers, to a hurricane moving at a constant velocity. The computations were made for a vertical section of the ocean oriented along the hurricane trajectory. The vertical velocity of the current at the depth of the discontinuity has the form of a track predicted by the Geisler linear theory. The first peak of the upwelling is at a distance of approximately 100 km from the hurricane center. The principal difference from the Geisler results is that allowance for turbulent mixing leads to an increase in the thickness of the upper homogeneous layer and a decrease in its temperature. After the passage of the hurricane the mixing between the layers ceases and the temperature of the mixed layer does not change, despite inertial-gravitational oscillations of its thickness.

More detailed results were obtained in the numerical experiments of Chang and Anthes [15] for a uniformly moving idealized eddy over a rectangular region of the ocean with a similar two-layer model. After passage of the vortex, at the ocean surface a zone of water cooled as a result of mixing remains on the ocean surface (in this study heat transfer into the atmosphere was not taken into account). The intensity of cooling increases with a decrease in the velocity of movement of the vortex.

An analysis of different factors in the cooling of the ocean surface, carried out within the framework of an axially symmetric model of interaction between the boundary layers of the ocean and the atmosphere in a tropical cyclone [9], confirmed the dominant role played during a storm by the entrainment into the upper homogeneous layer of colder water from the thermocline associated with turbulent mixing. Thus, for example, the extremal cooling of the ocean surface, attaining 6°C after the passage of hurricane Hilda [20], can be attributed to the greater duration of the effect and the intensity maximum of the hurricane in this place. The decrease in the temperature of the waters from the thermocline entrained into the mixed layer also favors cooling of the ocean surface. In addition, as was demonstrated in [9], the degree of cooling is essentially dependent on the initial heat content of the upper layer of the ocean, which in the region of maximum cooling, according to the data in [20], could be lower.

Recently the observational data obtained on the specialized expeditions of the State Committee on Hydrometeorology, "Tayfun-75" and "Tayfun-78," and on the 27th voyage of the scientific research ship "Akademik Kurchatov" in accordance with the POLIMODE program, considerably enriched our ideas concerning the structure of the track of a tropical cyclone in the ocean [1, 5, 6, 11, 13]. It was found that the changes in the temperature field can be traced not only in the upper layer of the

ocean, but also in the main thermocline in the ocean. An analysis of the change in the heat content of the upper layer of the ocean as a result of the passage of hurricane Ella (1978) indicated that the main role in this change is played by the vertical advection of heat under the central region of passage of the hurricane [3]. Thus, the circulation caused by the tropical cyclone is not closed in the upper layer of the ocean, as was theoretically demonstrated in [8]. Nevertheless, in clarifying the principal peculiarities of structure of the typhoon track in the upper layer of the ocean it is possible to neglect the processes transpiring below, in the main ocean thermocline, as is usually done [7, 9, 10, 15, 17]. On the other hand, the dynamics of currents in the main ocean thermocline can be analyzed without taking into account the vertical turbulent transfer of heat and salts in the upper layer of the ocean [8].

The modeling of the track of typhoon Tess (1975) within the framework of an integral model of the upper layer of the ocean [7] indicated that in those regions where the typhoon slowed its velocity of movement spots of the coolest water remained at the ocean surface. Thus, the observed "spotty" structure of the typhoon track in the ocean [5, 11] can be attributed to the nonuniformity of typhoon movement. In this study we give a description of this model and set forth the results of a numerical investigation of the formation of the track of a tropical cyclone in the upper layer of the ocean under the influence of a model distribution of wind stress and fluxes of apparent and latent heat. The results of the computations are compared with data from observations of the typhoon track in the ocean.

Integral Model of Upper Layer in Ocean

Data from observations in the ocean show that the upper layer usually consists of a mixed vertically quasi-homogeneous layer and a jump layer, where the water density increases sharply with depth (Fig. 1). These peculiarities in the density distribution in the upper layer of the ocean make it possible in the modeling of the variability of its structure to make effective use of the integral method widely employed in the theory of the turbulent boundary layer. Then the dependence of density only on temperature will be taken into account because the influence of salinity is taken into account similarly.

The basis for the model is the continuity equation and the heat balance equation

$$\nabla \mathbf{v} + w_z = 0, \tag{1}$$

$$T_t + \nabla T\mathbf{v} + (Tw)_z = -\Gamma_z, \tag{2}$$

where ∇ is the nabla differential operator in the system of horizontal coordinates x and y, v is the vector of horizontal current velocity, w is the vertical component of current velocity, the z-axis being directed downward, T is temperature, t is time, $\Gamma = \overline{w'T'}$ is the kinematic turbulent heat flux (the primes denote pulsations, the line denotes averaging).

Solar radiation in the typhoon region can be neglected.

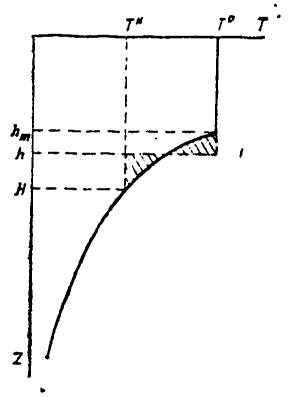

Fig. 1. Vertical temperature profile in upper layer of ocean.

Integrating equations (1), (2) along z from the ocean surface z = 0, where the boundary conditions w = 0, $\Gamma = \Gamma^0$ are satisfied, to the boundary of the upper turbulent layer of the ocean z = H(x, y, t), where $\Gamma = 0$, we obtain

$$\Gamma V = v^H \cdot \nabla H - w^H, \quad V = \int_0^H v\,dz, \tag{3}$$

$$Q_t + \nabla U = \Gamma^0 + T^H v_t, \quad Q = \int_0^H T dz, \quad U = \int_0^H T v\,dz. \tag{4}$$

Here the superscript H denotes the values at the boundary of the upper layer of the ocean, $v_e = H_t + v^H \cdot \nabla H - w^H \equiv a(v_n^s - v_n^w)$ is the rate of entrainment of water from the lower-lying thermocline into the upper layer of the ocean ($a = \sqrt{1 + (\nabla H)^2}$, $v_n^s = H_t a$ is the rate of movement of the surface z = H(x, y, t) along the normal to it, $v_n^w = (w^H - v^H \cdot \nabla H)/a$ is the water current velocity along the normal to this surface).

With expressions (3) taken into account, the rate of entrainment can be represented in the form

$$v_e = H_t + \nabla V. \tag{5}$$

With entrainment ($v_e > 0$) the temperature change at the boundary of the upper layer of the ocean is described by an expression derived from equation (2) for the surface z = H(x, y, t),

$$T_t^H + v^H \cdot \nabla T^H = -\gamma v_e, \quad \gamma = -T_z \text{ with } z = H. \tag{6}$$

Since in the mixed layer the temperature is vertically constant T = T°, the integration of equation (2), with allowance for (1), along z from the ocean surface to the boundary of the quasi-homogeneous layer z = h_m (x, y, t), leads to the expression

$$T_t + \bar{v} \cdot \nabla T = (\Gamma^\circ - \Gamma^m) w_m, \tag{7}$$

where

$$\bar{v} = \int_0^{h_m} v\, dz\, h_m$$

is the mean current velocity in the mixed layer,

$$\Gamma^m = \Gamma \text{ when } z = h_m.$$

The influence of the processes transpiring in the main thickness of the ocean on the dynamics of the upper layer is not considered here and therefore henceforth $v^H = 0$.

The heat content of the upper layer of the ocean can be expressed in the form

$$Q = hT^\circ + (H-h)T^H, \tag{8}$$

where the depth $h = h_m + \sigma(H - h_m)$ is determined from the condition of equality of the shaded areas in Fig. 1

$$\left(\gamma = \int_{h_m}^{H} (T - T^H)\, dz = (H-h_m)(T^\circ - T^H)\right).$$

Substituting expression (8) into equation (4) and also using (5)-(7), we obtain the condition in a jump layer of finite thickness in the following form:

$$(T^\circ - T^H)(h_t + \nabla V) - \Gamma^m = (1 - h/h_m)(\Gamma^\circ - \Gamma^m) + \gamma v_e (H - h) + (h\bar{v} - V) \cdot \nabla T^\circ + \nabla (T^\circ V - U). \tag{9}$$

According to the data in [14], $H/h_m = 1.4\text{-}1.8$, $\sigma = 0.2\text{-}0.3$, therefore $h/h_m = 1.1\text{-}1.2$ and with an accuracy adequate for the integral model it can be assumed that $h \approx h_m$, $h\bar{v} \approx V$, $T^\circ V \approx U$. In addition, usually $\gamma(H\text{-}h) \ll T^\circ - T^H$. Thus, all the terms on the right-hand side of expression (9) can be neglected even under conditions when the thickness of the jump layer has a finite value. Due to the steep drop of temperature in the jump layer, characterized by the σ value, the use of a simple expression at the jump is entirely justified

$$(T^\circ - T^H)(h_t + \nabla V) = \Gamma^m, \tag{10}$$

for whose derivation it is customary to apply the hypothesis of a negligibly small thickness of the jump layer. As in [14], the thickness of the entire upper layer will be assumed to be proportional to the value $h_m : H/h_m = \lambda$.

In this model we will take into account only the drift part of the current velocity, which, as indicated by an analysis of the results in [15, 17], plays the principal role in forming of the track in the ocean under a moving typhoon. The total flux of the horizontal current velocity in the upper layer of the ocean is determined directly from the wind stress τ°:

$$V_t + fk \times V = \tau^{\circ}/\rho. \tag{11}$$

Here f is the Coriolis parameter, k is the unit vector along the z-axis, ρ is water density.

Thus, for finding the parameters of the upper layer of the ocean T^H, T°, h, V we derived the system of equations (6), (7), (10), (11), in which the Γ^m value is determined taking into account the integral balance of kinetic energy of turbulence [9]:

$$\Gamma^m = -c_1\Gamma^{\circ} + c_2 v_*^3 \exp(-c_3 h v_* f)\, g\alpha h, \tag{12}$$

where $v_* = (|\tau^\circ|/\rho)^{1/2}$ is friction velocity, g is the acceleration of free falling, α is the thermal expansion factor, dependent on the temperature of the mixed layer, with the following values of the constants:

$$c_1 = 0.2; \quad c_2 = 1.0; \quad c_3 = 4.0.$$

The computations were made in a rectangular region in a grid with a 30-km interval. The points at which the total flow of the drift current was computed are shifted by a half-interval relative to the points at which the remaining parameters were computed with use of the "predictor-corrector" method, ensuring a second order of approximation in time and space. At those points of the boundary where the total flow V was directed within the region, the Neumann conditions were used for the temperature T° of the mixed layer. At the remaining points of the boundary use was made of a directed differences scheme. The time interval was 1 hour.

The initial values of the parameters in the upper layer of the ocean were selected close to the mean values of the background in the region of passage of typhoon Tess [5]: the temperature of the ocean surface was $T^\circ = 28.5°C$, the thickness of the mixed layer was h = 40 m, the temperature drop in the jump layer was $T^\circ - T = 4.5°C$, the vertical temperature gradient in the thermocline was $\gamma = 0.05°C/cm$, $\lambda = 1.6$.

Exchange of Momentum, Heat and Moisture Between Ocean and Atmosphere

During a storm the expenditures of heat on evaporation and turbulent heat transfer constitute the principal part of the heat flux at the ocean surface $\rho c_p \Gamma^\circ$. Its distribution, and also the flux of momentum τ°, were stipulated by the integral expressions

$$\rho c_p \Gamma^{\circ} = \rho_a c_{pa} c_E \Delta T u (1 + \mathrm{Bo}^{-1}), \quad \tau^{\circ} = \rho_a c_D u u,$$

where c_p and c_{pa} are the specific heat capacities of water and air, ρ_a is air density, Bo = 0.03 and $\Delta T = 0.4°C$ are the characteristic values of the Bowen number and the water-air temperature drop for the conditions of typhoon Tess [1], $u = u_{typh} + u_{wind}$ is the wind velocity at the level of the anemometer, being the sum of the velocity of movement of the typhoon u_{typh} and the wind velocity in the typhoon u_{wind}, whose radial and azimuthal components were determined from the empirical dependence [18]

[T = wind]

$$u_\tau^r = u_m (r/r_m)^\chi \sin\theta, \quad u_\tau^\varphi = u_m (r/r_m)^\chi \cos\theta,$$

$\chi = 1$, $\theta = 0$ with $r \leqslant r_m$; $\chi = -0.5$, $\theta = \theta_m(1 - r_m/r)$ with $r > r_m$.

Here u_m is the maximum wind velocity in the typhoon, r is the distance to the center of the typhoon, r_m is the radius of the maximum winds, $\theta_m = -30°$ is the angle of inflow on the periphery of the typhoon.

The most complete data on the coefficient of exchange of momentum up to a wind velocity of 50 m/sec are presented in [19], and hence we have

$$c_D = (1.2 + u/u_1) \cdot 10^{-3}, \quad u_1 = 40 \text{ m/sec with } u \leqslant 25 \text{ m/sec};$$
$$c_D = u/u_2 \cdot 10^{-3}, \quad u_2 = 14 \text{ m/sec with } u > 25 \text{ m/sec}.$$

The information on the coefficient of exchange of heat and moisture in the presence of stormy winds for the most part has an evaluatory character. The last chapter in [4] notes the possibility of a marked increase in this coefficient due to the generation of spray up to a value $c_E = 0.008$ with u = 40 m/sec. However, estimates of the fluxes of apparent and latent heat from the balance expressions on the basis of observations in a hurricane [21] and on the basis of the change in the heat content of the upper layer of the ocean, with allowance for the advection of heat by currents [3], give basis for assuming that the exchange coefficient increases somewhat more slowly, approximately as follows:

$$c_E = 1.2 \cdot 10^{-3} \quad \text{with } u \leqslant 12 \text{ m/sec},$$
$$c_E = u/u_3 \cdot 10^{-3}, \quad u_3 = 10 \text{ m/sec with } u > 12 \text{ m/sec}.$$

It should be noted that use of the Deardorff method [16] for stormy conditions gives values of the c_E coefficient close to these [10, 21].

Uniformly Moving Typhoon

The temperature anomalies and thicknesses of the mixed layer 96 hours after onset of operation of a typhoon having a maximum wind velocity $u_m = 40$ m/sec with $r_m = 100$ km and a velocity of movement $u_{typh} = 5$ m/sec are shown in Fig. 2. In the case of uniform movement of a typhoon a zone of cooled water is formed at the ocean surface. An upwelling develops behind the center of the typhoon and the thickness of the mixed layer becomes less than the initial thickness, despite the mixing in the rear region of typhoonal action. The inertial oscillations of thickness of the mixed layer (Fig. 2b), whose presence was demonstrated by Geisler [17], exert virtually no influence on its temperature, since after the passage of the region of winds of hurricane force in the typhoon the mixing and cooling are greatly weakened. The asymmetry of wind stress, associated with movement of the typhoon, leads to shifting of the region of maximum cooling and upwelling to the right of the trajectory of the center of the typhoon. These results essentially agree with the computations of Chang and Anthes [15] for a two-layer model with a somewhat different wind distribution and without allowance for the heat flux.

Allowance for the heat flux and the final thickness of the jump layer makes possible a real evaluation of the role of different factors in cooling of the ocean surface. For the section A-A (shown in Fig. 2), in Fig. 3 we give a comparison

of the contribution of the heat flux on the lower boundary of the mixed layer (1), heat transfer into the atmosphere (2) and horizontal advection (3) to change in the temperature of the ocean surface (equation (7)). As already noted, the principal mechanism of its cooling is convective-wind turbulent mixing in the region of winds of hurricane force, which leads to entrainment of colder water from the thermocline into the mixed layer through the jump layer. These computations show that heat loss into the atmosphere gives about one-third of the cooling of the mixed layer in the region of winds of hurricane force and about one-half on the typhoon periphery, thus playing a significant role in cooling of the ocean surface. The horizontal advection of heat exerts a significant effect in the region of high horizontal temperature gradients forming under the influence of the typhoon and leads to an increase in shifting of the region of the maximum cooling of the ocean surface to the right of the typhoon trajectory.

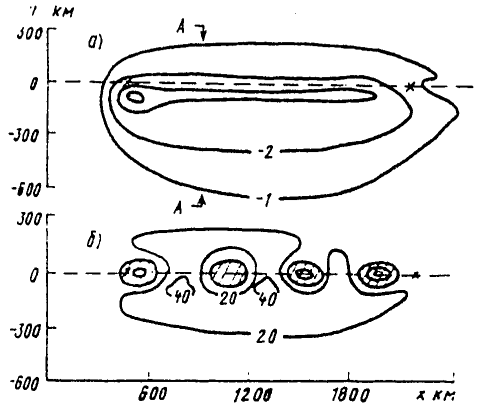

Fig. 2. Anomalies of temperature (a) and thickness (b) of upper homogeneous layer 96 hours after onset of operation of typhoon over ocean. The regions where the thickness is less than initially are shaded. Temperature isolines are drawn each 1° C; isolines of thickness are drawn each 20 m. The crosses represent the initial and final positions of the center of the typhoon, whose trajectory is indicated by a dashed line (movement from left to right).

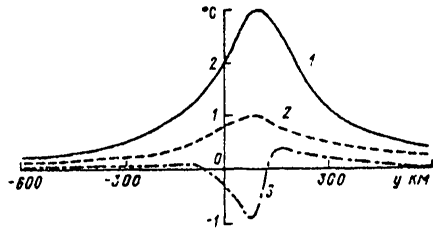

Fig. 3. Distribution of components of temperature anomaly of homogeneous layer in section A-A (see Fig. 2). 1) cooling as a result of entrainment, 2) cooling as a result of heat transfer from ocean surface, 3) change in temperature as a result of horizontal advection.

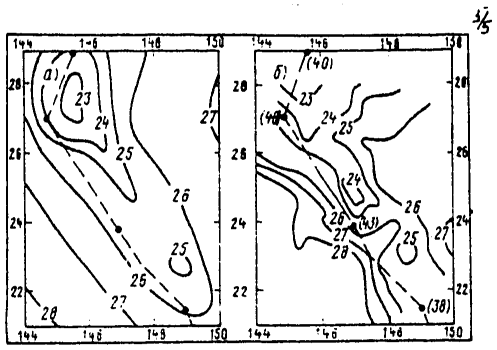

Fig. 4. Temperature of ocean surface in track of typhoon, computed from model for conditions close to conditions of passage of Tess (a) and on basis of observations [5] (b). The dashed line represents the trajectory of the center of the typhoon, the dots represent the position of its center after 24 hours. The maximum wind velocity (m/sec) is given in parentheses.

Modeling of Track of Typhoon Tess

The results of computations of the distribution of temperature at the ocean surface after the passage of a typhoon whose intensity and velocity of movement are stipulated in accordance with data on Tess [1] are given in Fig. 4a. A comparison of the computations with observational data taken from [5] (Fig. 4b) leads to the conclusion that the spotty structure of the Tess track on the ocean surface is associated with nonuniformity of typhoon movement.

In actuality, on the average the typhoon moved at a rate of 5 m/sec. The closed isotherm 25°C is associated with a slowing of the rate of movement of the typhoon to 3.5 m/sec and an increase in intensity (u_m = 43 m/sec) in this region. Then the typhoon increased its velocity of movement, but we do not know how it changed its velocity on the days which followed. In the computations in this sector the velocity of movement was stipulated constant (u_{typh} = 5 m/sec) and therefore there are no closed isotherms here (Fig. 4a), whereas in accordance with observational data, in Fig. 4b there is a closed isotherm. Then the typhoon reduced its velocity of movement by half and changed direction. The ocean surface was cooled to 23°C, which agrees with observations. It is therefore possible to express the hypothesis that the formation of the closed isotherm 24°C (Fig. 4b) was associated with a slowing of movement of the typhoon or a brief increase in its intensity over this region. In addition, the appearance of the isotherm 26°C in the region of passage of the maximum winds could be associated with a preliminary local increase in the velocity of typhoon movement.

These computations were made for an extremely idealized typhoon. To the left of the trajectory of the center the cooling, according to computations, was considerably more intense than according to observational data. Further improvement of the model requires more detailed observations, both in the ocean and in the atmosphere.

We note in conclusion that on the basis of the model of the upper layer of the ocean described above we carried out numerical experiments taking into account the inverse influence of the track in the ocean on the dynamics of a tropical cyclone [10]. With a velocity of movement of 5 m/sec the inclusion of interaction between the ocean and the atmosphere leads to a substantial decrease in the intensity of a tropical cyclone.

BIBLIOGRAPHY

1. Ivanov, V. N., Pudov, V. D., "Structure of the Thermal Track of Typhoon Tess in the Ocean and Evaluation of Some Parameters of Energy Exchange Under Stormy Conditions," TAYFUN-75 (Typhoon-75), Vol 1, Leningrad, Gidrometeoizdat, 1977.

2. MODELIROVANIYE I PROGNOZ VERKHNIKH SLOYEV OKEANA (Modeling and Prediction of the Upper Layers in the Ocean), edited by Ye. B. Kraus, translated from English, Leningrad, Gidrometeoizdat, 1979.

3. Ostrovskiy, A. G., Sutyrin, G. G., "Heat Balance of the Upper Layer of the Ocean During the Passage of a Hurricane," OKEANOLOGIYA (Oceanology), Vol 20, No 5, 1980.

4. PROTSESSY PERENOSA VBLISI POVERKHNOSTI RAZDELA OKEAN-ATMOSFERA (Transfer Processes Near the Ocean-Atmosphere Discontinuity), edited by A. S. Dubov, Leningrad, Gidrometeoizdat, 1974.

5. Pudov, V. D., Varfolomeyev, A. A., Fedorov, K. N., "Vertical Structure of a Typhoon Track in the Upper Layer of the Ocean," OKEANOLOGIYA, Vol 18, No 2, 1978.

6. Pudov, V. D., Petrichenko, S. A., "Thermodynamic Structure of the Track of Typhoon 7807 (Virginia) in the Ocean," TEZISY DOKLADOV XIV TIKHOOKEANSKOGO NAUCHNOGO KONGRESSA (Summaries of Reports at the 14th Pacific Ocean Scientific Congress), Khabarovsk, Ser FI, 1979.

7. Sutyrin, G. G., "Reaction of the Upper Layer of the Ocean to a Moving Typhoon," TEZISY DOKLADOV XIV TIKHOOKEANSKOGO NAUCHNOGO KONGRESSA, Khabarovsk, Ser FI, 1979.

8. Sutyrin, G. G., "Energy Resources of the Stratified Ocean Under an Unmoving Tropical Cyclone," IZV. AN SSSR, FIZIKA ATMOSFERY I OKEANA (News of the USSR Academy of Sciences, Physics of the Atmosphere and Ocean), Vol 15, 1979.

9. Sutyrin, G. G., Khain, A. P., Agrenich, Ye. A., "Interaction Between the Boundary Layers of the Ocean and Atmosphere in a Tropical Cyclone," METEOROLOGIYA I GIDROLOGIYA (Meteorology and Hydrology), No 2, 1979.

10. Sutyrin, G. G., Khain, A. P., "Interaction Between the Ocean and the Atmosphere in the Region of a Moving Tropical Cyclone," DOKLADY AN SSSR (Reports of the USSR Academy of Sciences), Vol 249, No 2, 1979.

11. Tunegolovets, V. P., "Transformation of the Temperature Field in the Ocean After the Passage of a Tropical Cyclone (in the Example of Typhoon Tess (1975)," METEOROLOGIYA I GIDROLOGIYA, No 12, 1976.

12. Fedorov, K. N., "Behavior of the Upper Active Layer of the Ocean Under the Influence of Tropical Hurricanes and Typhoons," OKEANOLOGIYA, Vol 12, No 3, 1972.

13. Fedorov, K. N., "Slow Relaxation of the Thermal Track of a Hurricane in the Ocean," DOKLADY AN SSSR, Vol 245, No 4, 1979.

14. Khar'kov, B. V., "Structure of the Upper Layer of the Ocean," OKEANOLOGIYA, Vol 17, No 1, 1977.

15. Chang, S. W., Anthes, R. A., "Numerical Simulation of the Ocean's Nonlinear, Baroclinic Response to Translating Hurricanes," J. PHYS. OCEANOGR., Vol 8, No 3, 1978.

16. Deardorff, J. W., "Parameterization of the Planetary Boundary Layer for Use in General Circulation Models," MON. WEATHER REV., Vol 100, No 2, 1972.

17. Geisler, J. F., "Linear Theory of the Response of a Two-Layer Ocean to a Moving Hurricane," GEOPHYS. FLUID DYN., Vol 1, 1970.

18. Gray, W. M., Shea, D. J., "The Hurricane's Inner Core Region. 2. Thermal Stability and Dynamic Characteristics," J. ATMOS. SCI., Vol 30, No 8, 1973.

19. Kondo, J., "Air-Sea Bulk Transfer Coefficients in Diabatic Conditions," BOUND. LAYER METEOROL., Vol 9, No 1, 1975.

20. Leipper, D. L., "Observed Ocean Conditions and Hurricane Hilda, 1964," J. ATMOS. SCI., Vol 24, No 2, 1967.

21. Moss, M. S., Rosenthal, S. L., "On the Estimation of Planetary Boundary Layer Variable in Mature Hurricanes," MON. WEATHER REV., Vol 103, No 11, 1975.

UDC 551.461.(261)

COMPUTATION OF THE OCEAN LEVEL

Moscow METEOROLOGIYA I GIDROLOGIYA in Russian No 9, Sep 80 pp 71-80

[Article by Professor A. S. Sarkisyan, Yu. L. Demin and A. M. Gurina, Institute of Oceanology USSR Academy of Sciences, submitted for publication 29 Jan 80]

[Text]

Abstract: On the basis of the most complete and detailed observational data (in comparison with those used previously) the authors made a series of numerical experiments for the northern part of the Atlantic Ocean based on schemes with different orders of approximation. An evaluation of the influence of refinements of the model and the numerical method on the accuracy of computing the level and currents in the ocean is presented.

As is well known, level is one of the important hydrodynamic characteristics of the ocean. Being of independent oceanographic interest as a characteristic of surface gradient currents, the level field, in addition, is the principal integral function in many models of oceanic circulation [9]. Accordingly, the accuracy in computing level to a great extent governs the accuracy in computing the field of currents. The accuracy and correctness in computing level are of particularly great importance in prognostic problems. To be sure, at the present time such problems are based on the "total flows" function. However, in some cases models based on the level function are preferable (for example, in an investigation of equatorial circulation [10] and in global computations of currents in multiply connected regions [6]).

In our research, on the basis of the most complete and detailed observational data (in comparison with those used earlier) we carried out a series of numerical experiments for the North Atlantic based on schemes with different orders of approximation. We will formulate both an oceanographic problem -- obtaining more precise and detailed information on the ocean level and comparison with earlier results, and a methodological problem -- an evaluation of the influence of refinements of the model and the numerical method on the accuracy of computations of the level and currents.

The computations made here are based on the quasi-geostrophic model given in [9]. In this model the pressure gradient is balanced by the Coriolis force and vertical turbulent viscosity. It is well known that a quasi-geostrophic approximation is completely justified when computing macroscale currents of the extra-equatorial zones of the ocean [9]. The basis for this model is the following boundary-value problem for the level:

Level equation

$$\frac{1}{2\alpha}\Delta\zeta+\frac{1}{\sin\theta}\left(\frac{\partial H}{\partial\theta}+H\operatorname{tg}\theta\right)\frac{\partial\zeta}{\partial\lambda}-\frac{1}{\sin\theta}\frac{\partial H}{\partial\lambda}\frac{\partial\zeta}{\partial\theta}=$$

$$=\frac{a}{\rho_0 g}\left(\frac{\partial\tau_\lambda}{\partial\theta}+\tau_\lambda\operatorname{ctg}\theta-\frac{1}{\sin\theta}\frac{\partial\tau_\theta}{\partial\lambda}\right)-\frac{1}{2\alpha\rho_0}\int_0^H\Delta\rho\,dz- \tag{1}$$

$$-\frac{1}{\rho_0\sin\theta}\left(\frac{\partial H}{\partial\theta}\int_0^H\frac{\partial\rho}{\partial\lambda}\,dz-\frac{\partial H}{\partial\lambda}\int_0^H\frac{\partial\rho}{\partial\theta}\,dz\right)-$$

$$-\frac{1}{\rho_0\cos\theta}\int_0^H(H-z)\frac{\partial^2\rho}{\partial\lambda^2}\,dz.$$

Boundary conditions for meridional sectors of the contour

$$\left(1-\frac{1}{2\alpha H}\right)\frac{\partial\zeta}{\partial\theta}=-\frac{1}{\rho_0 H}\int_0^H(H-z)\frac{\partial\rho}{\partial\theta}\,dz+\frac{a}{\rho_0 gH}\tau_\theta+\frac{2a\omega\cos\theta}{gH}V_\lambda+ \tag{2}$$

$$+\frac{1}{2\alpha\rho_0 H}\int_0^H\left(\frac{\partial\rho}{\partial\theta}+\frac{1}{\sin\theta}\frac{\partial\rho}{\partial\lambda}\right)dz+\frac{1}{2\alpha H\sin\theta}\frac{\partial\zeta}{\partial\lambda};$$

for the zonal sectors of the contour

$$\left(1-\frac{1}{2\alpha H}\right)\frac{\partial\zeta}{\partial\lambda}=-\frac{1}{\rho_0 H}\int_0^H(H-z)\frac{\partial\rho}{\partial\lambda}\,dz+\frac{a\sin\theta}{\rho_0 gH}\tau_\lambda- \tag{3}$$

$$-\frac{2a\omega\sin\theta\cos\theta}{gH}V_\theta+\frac{1}{2\alpha\rho_0 H}\int_0^H\left(\frac{\partial\rho}{\partial\lambda}-\sin\theta\frac{\partial\rho}{\partial\theta}\right)dz-\frac{\sin\theta}{2\alpha H}\frac{\partial\zeta}{\partial\theta}.$$

Notations: H is ocean depth; ρ is the density anomaly, $\tau_\lambda, \tau_\theta$ are the components of wind shearing stress; $\zeta = \zeta_1 + P_a/\rho_0 g$ is the reduced level (ζ_1 is the physical level, P_a is atmospheric pressure, g is the acceleration of free falling); a is the earth's mean radius; ρ_0 is some constant density value (here $\rho_0 = 1.028$ g/cm^3); $\alpha = (\omega\cos\theta/\nu)^{1/2}$ is the Ekman parameter (ω is the angular velocity of the earth's rotation, ν is the coefficient of vertical turbulent viscosity); λ is longitude; $\theta = \pi/2 - \varphi$ is the polar angle (φ is latitude);

$$V_\lambda=\int_0^H v_\lambda\,dz,\quad V_\theta=\int_0^H v_\theta\,dz,$$

are the integral water discharges;

$$\Delta=\partial^2/\partial\theta^2+\operatorname{ctg}\theta\,\partial/\partial\theta-\partial^2/\partial\lambda^2/\sin^2\theta$$

is the Laplace operator in a spherical coordinate system.

The λ axis is directed eastward, θ is directed southward, z is directed vertically downward.

We will reduce this problem to a problem for reduced pressure at the bottom [3, 7], introducing

$$\zeta = \zeta_g + \zeta'. \tag{4}$$

where $\zeta_g = -\frac{1}{\rho_0}\int_0^H \rho\, dz.$

Substituting (4) into (1)-(3), we obtain an equation for pressure at the bottom

$$\frac{1}{2\gamma}\Delta\zeta' - \frac{1}{\sin\theta}\left(\frac{\partial H}{\partial\theta} + H\operatorname{tg}\theta\right)\frac{\partial\zeta'}{\partial\lambda} - \frac{1}{\sin\theta}\frac{\partial H}{\partial\lambda}\frac{\partial\zeta'}{\partial\theta} =$$

$$= \frac{a}{\rho_0 g}\left(\frac{\partial\tau_\lambda}{\partial\theta} + \tau_\lambda\operatorname{ctg}\theta - \frac{1}{\sin\theta}\frac{\partial\tau_\theta}{\partial\lambda}\right) + \frac{1}{\rho_0\cos\theta}\frac{\partial}{\partial\lambda}\int_0^H z\rho\, dz + \tag{5}$$

$$+ \frac{1}{2\gamma\rho_0}\left[\rho_H\Delta H + 2\left(\frac{\partial H}{\partial\theta}\frac{\partial\rho_H}{\partial\theta} + \frac{1}{\sin^2\theta}\frac{\partial H}{\partial\lambda}\frac{\partial\rho_H}{\partial\lambda}\right)\right]$$

with the boundary conditions

$$\left(1 - \frac{1}{2\gamma H}\right)\frac{\partial\zeta'}{\partial\theta} = \frac{1}{\rho_0 H}\frac{\partial}{\partial\theta}\int_0^H z\rho\, dz + \frac{a}{\rho_0 g H}\tau_\theta + \frac{2a\omega\cos\theta}{gH}V_\lambda + \tag{6}$$

$$+ \frac{1}{2\gamma H\sin\theta}\frac{\partial\zeta'}{\partial\lambda},$$

$$\left(1 - \frac{1}{2\gamma H}\right)\frac{\partial\zeta'}{\partial\lambda} = \frac{1}{\rho_0 H}\frac{\partial}{\partial\lambda}\int_0^H z\rho\, dz + \frac{a\sin\theta}{\rho_0 g H}\tau_\lambda -$$

$$- \frac{2a\omega\sin\theta\cos\theta}{gH}V_\theta - \frac{\sin\theta}{2\gamma H}\frac{\partial\zeta'}{\partial\theta}. \tag{7}$$

Neglecting the derivatives of ζ' along the normal to the contour and substituting into (6) and (7) the expressions for the water discharges, obtained by the quasi-dynamic method

$$V_\lambda = -\frac{g}{2a\rho_0\omega\cos\theta}\frac{\partial}{\partial\theta}\int_0^H z\rho\, dz,\quad V_\theta = \frac{g}{2a\rho_0\omega\cos\theta\sin\theta}\frac{\partial}{\partial\lambda}\int_0^H z\rho\, dz, \tag{8}$$

in place of (6), (7), we arrive at the expressions

$$\frac{\partial\zeta'}{\partial\lambda} = \frac{a\sin\theta}{\rho_0 gH}\tau_\lambda, \tag{9}$$

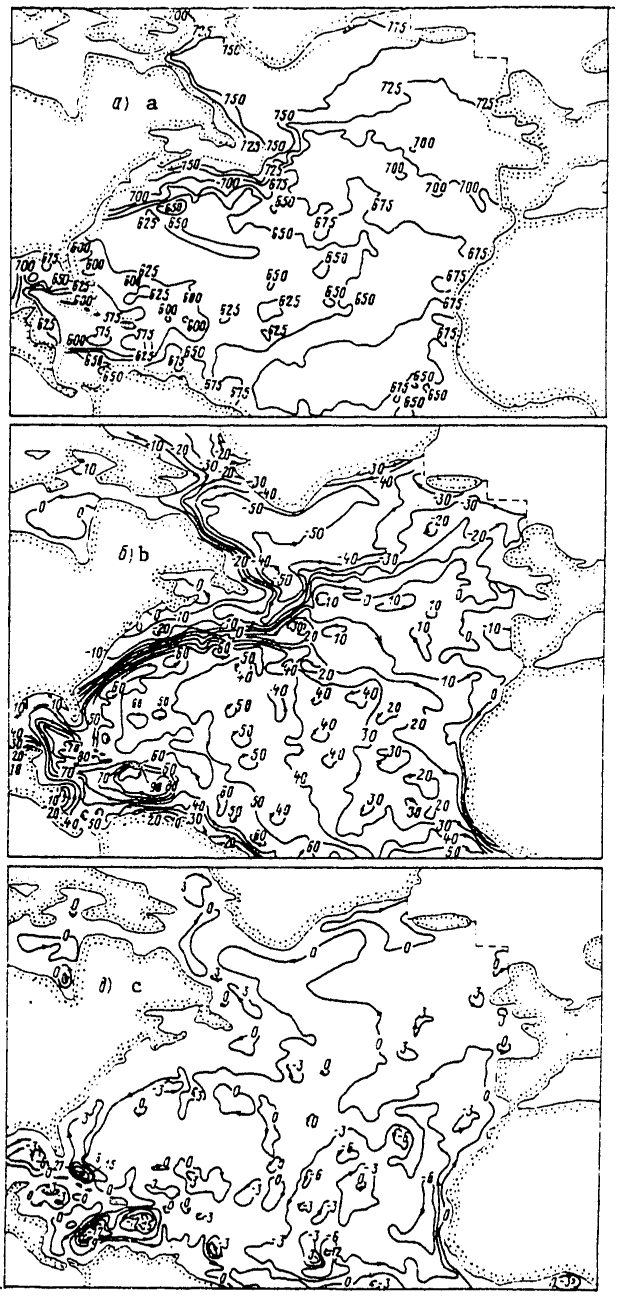

Fig. 1. Density field at a depth of 200 m (the values of the isolines correspond to $\rho' = 10^5 (\rho_1 - 1.02)$ (a), level surface of the North Atlantic, cm (b) and field of reduced pressure at bottom, cm (c).

$$\frac{\partial \zeta'}{\partial n} = \frac{\tau}{\rho g H} \tau_\theta \cdot \qquad (10)$$

The very insignificant role of the normal derivatives of ζ' has been repeatedly demonstrated by computations of macroscale circulation made earlier (at least with grid intervals 1° or more [9]). However, allowance for these terms sharply increases the time expenditures on an electronic computer. With respect to stipulation of the water discharges by the quasidynamic method, for the time being there is no other more acceptable method for their stipulation. It is known (and this will be seen from the computed data) that the quasidynamic method is a good approximation in computing the level. We then note that since we are considering a stationary problem, integrated along the contour, the discharge must be equal to zero. As a result of neglecting the normal derivatives of ζ' and stipulation of the discharges by the quasidynamic method, this condition, generally speaking, is not satisfied. The balancing of the discharge is accomplished by a method proposed in [1]. We emphasize here that in diagostic problems the satisfaction of this condition is not so important since the influence of the boundary conditions in these problems is localized near the boundaries of the basin and the errors in the boundary conditions to all intents and purposes are not reflected in the solution within the region [9].

The advantage of this approach is that the main part of the solution ζ_g is computed precisely, using an explicit formula (including the boundary of the region), whereas for ζ' we obtain a less unwieldy problem, and accordingly, one which is simpler to solve on an electronic computer. In contrast to [3, 7], conversion to the problem for ζ' has been done precisely, with preservation of the bottom friction effect (the underlined term in (5)).

The "directional differences" method is used in constructing the difference scheme. The solution of the difference problem was found by the Gauss-Seidel method. The computations were carried out in three stages. In the first stage we found a solution in the initial grid using the directional differences scheme, that is, with a first order of approximation. In the second stage a solution was found by the same method, but in a grid with an interval half as great. The "input" data in this case were determined by interpolation of the initial data. Finally, in the third stage a corrector in the form

$$\zeta^h = 2\zeta^{h/2} - \zeta^h. \qquad (11)$$

was obtained.

As a result, in the initial grid the solution was obtained with a second order of accuracy. The described procedure for increasing the order of approximation of the difference schemes is one of the variants of the embedded grids method and was proposed in [5]. The iteration process for solution of the difference problem was continued until satisfaction of the condition $\max|\zeta_{n+1} - \zeta^n| < \varepsilon$, where n is the number of the iteration. On the basis of numerical experiments the ε value was assumed equal to 10^{-3}. The results in this case are not dependent on the initial approximation. The coefficient of vertical turbulent viscosity ν was assumed equal to 10 cm^2/sec.

The computations were made for the North Atlantic. The greatest number of diagnostic computations were evidently made for this region of the world ocean. The southern boundary of the considered region was situated at 3.5°N and the northern boundary at 72.5°N. In the eastern part of the basin it passes through the shallow waters in the neighborhood of the Danish straits (shown in the figures by a dashed line). The grid interval is 1° and the number of computation horizons is 31, from the surface to 6,000 m. The basis for the computations was information on the mean long-term temperature and salinity distribution for the summer season. Data on temperature and salinity, as well as the mass of averaged ocean depths, were prepared at Princeton University in the United States. The density anomaly ρ was determined, in accordance with [9], as $\rho(\lambda, \theta, z) = \rho_1(\lambda, \theta, z) - \bar{\rho}(z)$, where ρ_1 is density and $\bar{\rho}(z)$ is the standard mean vertical distribution of density. The "input" data on the components of wind shearing stress were prepared using the Hellerman tables [11]. Thus, in this study we examine the climatic circulation of waters of the North Atlantic in summer. An example of the density field is shown in Fig. 1a. We note that this map, like the subsequent maps, was constructed using a CALCOMP curve plotter.

Figure 1b shows the level surface field obtained with a second order of accuracy. The level map is more characteristic of subsurface than surface circulation because it does not reflect drift transfer. Accordingly, in particular, on this map, as in other diagnostic level computations (see [9]), there is no North Trades Current. However, the macroscale circulation elements expressed in the density field are represented rather clearly. The level drop in the Gulf Stream is more than 90 cm, in the Guinea, Guiana and Labrador Currents -- 40-50 cm, in the East and West Greenland Currents -- 20-30 cm. The total level drop was about 1.5 m. The very well-developed circulation systems of the Caribbean Sea and the Gulf of Mexico are the sources of the Gulf Stream. In general, however, with the exception of the Guinea, West Greenland and Canaries Currents, located along the eastern coast, and also the Inter-Trades Countercurrent and the North Atlantic Current, passing through the ocean from west to east, all the most powerful systems of currents are situated along the western shore — a clear illustration of the role of the β-effect. One of the most interesting peculiarities of Fig. 1b is the representation of a clearly expressed flow of Labrador waters toward the shores of America, driving the Gulf Stream away from the shore.

In comparison with the diagnostic computations made earlier (for example, see [9]), the presented map is more detailed and informative. In [2], where one of the authors earlier made computations in a 5° grid, the level drop in the Gulf Stream is 1 1/2 times less than in this study, the flow is considerably broader and the velocity is much weaker. The fundamental, global characteristics of circulation coincide qualitatively but in [2] many detailed characteristics are absent and narrow flows, such as the Guinea Current, are expressed very weakly. The circulation in the Caribbean Sea is far less developed. The principal reasons for these differences, to be sure, are the grid interval and the detail of the density field. However, in addition to the quality of the density field, an important role is also played by the peculiarities of the model and the numerical method.

For example, in [8], in which a quasi-geostrophic model and approximately the same grid interval (1°15') are used, the level map differs appreciably from that presented here. The subpolar cyclonic circulation is poorly expressed and the flow

of Labrador waters toward the shores of America is completely absent: the Gulf Stream occupies the entire coastal region. One of the principal reasons for these discrepancies is methodological: in the numerical realization of the model there was a strong exaggeration of the "baroclinic" effect of bottom relief, which led to a suppression of "anomalous" coastal currents. Labrador waters are also absent on the level map in [12], where the computations were made using a nonlinear model in a grid with a 1° interval. It is interesting that the level drop across the flow of the Gulf Stream is the same as in these computations (90 cm). However, other jet currents were expressed extremely weakly. In general the map is rather close to that obtained in a 5° grid in [2]. To a considerable degree this is associated, in our opinion, with the strong smoothing effect of horizontal viscosity (as a result of the high value A_ξ equal to $4 \cdot 10^8$ cm^2/sec).

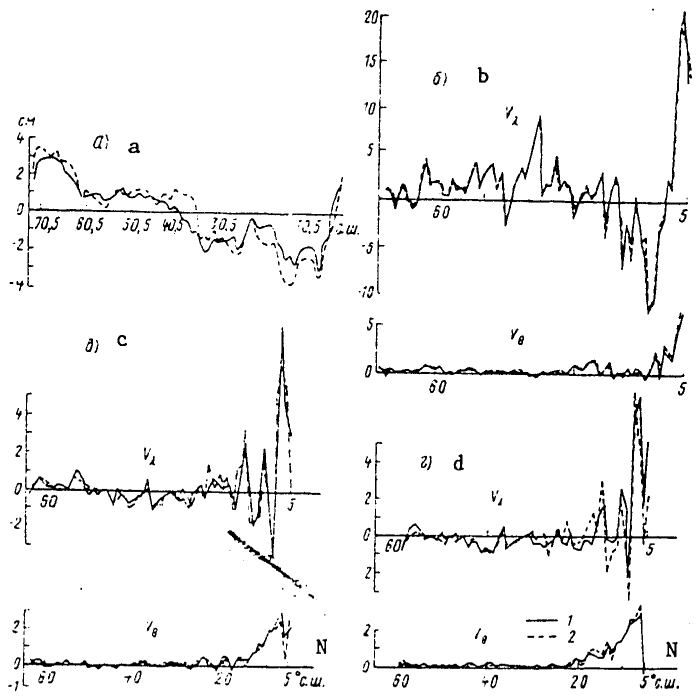

Fig. 2. Distribution of mean latitudinal values of reduced bottom pressure (a), zonal (v_λ) and meridional (v_θ) velocity components at horizons 50 m (b), 1,500 m (c), 3,000 m (d). 1) variant of computations with second order of accuracy, 2) with first order of accuracy.

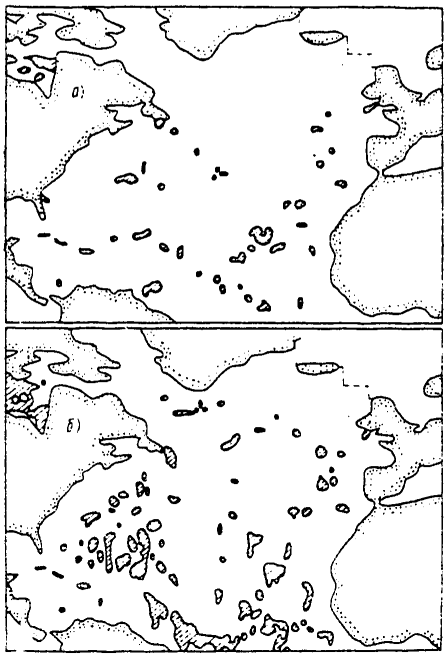

Fig. 3. Fields of Reynolds difference numbers. a) $r^{(\lambda)}$, b) $r^{(\theta)}$. In the shaded regions $r^{(\lambda)}$, $r^{(\theta)} \leqslant 10$.

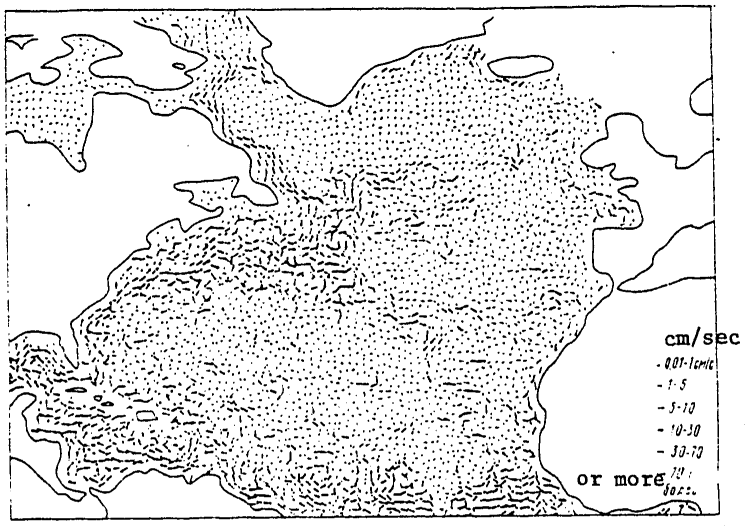

Fig. 4. Surface gradient currents in North Atlantic.

Figure 1b shows a considerable number of relatively small circulations. An attempt at smoothing them by means of a Tukey cosine filter led to a dual result. On the one hand, the number of small eddies considerably decreased, but on the other hand, there was a considerable weakening of jet currents. The Gulf Stream became broader and the velocities in it decreased appreciably. The narrow Guinea Current, in particular, "suffered." The double use of the filter leads to a pattern extremely close to that obtained in a 5° grid in [2].

Figure 1c represents the field of reduced bottom pressure obtained using the corrector. It is some dynamic characteristic of deep and bottom currents. The total drop ζ' is about 40 cm, that is, approximately 25% of the drop ζ. The most developed circulatory systems are in the southwestern part, in the region of the Caribbean Sea, Gulf of Mexico and to the north of the West Indies. A chain of circulations can also be seen in the neighborhood of the Mid-Atlantic Ridge. The intensive bottom circulation in these zones is evidently caused by the very nonuniform bottom relief. The most interesting characteristic of this map is that it graphically demonstrates a virtually universal tendency of oceanic currents to be restructured with depth. An extensive cyclonic system is formed in the area of the subtropical anticyclonic circulation; it, joining with the subpolar cyclonic circulation, forms a gigantic cyclonic ring occupying almost the entire North Atlantic. The tendency to the formation of countercurrents is manifested in most circulatory systems in the ocean: in the neighborhood of the Gulf Stream, Laborador and East Greenland Currents, the currents in the Caribbean Sea and the Gulf of Mexico, and others. A countercurrent is very well expressed along the shores of Northwest Africa. It is known [13] that a deep countercurrent, directed poleward, is an important component of the dynamics of the coastal upwelling, whose zone is the region in question. One of the few systems where the direction does not change with depth is the Inter-Trades Countercurrent. The latter peculiarity, like the restructuring of the subtropical anticyclonic circulation with depth, was noted earlier in [1] in an investigation of the dependence of integral circulation on the thickness of the baroclinic layer. It is interesting that on the bottom pressure map, in contrast to the level map, the western intensification cannot be traced. Along the shores of Africa, for example, the bottom pressure gradient is much greater than in the Gulf Stream region, that is, the bottom relief effect successfully competes here with the β-effect.

Computation of the values of the terms on the right-hand side of (5) shows that the "weight" of the term expressing the bottom friction effect, taken into account in this problem, is approximately the same as the "weight" of the wind term. And although the density term on the right-hand side of (5) is the most important, even on the average it exceeds the other two terms by less than an order of magnitude. Thus, in correct computations of bottom pressure it is necessary to take all three terms into account.

The solutions for ζ', obtained with the first and second orders of accuracy, were qualitatively extremely close. However, the quantitative refinements were considerable. This can be seen even from a comparison of the mean ζ' profiles constructed for a "meridional ocean" (Fig. 2a). The differences in the level fields were far less considerable, as is understandable; indeed, the principal part of the solution, ζ_g, is the same in both variants. It is interesting to note that the mean

zonal level profile is diametrically opposite the bottom pressure profile: if the ζ ' surface is tilted from north to south, the level drops from south to north. This is still another illustration of the fact that countercurrents are a distinguishing characteristic of the ocean.

It is known [4] that schemes of the first and second orders of approximation give close results if the Reynolds difference numbers are much greater than unity. In this case these numbers have the form

$$r^{(\theta)} = h\alpha \left| \frac{H}{\cos\theta} + \frac{1}{\sin\theta} \frac{\partial H}{\partial \theta} \right|; \quad r^{(\lambda)} = h\alpha \left| \frac{1}{\sin\theta} \frac{\partial H}{\partial \lambda} \right|, \tag{12}$$

where h is the grid interval.

The results of computations of $r^{(\lambda)}$ and $r^{(\theta)}$ are represented in Fig. 3. It can be seen that the sectors where the use of schemes of an increased order of approximation can give a substantial refinement of the solution occupy a relatively small part of the region. As a rule, these are regions with a small bottom relief slope. In general, it can be concluded that the resolution of a 1° grid is nevertheless inadequately high for it to be possible to obtain a full manifestation of the advantage of precise schemes.

Nevertheless, in the computation of currents even relatively small quantitative refinements of level were extremely important. The discrepancies in the fields of currents increase appreciably with an increase in depth and at 3,000 m, for example, in some regions even have a qualitative character. The dependence of the results of computations of currents on depth is illustrated in Fig. 2b,c,d, where it is possible to see the mean zonal profiles of the velocity components, computed from two level fields at the horizons 50, 1,500 and 3,000 m. The velocities were computed from the quasi-geostrophic expressions cited in [9]. The values of the velocity components were determined at the points of intersection of a "chessboard" grid, that is, at the centers of elementary grid units of the initial grid. This procedure increases the accuracy of the difference representation of the level and density derivatives, that is, in the last analysis, the accuracy in computing velocity. This is particularly important for narrow flows.

As a quantitative illustration of the level field, Fig. 4 is a map of surface gradient currents. It shows even detailed peculiarities of circulation represented on the level map. To a considerable degree this is attributable to the use of a chessboard grid. However, with the usual approximation of the derivatives by central differences some of the information is lost in the computation of velocities. For example, the flow of Labrador waters toward the shores of America is very poorly expressed in this case, although it is reliably represented on the level map. It is interesting to note that the level map itself does not give a full idea concerning the intensity of the currents. Thus, at the equator the level gradients are relatively small, but the velocity values, as a result of the smallness of the Coriolis parameter, are extremely considerable. In the Inter-Trades Countercurrent and the Guinea Current, like in the Gulf Stream, they are more than 80-90 cm/sec.

BIBLIOGRAPHY

1. Brekhovskikh, A. L., Demin, Yu. L., "Integral Circulation of Waters in the Atlantic Ocean," OKEANOLOGIYA (Oceanology), Vol XVIII, No 6, 1978.

2. Bulatov, R. P., Demin, Yu. L., Polyakov, S. G., "Principal Characteristics of the Three-Dimensional Field of Currents in the Atlantic Ocean (Climatic Circulation)," OKEANOLOGICHESKIYE ISSLEDOVANIYA (Oceanological Research), No 31, 1979.

3. Kozlov, V. F., "On the Method for Computing Ocean Currents from the Stipulated Density Field," METEOROLOGIYA I GIDROLOGIYA (Meteorology and Hydrology), No 1, 1973.

4. Kozlov, V. F., "Use of Monotonic Difference Schemes in Diagnostic Computations of Sea Currents," IZV. AN SSSR, FIZIKA ATMOSFERY I OKEANA (News of the USSR Academy of Sciences, Physics of the Atmosphere and Ocean), Vol 13, No 7, 1977.

5. Kochergin, V. P., Sherbakov, A. V., "Investigation of Difference Schemes for an Elliptical Equation With a Small Parameter With a Higher Derivative," CHISLENNYYE MODELI OKEANICHESKIKH TSIRKULYATSIY (Numerical Models of Ocean Circulations), Novosibirsk, VTs SO AN SSSR, 1972.

6. Kochergin, V. P., TEORIYA I METODY RASCHETA OKEANICHESKIKH TECHENIY (Theory and Methods for Computing Ocean Currents), Moscow, Nauka, 1978.

7. Perederey, A. I., Sarkisyan, A. S., "Precise Solutions of Some Transformed Equations of Dynamics of Sea Currents," IZV. AN SSSR, FIZIKA ATMOSFERY I OKEANA, Vol 8, No 10, 1972.

8. Sarkisyan, A. S., Keondzhiyan, V. P., "Computation of the Level Surface and the Full Flows Function for the North Atlantic," IZV. AN SSSR, FIZIKA ATMOSFERY I OKEANA, Vol 8, No 11, 1972.

9. Sarkisyan, A. S., CHISLENNYY ANALIZ I PROGNOZ MORSKIKH TECHENIY (Numerical Analysis and Prediction of Sea Currents), Leningrad, Gidrometeoizdat, 1977.

10. Demin, Yu. L., Sarkisyan, A. S., "Calculation of Equatorial Currents," J. MARINE RES., Vol 35, No 2, 1977.

11. Hellerman, S., "An Updated Estimate of the Wind Stress on the World Ocean," MON. WEATHER. REV., Vol 95, No 9, 1967.

12. Holland, W. R., Hirschman, A. D., "A Numerical Calculation of the Circulation in the North Atlantic Ocean," J. PHYS. OCEANOGR., Vol 2, No 4, 1972.

13. O'Brien, J. J., "Models of Coastal Upwelling," NUMERICAL MODELS OF OCEAN CIRCULATION, NAS, Washington, D.C., 1975.

UDC 551.326.7

NUMERICAL MODELING OF ICE DRIFT IN THE COASTAL ZONE OF THE SEA

Moscow METEOROLOGIYA I GIDROLOGIYA in Russian No 9, Sep 80 pp 81-85

[Article by B. M. Taran, Moscow State University, submitted for publication 18 Dec 79]

[Text]

Abstract: The author proposes a hydrodynamic model of drift of the ice cover in the coastal zone of the sea. The model makes it possible to formulate correctly the boundary conditions for the drift velocity of ice in a closed region, compute the detailed characteristics of drift and even detect narrow coastal polynias. A numerical solution of the problem is obtained using the method of splitting with respect to physical factors and the "coarse particles" method. The article gives an example of computations of the dynamics of the ice cover when an offshore wind is prevailing. The results of the computations are compared with the actual ice conditions under similar hydrometeorological conditions. The width of the computed polynia is approximately the same as is actually observed.

There are a great number of hydrodynamic models of ice drift which make it possible to compute the dynamics of the ice cover. In these models the authors for the most part deal with problems relating to ice drift in basins commensurable with the extent of an arctic sea or the entire Arctic Ocean. In this article an attempt is made to formulate a model of ice drift in a closed coastal region occupying part of the arctic sea. We will examine the coastal zone of an arctic sea, knowing that in a definite hydrometeorological situation polynias exist here beyond the shore ice. We will assume that the wind regime is the principal cause of the formation and regime of a polynia, as described by V. N. Kupetskiy [2].

We will represent the coastal region in the form of a rectangular region (Fig. 1) bounded on the west, east and south by the solid part of the boundary contour and on the north by the liquid part of the boundary. Such an approximation occurs, for example, along the coast of the Laptev Sea where the shore ice along the eastern

shores of the Taymyr Peninsula, along the sea shores and the western edge of the shore ice of the Novosibirskiye Islands form the solid part of the boundary and the northern part of the boundary of this region -- the fluid part -- is situated at a distance of 200 km from the southern part of the solid boundary (Fig. 2).

We will assume that the area of averaging ω is far greater than the dimensions of the floes and the spatial scale of the problem is considerably greater than the linear dimensions of the area ω. We will examine the movement of an ice cover consisting of individual floes within the framework of a two-dimensional continuous model. The laws of conservation of momentum and mass of the ice cover are written in the form

$$\frac{d\vec{u}}{dt} = \vec{F} - \frac{1}{\rho} \operatorname{grad} p + A \Delta \vec{u}, \tag{1}$$

$$\frac{\partial s}{\partial t} + \operatorname{div} (s\vec{u}) = 0, \tag{2}$$

where $\rho = \rho_{ice} hs$ is the surface density of the ice [1], g/cm^2; ρ_{ice} is the density of the ice, g/m^3; h is ice thickness (h = const), cm; s(t, $\vec{x}$) is the ice continuity (packing) function [5]; $\vec{u}$(t, $\vec{x}$) is ice drift velocity, cm/sec; $\vec{F}$ is the density of external mass forces, cm/sec^2; p is the analogue of hydrostatic pressure [6], g/sec^2; A is the lateral exchange coefficient [3], cm^2/sec;

$$\Delta = \frac{\partial^2}{\partial x^2} + \frac{\partial^2}{\partial y^2}$$

is the two-dimensional Laplacian symbol.

Adhering to [6], we will represent the dependence of pressure on ice continuity in the form

$$p = p_0 \left(\frac{s}{s_0}\right)^{\chi} \Theta \left(\frac{ds}{dt}\right), \tag{3}$$

$$\Theta \left(\frac{ds}{dt}\right) = \begin{cases} \text{when} & \frac{ds}{dt} > 0 \\ \text{when} & \frac{ds}{dt} \leq 0; \end{cases}$$

$$p_0 = 10^5\text{-}10^7 \text{ g/sec}^2; \ \chi = 4;$$

s_0 is the value of the continuity function in the case of dense packing of the floes.

The system of equations (1)-(3) is closed. We will formulate the boundary conditions. On the solid part of the boundary contour for the velocity we stipulate the condition

$$\vec{u}|_L = 0, \tag{4}$$

and the continuity function here will be assumed equal to zero:

$$s|_L = 0, \tag{5}$$

where L is the solid part of the boundary contour.

On the liquid part of the boundary we stipulate the condition

$$\frac{\partial v}{\partial n} = 0, \tag{6}$$

where n is the normal to the liquid part of the boundary.

At the initial moment in time the Ω region occupied by the ice is known, velocity is absent and the continuity function is stipulated:

$$\Omega(0, \vec{x}) = \Omega_0(\vec{x}), \quad \vec{u}(0, \vec{x}) = 0, \quad s(0, \vec{x}) = s_0(\vec{x}), \quad \vec{x} \in \Omega_0(\vec{x}).$$

It is necessary to find the region $\Omega(t, \vec{x})$ and the function $\vec{u}(t, \vec{x})$, $s(t, \vec{x})$, $p(t, \vec{x})$ satisfying the system of equations (1)-(3) with the boundary conditions (4)-(6) with $t \geqslant 0$.

With the wind drift of ice relative to motionless water the external mass forces represent the sum of the frictional forces between the upper surface of the ice and the air flow, the lower surface of the ice and the water and Coriolis force. The shearing stresses at the upper (τ^a) and lower (τ^w) surfaces of the ice cover can be computed using the formulas [1]:

$$\tau^a = K_1 \rho_a w |w|, \quad \tau^w = K_2 \rho_w u |u|, \tag{7}$$

where K_1, K_2 are the coefficients of resistance of the upper surface of the ice to the air flow and the lower surface of the ice to the water respectively; ρ_a, ρ_w are the densities of the air and water, g/cm^3; w, u are the velocities of the wind and ice drift, cm/sec.

For numerical solution of the problem (1)-(6) we will use a variant of the splitting method with respect to the physical factors [4, 7].

Assuming the movement to be steady, equation (1) is written in the form

$$f\vec{u} = \frac{1}{\rho} \operatorname{grad} p - \frac{s}{\rho}(\tau^a - \tau^w) - A\Delta\vec{u}, \tag{8}$$

where $f = f_0 + \beta y$ is the Coriolis parameter, 1/sec.

Applying the splitting method to equation (2), we obtain two equations:

$$\frac{\partial \tilde{s}}{\partial t} = -\tilde{s} \operatorname{div} \vec{u}, \tag{9}$$

$$\frac{ds}{dt} = 0. \tag{10}$$

Equation (9) describes the compressibility of the ice cover. With its solution we obtain intermediate values of the continuity function $\tilde{s}$, which are used in the transfer equation (10). After the solution of (10) we have the final values of the continuity function s.

We will break the computation region down into rectangular fixed areas in the process of solution of the grid element. Within the grid units there are moving particles modeling elements of the continuous medium. The integration of system

(1)-(3) is accomplished in time intervals in two stages.

In the first stage we compute the adaptation of the properties of the medium under the influence of frictional forces, the Coriolis force and the pressure gradient. At the initial moment in time at the points of intersection of the fixed grid there are "coarse particles" having the properties of the medium for a particular point of intersection. On the basis of the known initial values of the continuity function $s_0(\vec{x})$, by the solution of equation (3) we determine the pressure. Solving equation (8) with the boundary conditions (4), (6) we determine the velocities at the grid points of intersection. By solution of equation (9) we find the intermediate values of the continuity function at the grid points of intersection.

In the second stage we compute the transfer of the properties of the medium by the particles. In our case we will determine only the evolution of the continuity function by solution of equation (10) with the boundary condition (5). We introduce the new variables X and Y -- the coordinates of the particles relative to the fixed grid. In Lagrangian coordinates the transfer equation (10) is written as follows:

$$\frac{dX}{dt} = u, \quad \frac{dY}{dt} = v, \tag{11}$$

where u, v are the velocities found by solution of equation (8).

Assuming that during one time interval δt the particles transport the values of the continuity function along the trajectories of movement without changes, we find from (11) the distances (ΔX, ΔY) by which the particles move during δt. Here we will assume that there is satisfaction of the Courant test $|\vec{u}|\delta t/h < 1$, where u is the velocity of the particle, h is the interval of the difference grid. If we now interpolate the values of the continuity function from the points to which the particles were moved to the nearest points of intersection of the fixed grid we obtain the final values of the continuity function. These will be the initial values for the next integration interval. In each integration interval the particles begin their movement from the grid points of intersection. In each time interval we deal with different particles arriving in a particular grid unit with their values of the continuity function. The continuity function is assumed to be continuous in the entire integration region. The isoline $s \simeq 0$ corresponds to the ice-water edge.

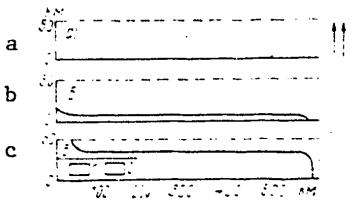

Fig. 1. Formation and development of polynia beyond the shore ice five and ten days after onset of offshore wind. a) t = 0, b) t = 5 days; c = 10 days. The wind velocity is 5 m/sec (Δx = 30 km, Δy = 10 km, Δt = 12 hours, $s_0(x)$ = 0.4, A = 10^8 cm^2/sec, p_0 = 10^5 g/sec^2); 1) drifting ice, 2) clear water. The arrows indicate wind direction.

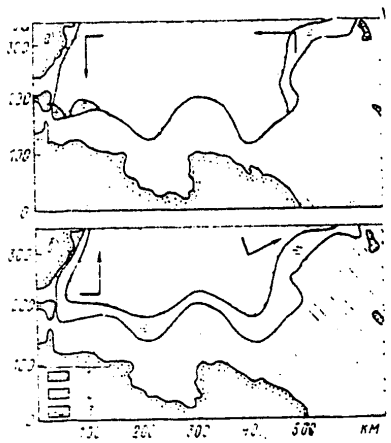

Fig. 2. Formation of polynia beyond shore ice in spring of 1959 in southern part of Laptev Sea. a) ice conditions at end of May, b) ice conditions at beginning of June; 1) shore ice, 2) drifting ice, 3) clear water. The arrows indicate the direction and velocity (5 m/sec) of the prevailing wind.

Figure 1 shows an example of computation of the dynamics of the ice cover in the coastal region of the sea, completely filled with ice at the initial moment, under the influence of a southerly offshore wind. The polynia forming in this case after being under the influence of the wind for 10 days attains a width of 30 km. In the computations we used a model region with a latitudinal extent of 600 km and a meridional extent of 200 km. Figure 1 shows the southern part of this region.

Figure 2 shows ice conditions in the southern part of the Laptev Sea under hydrometeorological conditions similar to the model conditions. Approximately after the same length of exposure to a southerly offshore wind the width of the polynia beyond the shore ice attains 14-40 miles (25-70 km).

A comparison of the computed and real data indicates some nonagreement which can be attributed to different initial conditions. In general, however, the model ice conditions reliably reflect the essence of the process of movement of the ice cover under the influence of the offshore wind -- the outward movement of the drifting ice from the shore ice and the formation of a polynia beyond the shore ice of approximately the same width as in nature.

Numerical experiments make it possible to draw the conclusion that the proposed model can describe the dynamics of the ice cover, including in a closed region.

The author expresses appreciation to Ye. V. Semenov for great assistance in the work.

BIBLIOGRAPHY

1. Doronin, Yu. P., Kheysin, D. Ye., MORSKOY LED (Sea Ice), Leningrad, Gidrometeoizdat, 1975.

2. Kupetskiy, V. N., "Stationary Polynias in Freezing Seas," VESTNIK LGU, SERIYA GEOL. I GEOGR. (Herald of Leningrad State University, Series on Geology and Geography), Vol 2, No 12, 1958.

3. Laykhtman, D. L., "Wind Drift of Ice Fields," TRUDY LGMI (Transactions of the Leningrad Hydrometeorological Institute), No 7, 1958.

4. Leys, S. Ye., "Numerical Modeling of the Earth's Atmosphere," CHISLENNYYE METODY RESHENIYA ZADACH DINAMIKI ATMOSFERY I OKEANA (Numerical Methods for Solving Problems in Atmospheric and Oceanic Dynamics), Leningrad, Gidrometeoizdat, 1968.

5. Nikiforov, Ye. G., "Change in the Continuity of the Ice Cover in Relation to its Dynamics," PROBLEMY ARKTIKI (Problems of the Arctic), No 2, 1957.

6. Ovsiyenko, S. N., "Numerical Modeling of Ice Drift," IZV. AN SSSR, FIZIKA ATMOSFERY I OKEANA (News of the USSR Academy of Sciences, Physics of the Atmosphere and Ocean), Vol XII, No 11, 1976.

7. Seidov, D. G., "Numerical Eulerian - Lagrangian Model of Currents in a Nonhomogeneous Ocean," IZV. AN SSSR, FIZIKA ATMOSFERY I OKEANA, Vol XII, No 10, 1976.

UDC 556.16.044"321"

METHOD FOR COMPUTING THE LAYER OF SPRING RUNOFF OF SMALL WATERCOURSES

Moscow METEOROLOGIYA I GIDROLOGIYA in Russian No 9, Sep 80 pp 86-91

[Article by Candidate of Technical Sciences V. Ye. Vodogretskiy, State Hydrological Institute, submitted for publication 21 Mar 80]

[Text]

Abstract: Results were obtained on the basis of an analysis of the dependence of slope runoff on soil-botanical factors. A method was developed for the differentiated allowance for slope runoff from different elements of the underlying surface with its subsequent integration over the area of the drainage basin. A formula was derived for refining computations of the layer of spring runoff from slopes and in small watercourses in comparison with the existing recommendations.

In the practice of planning of agricultural water supply an important place is occupied by the use of local slope runoff and the runoff of small watercourses by its accumulation in different artificial water bodies: reservoirs, ponds, pools and tanks.

In regions of inadequate moistening and with limited possibilities for the use of ground water the construction of the mentioned water bodies assumes particular importance. They are used not only for the watering of cattle, fish cultivation and irrigation of adjacent lands, but also for industrial and domestic water supply of populated places.

At the present time in computations of the volume of spring high water in unstudied rivers the recommendations call for the use of a map of the layer of spring runoff constructed on the basis of observational data on runoff primarily in medium and large rivers.

Using such a map the runoff layer is determined independently of the area of the drainage basin with the exception of the arid and semidesert regions of Western Siberia and Kazakhstan. The accuracies in computing the layer of spring runoff in the small watercourses is 24% in the forest zone, 32% in the wooded steppe zone, 44% in the steppe zone of the European USSR and 50% in the steppe zone of Northern Kazakhstan.

For a more precise (reliable) evaluation of local (slope and channel) runoff in small watercourses an attempt was made at development of a method for differentiated allowance for slope runoff from different elements of the underlying surface with its subsequent integration over the area of the drainage basin.

The method for computing the spring runoff of small watercourses was developed on the basis of an analysis of data on slope runoff in runoff areas and in small channels at water balance stations and at hydrometeorological observatories situated in different natural zones of the USSR and belonging to the State Committee on Hydrometeorology and other departments.

As a basis we used a dependence in the form

$$\alpha = \frac{y}{S+x} = f(U_{0-100},\ \Sigma - t,\ \Pi,\ M,\ I), \tag{1}$$

where α is the coefficient of winter-spring slope runoff; y is slope runoff; S + x are the maximum snow reserves and liquid precipitation during the period of slope runoff; U_{0-100} are the moisture reserves in the meter snow layer during the period preceding snow thawing and runoff; $\sum$ - t is the sum of negative air temperatures from the date of stable transition of air temperatures through 0°C to 1 January or to mid-February for the steppe zone of the European USSR, that is, during the period of maximum cementation of the ground and soil prior to the onset of runoff; Π is the nature of the underlying surface (З is idle land, steppe, virgin lands, π is cultivated land; л is forest); M is the mechanical composition of the soil and ground with their separation into sandy loam and light clayey loam soils, clayey loam and heavy clayey loam soils; I is the slope in promille.

A dependence in the form of graphs was constructed for each natural zone (forest, wooded steppe and steppe) and for years with different water volumes (years with abundant, intermediate and little water). The years with abundant water include years with a runoff having a probability P< 25%; years with intermediate water volume -- years with a runoff having a probability 25% < P < 75%; years with a low water volume -- years with a runoff having a probability P> 75%.

As an example, a dependence of the mentioned type for virgin land and cultivated slopes was given in [2].

The dependence is a multiple nonlinear correlation of three variable parameters

$$\alpha = f(U_t,\ I), \tag{2}$$

where U_t is the index characterizing the degree of moistening in the meter layer and the freezability of the soil and ground during the period preceding the runoff; the remaining notations are as before.

The U_t index is the index of permeability of the soil and ground. The greater the index, the higher is the runoff coefficient and vice versa.

The greatest values of the index correspond to years with abundant water with active slope runoff and, vice versa, minimum values of the index correspond to years with little water, with great losses of runoff with soaking into the soil and ground. A more detailed explanation of structure of the index was given in [2].

Here it need only be added that for constructing the empirical dependences the structure of the index in such a variant can be applicable. One and the same value of the index with different combinations of its components (U) and ($\sum$- t) corresponds to a definite value of the runoff coefficient.

The total correlation coefficient of dependence (2) is 0.80-0.90 with a relative mean square error 12-17%.

On the basis of the mentioned interpolation dependences it was possible to determine the coefficient of slope runoff in land-use areas in ranges of slopes not covered by data from actual measurements.

Table 1 gives the coefficients of spring runoff from different land-use areas (virgin land or idle land, cultivated land, forest) on slopes with different degrees of slope and in years with different abundance of water. Within the limits of each natural zone data are cited for the characteristics of soil and ground and different degrees of slope.

The cited data are recommended as computational data. When using the tables it must be remembered that the recommendations apply to slopes which are plowed in autumn by the usual method, that is, with a depth not greater than 22 cm. Accordingly, for slopes with plowing greater than 22 cm it is necessary that the value of the runoff coefficient α_{π} taken from the tables be divided by a factor of 1.5, whereas for slopes with deep plowing (25-37 cm) and where antierosion measures have been taken (such as the forming of ridges and dams, contour and combined plowing, etc.), by a factor of 1.7. This is convincingly demonstrated by the results of experimental investigations under productive conditions, generalized in a study by M. I. L'vovich [6], N. I. Koronkevich [5] and supplemented by V. N. Kaulin [4].

Computations of the magnitude of water inflow into an artificial water body (pond, pond-tank, tank) due to slope runoff are made in the following sequence.

1. We determine the area of land-use areas in the drainage basin, taking into account the variety of soil and ground (sandy loam, clayey loam) in percentage of the total area of the water-collecting part of the water body.

2. We compute the mean weighted degree of slope in the drainage basin within the limits of sectors with sandy loam (f_{sl}) or clayey loam (f_{cl}) soil and ground in each land-use area (idle land, cultivated land, forest). The slope is determined from large-scale maps in accordance with the recommendations existing for these purposes.

3. We compute the mean weighted coefficient of slope runoff (inflow)

$$\bar{\alpha} = [(\alpha_з f_{сп} + \alpha_з f_{сг}) + (\alpha_л f_{сп} + \alpha_л f_{сг})] K_{лсп} + (\alpha_з f_{сп} + \alpha_з f_{сг}) + \alpha_г f_г, \quad (3)$$

where $\alpha_з$, $\alpha_п$, $\alpha_л$, $\alpha_г$ are the coefficients of slope runoff from idle land (virgin land), cultivated land, forest and the hydrographic network (slopes along channels); f is the area of land-use areas, taking into account the differences in soil and ground in fractions of the area of the drainage basin; $K_{лсп}$ is the coefficient of decrease in slope runoff under the influence of shelterbelts in the drainage basin of an artificial water body.

$$K_{лсп} = 1 - 0.01(1.0\text{–}1.4) f_{лсп}, \quad (4)$$

where $f_{лсп}$ is the area in shelterbelts in percent of the area of the drainage basin. With a cross arrangement of the shelterbelts in the drainage basin a value 1.0 is used in the computations and when the shelterbelts are laid out across the slope -- 1.4. The coefficients of slope runoff from different land-use areas are included in Table 1 on the basis of data on the mean weighted slopes in the range from f_{s1} and f_{c1}; $\alpha_г$ in all cases is assumed to be equal to 0.7-0.8 [5, 6].

The mean weighted coefficients of slope runoff are determined from Table 1.

With the availability of recommendations for computing the slope runoff from swamps and swampy lands the computation of mean weighted $\bar{\alpha}$ can also be carried out for swampy drainage basins.

4. We determine the mean weighted value of the maximum water supplies in snow and precipitation during a period of slope runoff (S + x) in the drainage basins of the water body:

$$(\bar{S} + \bar{x}) = (\bar{S} + \bar{x})_з f_з + (\bar{S} + \bar{x})_п f_п + (\bar{S} + \bar{x})_л f_л + (\bar{S} + \bar{x})_г f_г, \quad (5)$$

where $f_з$, $f_п$, $f_л$, $f_г$ are the areas of the land-use areas in the drainage basin in virgin land, cultivated land, forest and the hydrographic network. In the absence of large-scale plans or maps the area $f_г$ can be assumed to be approximately 30% of the area of the drainage basin not in agricultural use [6].

The maximum water supplies S in the snow in the sectors (land-use areas) are determined from the map, taking into account the factors for conversion from snow reserves in the predominant landscape (land-use area) to other landscapes.

The quantity of liquid precipitation during the period of snow melting and slope runoff (X) is small. In the forest zone it can be neglected, in the wooded steppe and steppe zones it can be 20 and 15% respectively, and in the southwestern part of the steppe zone of the European USSR — 30-40% of the total mean long-term S value respectively.

Computations of the total slope runoff (water inflow into an artificial water body) with a stipulated probability are made using the formula

$$V_o = 10^3 \bar{\alpha} (\bar{S} + \bar{x}) \lambda_p F, \quad (6)$$

Table 1

Coefficients of Mean Long-Term Spring Slope Runoff from Idle Lands and Virgin Lands ($\alpha_з$), Autumn-Plowed Fields ($\alpha_п$), Forest ($\alpha_л$)

Characteristic	Slope, o/oo										
	5	10	20	30	40	50	60	80	100	150	200
Forest zone (sandy loam soil)											
$\alpha_з$	0,07	0,13	0,18	0,22	0,26	0,30	0,37	0,43	0,55		
$\alpha_п$	0,05	0,11	0,15	0,19	0,23	0,27	0,33	0,40	0,52		
$\alpha_л$	0,01	0,02	0,04	0,06	0,08	0,11	0,16	0,21	0,35		
Forest zone (clayey loam soil)											
$\alpha_з$	0,11	0,20	0,28	0,34	0,40	0,44	0,51	0,56	0,65	0,70	
$\alpha_п$	0,09	0,13	0,26	0,32	0,38	0,41	0,48	0,54	0,62	0,69	
$\alpha_л$	0,00	0,02	0,06	0,10	0,12	0,18	0,27	0,35	0,51	0,58	
Wooded steppe zone (clayey loam soil)											
$\alpha_з$	0,13	0,24	0,33	0,41	0,46	0,52	0,61	0,67	0,78	0,83	
$\alpha_п$	0,10	0,19	0,27	0,34	0,38	0,43	0,51	0,57	0,69	0,76	
$\alpha_л$	0,00	0,01	0,02	0,03	0,05	0,07	0,11	0,15	0,26	0,37	
Steppe zone European USSR (clayey loam soil)											
$\alpha_з$	0,13	0,24	0,33	0,41	0,46	0,52	0,61	0,67	0,78	0,8	
$\alpha_п$	0,07	0,15	0,20	0,26	0,32	0,37	0,45	0,52	0,61	0,6	
Steppe zone — Northern Kazakhstan (sandy and light clayey loams)											
$\alpha_з$	0,07	0,13	0,21	0,25	0,30	0,32	0,34				
$\alpha_п$	0,04	0,07	0,15	0,17	0,22	0,24	0,26				
Steppe zone — Northern Kazakhstan (clayey and medium clayey loams)											
$\alpha_з$	0,10	0,16	0,23	0,27	0,30	0,32	0,34				
$\alpha_п$	0,03	0,08	0,12	0,15	0,17	0,19	0,20				

[з = idle and virgin lands; п = autumn-plowed fields; л = forest]

Table 2

Factors (λ_p) for Conversion from Mean Long-Term Values of Layer of Spring Runoff to Layers of Runoff of Different Probability

Natural zone	Probability, %					
	1	5	10	20	75	95
Forest	3.5	2.5	2.0	1.5	0.5	0.2
Wooded steppe	4.0	3.0	2.0	1.5	0.3	0.1
Steppe European USSR and Northern Kazakhstan	6.5	3.5	2.5	1.8	0.1	0.0

where λ_p is the factor for conversion from the mean long-term values of the layer of spring runoff to layers of different probability. The remaining notations are as before. The λ_p factors were computed on the basis of the spring runoff layer probability curves constructed on the basis of data for runoff areas and small watercourses within the regions of water balance stations and generalized for natural zones (Table 2).

Table 3

Factors for Conversion from Slope Runoff to Total Channel Runoff in Drainage Basins with F< 200 km^2

Natural zone	Mean degree of slope in drainage basin	Probability of annual excess P, %			
		1	5	50	75
Forest	> 80	1.0	1.0	1.9	
	< 80	1.6	1.8	3.0	
Wooded steppe	> 80	1.0	1.0	1.2	
	< 80	1.3	1.4	2.7	
Steppe zone of European USSR and Northern Kazakhstan		1.3	1.3	1.9	

Notes. 1. In the steppe zone the dependence of the values of the coefficients on the mean degrees of slope in the drainage basin were not determined. The cited data are characteristic for degrees of slope less than 80°/oo. 2. In drainage basins with slopes greater than 80°/oo when there is ground water runoff in the channel the value of the factor is obtained by interpolation between the values for slopes more or less than 80°/oo.

The total volume of the runoff in small watercourses with an area of the drainage basins less than 200 km^2 is computed using formula (6) with the introduction of an additional factor (the coefficient K) into the computations, that is

$$V_p = 10^3 \bar{z} (\bar{S} + \bar{x}) \lambda_p KF. \quad (7)$$

The K coefficient represents the relationship between the actual (complete) runoff of the watercourse and slope runoff from the drainage basin, computed using formulas (3), (5) and (6). The numerical values of the coefficient were obtained for all watercourses within the regions of the water balance stations and the hydrometeorological observatories situated in the forest, wooded steppe and steppe zones of the European USSR and the steppe zone of Northern Kazakhstan.

The K coefficient is dependent on the mean slope in the drainage basins and the probability of the annual exceeding of the volume of slope runoff. The generalized values of the factors for conversion from the volume (layer) of slope runoff to the total runoff from the drainage basin are given in Table 3.

In years of a rarer frequency of recurrence the relationship of the total channel and slope runoffs in small watercourses approaches unity. This was expressed most clearly in watercourses with slopes > 80°/oo. Such a character of the relationship

indicates that during years with a rare frequency of recurrence the runoff volume during the spring in the channels of small rivers is formed almost completely by slope runoff.

In years which are average with respect to water volume and during years with little water the slope runoff in the drainage basins totals 25-50% of the total channel runoff. The remaining part of the spring runoff is formed from ground water and also the accumulation of snow and its thawing in the channels of tributaries.

The results of comparison of computations of the layer of spring runoff in some watercourses of water balance stations on the basis of this method and the recommendations in the Handbook [7] indicate a higher accuracy of computations of the layer of spring runoff on unstudied rivers with $F<200$ km^2 by the proposed method. The accuracy of the computations is increased on the average by a factor of almost 2 in comparison with computations in accordance with the recommendations in the Handbook [7], that is, from the map of the layer of runoff, but for individual watercourses by a factor of 5-6 or more. In addition, in the mentioned Handbook there are no recommendations at all on computing the water resources of local slope runoff, which makes difficult the solution of practical problems involved in the planning of agricultural water supply.

BIBLIOGRAPHY

1. Alekseyev, G. A., OB"YEKTIVNYYE METODY VYRAVNIVANIYA I NORMIROVANIYA KORRELYATSIONNYKH SVYAZEY (Objective Method for the Balancing and Normalization of Correlations), Leningrad, Gidrometeoizdat, 1971.

2. Vodogretskiy, V. Ye., VLIYANIYE AGROLESOMELIORATSIY NA GODOVOY STOK (METODIKA ISSLEDOVANIY, OTSENKA I UCHET) (Influence of Agricultural Melioration Work on Annual Runoff (Research, Evaluation and Allowance Methods)), Leningrad, Gidrometeoizdat, 1979.

3. Voskresenskiy, K. P., NORMA, IZMENCHIVOST' GODOVOGO STOKA REK SSSR (Norms and Variability of Annual Runoff of Rivers in the USSR), Leningrad, Gidrometeoizdat, 1962.

4. Kaulin, V. N., "Influence of Agricultural Melioration Measures on the Runoff of Melt Water from Small Drainage Basins," MATERIALY PO VOPROSAM EKSPERIMENTAL'NOGO IZUCHENIYA STOKA I VODNOGO BALANSA RECHNYKH VODOSBOROV (Materials on Problems in the Experimental Study of Runoff and the Water Balance of River Drainage Basins), Valday, 1965.

5. Koronkevich, N. I., PREOBRAZOVANIYE VODNOGO BALANSA (Transformation of the Water Balance), Moscow, Nauka, 1973.

6. L'vovich, M. I., VODNYY BALANS SSSR I YEGO PREOBRAZOVANIYE (Water Balance of the USSR and its Transformation), Moscow, Nauka, 1969.

7. RUKOVODSTVO PO OPREDELENIYU RASCHETNYKH GIDROLOGICHESKIKH KHARAKTERISTIK (Handbook on Determining Computed Hydrological Characteristics), Leningrad, Gidrometeoizdat, 1973.

UDC 556.(115:582+18)(282.247.32)

HYDROLOGICAL CONDITIONS FOR THE 'BLOOMING' OF WATER IN THE RESERVOIRS OF THE DNEPR CASCADE

Moscow METEOROLOGIYA I GIDROLOGIYA in Russian No 9, Sep 80 pp 92-96

[Article by Candidate of Technical Sciences V. M. Shmakov, Institute of Hydrobiology Ukrainian Academy of Sciences, submitted for publication 20 Feb 80]

[Text]

Abstract: The creation of a cascade of reservoirs on the Dnepr has led to a change in the hydrological regime and has exerted an influence on formation of water quality. Under conditions of a warm climate and a highly developed national economy in this region this has led to an impairment of the ecological equilibrium, manifested in an intensification of the development of different species of algae, especially blue-green algae, which is observed in the form of water "blooming."

The problem of contending with the "blooming" of water is timely with respect to water bodies (reservoirs, lakes, seas and even individual sectors of some oceans) situated outside the polar and arctic zones. This problem is attributable to anthropogenic factors intensifying the development of different types of algae, especially blue-green algae. In our country the problem is most acute on the Dnepr. Here, in the average productive year, the quantities of organic mass during the time of "blooming" of the water, exceed 200,000 tons of dry matter [8]. During a period of intensive "blooming" (June-September, especially July-August) there is a marked deterioration of water quality and sometimes its consumption and even recreation along the shores in places where "blooming" is observed become unsafe.

According to the data of the All-Union Scientific Research Institute of Hydroengineering imeni Vedeneyev, the annual losses due to the "blooming" of water in the Dnepr reservoirs are about 12 million rubles (without taking into account the deterioration of the quality of water, which at the present time cannot be economically evaluated) [5].

One of the principal factors responsible for the "blooming" of water in the Dnepr reservoirs is a change in the hydrological conditions as a result of creation of the cascade.

The Dnepr is the principal water artery of the Ukraine, ensuring 75% of the water supply for the national economy of the republic. The great national economic importance of the Dnepr, the limitation on the water resources in the region and the need for their most complete and multisided use led to the creation of a cascade including six reservoirs. The total length of the reservoirs in the cascade is 855 km, the total volume is 43.8 km^3 and the surface area is 6,974 km^2. Reservoirs with dams have a head from 11.5 to 38.7 m; the total head is 114.4 m [2].

The creation of the cascade caused a change in the hydrological characteristics of the Dnepr [6], the most important of which are given in the table. The change in the indicated hydrological characteristics, as well as a number of other parameters, exerted a substantial influence on the hydrological regime of the Dnepr and on the dynamics of hydrobiological processes.

With creation of the cascade of reservoirs the predominating current velocities decreased from 0.6-0.8 to 0.3-0.02 m/sec. The decrease in current velocities in the reservoirs resulted in a more intensive sedimentation of suspended particles on the bottom and this exerted an effect on water transparency. In the cascade there is a gradual increase in water transparency: in each lower-lying reservoir it is 0.1-0.3 m greater than in the above-lying reservoir. In general, with the creation of the cascade the water transparency during the period when ice had not formed increased from 0.4-0.6 to 1.2-3.0 m.

The increase in water transparency caused an increase in the depth of penetration of solar radiation from 1.0-1.5 to 2.5-6.0 m, which resulted in a lowering of the boundary of the layer of photosynthesis by 1.5-4.5 m. The horizontal extent of this zone increased from 442 to 2,062 km^2 (see table). Therefore, the creation of the cascade of reservoirs caused a considerable increase in the zone of photosynthesis, which led to an increase in biological productivity, including an increase in the mass of blue-green algae.

The creation of the cascade of reservoirs caused a marked decrease in through flow and water exchange. For example, in the Kremenchugskoye Reservoir, intended for seasonal regulation, the water is replaced 3.5 times each year, whereas prior to the creation of the reservoir within its boundaries under these same conditions the water was replaced 83.9 times. The intensity of water exchange here decreased by a factor of 24. In the Kakhovskoye Reservoir this decrease was by a factor of 19.6 (see table), whereas for the Kiyevskoye Reservoir it was by a factor of 13, etc.

All other conditions being equal, hydrobiological processes develop most intensively in parts of water bodies without or with little through flow, characterized by a total absence of a current or currents with low velocities, little water exchange and weak turbulent mixing [4]. After creation of the cascade of reservoirs the Dnepr was transformed into a system of water bodies with little through flow, which caused an intensification of the development of different water organisms in them, including blue-green algae.

The decrease in water flow velocities in the reservoirs exerted an influence on the quantity and quality of bottom deposits. In the course of formation of these deposits their differentiation is observed: large particles are deposited in the

Table 1

Change in Hydrological Characteristics of Dnepr With Construction of Cascade of Reservoirs

Reservoir	Channel capacity, km^3			Surface area, km^2		
	with dam	before construction	increase	with dam	before construction	increase
Kiyevskoye	3.73	0.287	3.43	922	94.6	827
Kanevskoye	2.62	0.430	2.19	675	144	531
Kremenchugskoye	13.5	0.567	12.93	2250	188	2062
Dneprodzerzhinskoye	2.45	0.471	1.98	576	134	442
Zaporozhskoye	3.30	0.532	2.77	410	152	258
Kakhovskoye	18.2	0.943	17.26	2150	269	1881
Total						

Reservoir	Mean depth, m			Water exchange, times/year		
	with dam	before construction	increase	with dam	before construction	increase
Kiyevskoye	4.0	3.03	0.97	8.9	115.2	13.0
Kanevskoye	3.9	2.99	0.91	16.7	101.8	6.1
Kremenchugskoye	6.0	3.06	2.94	3.5	83.9	24.0
Dneprodzerzhinskoye	4.3	3.52	0.78	21.1	109.7	5.2
Zaporozhskoye	8.0	3.50	4.50	15.7	97.7	6.4
Kakhovskoye	8.5	3.50	5.01	2.9	55.1	19.6
Total	---	----	----	----	-----	----

FOR OFFICIAL USE ONLY

APPROVED FOR RELEASE: 2007/02/08: CIA-RDP82-00850R000300080007-3

zone of edging-out of the backwaters of rivers flowing into a reservoir and in the upper reservoirs of the cascade, whereas the finer particles move into the depths of the reservoir proper and into the lower-lying reservoirs. With the creation of the cascade of reservoirs there was an increase in the intensity of the deposition of the fine fractions on the bottom and the accumulation of silts. The thickness of the layer of silts in the Zaporozhskoye Reservoir is about 30 cm. The silting of the reservoirs in the cascade occurs at a rate of 0.5-0.9 cm/year. The bottom deposits are the site of wintering of blue-green algae. The silts create favorable conditions for the maintenance of vital functions of the blue-green algae during the prolonged presence of these water organisms there, in actuality without light, at a temperature of about 4°C.

Blue-green algae are characterized by a diurnal migration: during the daytime from the depths to the surface of the water, at nighttime from the surface into the depths. With the construction of the reservoirs there has been an intensification of the role of hydrological factors intensifying these migration processes.

An increase in depths and the associated decrease in the penetration of solar radiation into the bottom layers of water led, especially in deep-water sectors with little turbulent mixing, to an increase in the water temperature difference at the surface and in the depths. During anticyclonic weather in the summer months in the upper water layer there is a diurnal change in stratification: during the daytime and in the evening -- direct, at nighttime and in the early morning -- the reverse. Such a change in stratifications causes convective movements of the water particles and exerts a positive influence on migration processes.

A considerable increase in the surface areas of the reservoirs created favorable conditions for an increase in wind velocities and wave fetch, as well as an intensification of wind waves. The height of the waves increased from 0.3-0.6 to 0.7-1.9 m. The wave disturbances in the deep-water parts of the reservoir began to be propagated to a depth as great as 12 m and exerted an influence on the specifics of turbulent mixing of water. In this mixing there was an intensification of the role of water particles moving in a plane close to vertical. An intensification of the role of convective and wave phenomena in the turbulent mixing of water exerted an intensifying influence on the processes of migration of blue-green algae and on their development.

A decrease in the amplitude of the variation of water level results in a contraction of the coastal zones of drying-out (when the level drops), and this exerts a favorable effect on the development of hydrological processes [4]. An increase in channel capacity with the creation of the cascade of reservoirs by 40.6 km^3 (see table) made it possible to carry out regulation of runoff and a reduction in the amplitude of water level variation from 6-10 m to the height of the regulating prisms of the reservoirs.

With the creation of the cascade of reservoirs there was a change in the conditions for the formation of the quality of water in the reservoirs, which also intensified the processes of "blooming" of water. The Dnepr flows through a densely populated region with a well-developed industry and agriculture in which different chemicals are used extensively. The region is characterized by extremely great volumes of

industrial and domestic effluent rich in biogenous substances. With an increase in the use of chemicals in agriculture there has been an increase in their content in the runoff, especially in surface runoff. It has been computed that in the course of a year from 1 hectare of water-collection area about 0.2 kg of phosphorus, about 2 kg of nitrogen, etc. enter into the system of reservoirs. Scaled to per capita of population, this gives from 0.75 to 5 g of phosphorus and 8 g of nitrogen which are discharged daily with waste water [9].

Prior to creation of the cascade of reservoirs some of the runoff of solid and chemical substances was held by the abundant vegetation on the floodplain (grass, scrub and forests). After filling of the reservoirs most of the floodplain was inundated and the natural filter disappeared or its role was considerably decreased. There was also a decrease in the quantity of forest in the coastal zone and an increase in the area of the worked agricultural fields. For these reasons the entry of chemical substances into reservoirs, including biogenous substances, increased and this exerted a negative influence on formation of the quality of water and intensified hydrobiological processes.

With the filling of the reservoirs of the cascade about 6,000 km^2 of lands with fertile soils and vegetation were inundated. A total of 134,000 tons of organic material, 42,000 tons of nitrogen, 2,000 tons of phosphorus, etc., entered the reservoirs [8]. The inundated fertile lands and the biogenous substances entering the reservoirs from them exerted the most serious influence on the processes of development of different types of water organisms, including algae.

The creation of the cascade of reservoirs caused the formation of great areas of shallow waters which occupy the following percentages of the total areas of the reservoirs: Kiyevskoye -- 40%, Kanevskoye -- 24%, Kremenchugskoye -- 18%, Dneprodzerzhinskoye -- 31%, Zaporozhskoye -- 36%, Kakhovskoye -- 5% [3]. The shallow waters are characterized by poorer conditions for turbulent mixing and water exchange, a greater occurrence of phytocoenoses and better heating of the water masses. Investigations show that the water temperature in them is 0.5-1.5°C higher, and in some phytocoenoses -- 3-4° higher, than in the deep-water sectors of the reservoir. An increase in water temperature over great areas of shallow waters accelerated all the exchange processes and the rate of reproduction of populations [4] and exerted an influence on the quality of the water and on the course of hydrobiological processes in reservoirs.

In discussing the "blooming" of water it must be noted that this phenomenon is not observed over the entire surface area of the reservoirs of the cascade, but in individual spots [1]. These "blooming spots" are situated for the most part in the lower sectors of the reservoirs. For example, in the Kremenchugskoye Reservoir in July 1961 the biomass of blue-green algae in the sector near the dam attained 7,166 mg/m^3, in the middle sector -- 2,177 mg/m^3 and in the upper part -- 150 mg/m^3. Approximately the same picture was observed in July 1962 and 1963 [7].

Accordingly, "blooming spots" in reservoirs were associated with places of occurrence of great depths, small current velocities, increased transparency, maximum thickness of the layer of silts, and also slowed water exchange and flowthrough, that is, those places where the hydrological regime experienced the greatest changes.

The intensity of development of blue-green algae in individual years is extremely different and is governed for the most part by hydrometeorological factors. During the first years after filling of the reservoir there is an increase in the intensity of "blooming." During subsequent years the intensity of this process in general decreases somewhat. For example, in the Kakhovskoye Reservoir, filled in 1956, the total biomass of blue-green algae in August was: in 1956 -- 7,100 mg/m^3, in 1957 -- 9,429, in 1958 — 2,969, in 1963 -- 2,319 mg/m^3 [7]. An increase in the intensity of development of blue-green algae usually coincides with the years of positive water temperature anomalies, weakened wind activity and turbulent mixing of the water and increased water transparency, that is, with years of development of anticyclonic weather conditions.

Summary

The creation of the cascade of reservoirs on the Dnepr caused a change in its hydrological characteristics and related conditions of formation of the hydrological regime. There have been considerable increases in channel capacity, surface area and mean depths. In this connection there have been substantial changes in current velocity and water transparency, flowthrough, water exchange and conditions for the formation of bottom deposits, penetration of solar radiation into the water and its propagation there and formation of the thermal regime. Extensive areas of lands from which a great quantity of organic material and biogenous substances entered the reservoirs were flooded. The conditions for the formation of water quality changed with the disappearance or considerable contraction of the areas of the floodplains and also with the formation of extensive zones of shallow waters.

All these changes under conditions of a warm climate and the highly developed national economy of the region led to a disruption of the ecological equilibrium, manifested in an intensification of the development of different species of algae, and in particular, blue-green algae, as is observed in the form of "blooming" of water.

BIBLIOGRAPHY

1. Braginskiy, L. P., Bereza, V. D., et al., "'Blooming Spots,' Wind-Driven Masses, Surges of Blue-Green Algae and the Biological Processes Transpiring in Them," "TSVETENIYE" VODY (Water "Blooming"), Kiev, Naukova Dumka, 1968.

2. GIDROMETEOROLOGICHESKIY REZHIM OZER I VODOKHRANILISHCH SSSR. KASKAD DNEPROPETROVSKIKH VODOKHRANILISHCH (Hydrological Regime of Lakes and Reservoirs in the USSR. Cascade of Dnepropetrovsk Reservoirs), Leningrad, Gidrometeoizdat, 1976.

3. Zerov, K. K., Korelyakova, I. L., "Physiographic Description of the Dnepr and its Valley," GIDROBIOLOGICHESKIY REZHIM DNEPRA V USLOVIYAKH ZAREGULIROVANNOGO STOKA (Hydrobiological Regime of the Dnepr Under Conditions of Regulated Runoff), Kiev, Naukova Dumka, 1967.

4. Konstantinov, A. S., OBSHCHAYA GIDROBIOLOGIYA (General Hydrobiology), Moscow, 1979.

5. Makarov, A. I., Liguk, O. S., "Validation of the Economic Effectiveness of Measures for Regulating the 'Blooming' of Water in Dnepr Reservoirs," VOPROSY KOMPLEKSNOGO ISPOL'ZOVANIYA VODOKHRANILISHCH: TEZISY DOKLADOV VSESOYUZNOGO SOVESHCHANIYA (Problems in the Multisided Use of Reservoirs: Summaries of Reports at the All-Union Conference), Kiev, Naukova Dumka, 1971.

6. Pikush, N. V., Sukhoyvan, P. G., "On Evaluation of Fish Productivity in Dnepr Reservoirs," GIDROBIOLOGICHESKIY ZHURNAL (Hydrobiological Journal), No 4, 1978.

7. Priymachenko, A. D., Litvinova, M. A., "Distribution and Dynamics of Blue-Green Algae in Dnepr Reservoirs," "TSVETENIYE" VODY, Kiev, Naukova Dumka, 1968.

8. Sirenko, L. A.,"Extraction of Seston in a Period of Water 'Blooming'," VESTNIK AN UkrSSR (Herald of the Ukrainian Academy of Sciences), No 5, 1976.

9. Topachevskiy, A. V., Sirenko, L. A., Priymachenko-Shevchenko, A. D., "'Blooming' of Water in Reservoirs and Ways to Regulate It," VOPROSY KOMPLEKSNOGO ISPOL'ZOVANIYA VODOKHRANILISHCH: TEZISY DOKLADOV VSESOYUZNOGO SOVESHCHANIYA, Kiev, Naukova Dumka, 1971.

UDC 551.326.83

EXPERIENCE IN USING A KINETIC EQUATION FOR DESCRIBING THE PROCESS OF FORMATION OF FRAZIL ICE AND SLUSH

Moscow METEOROLOGIYA I GIDROLOGIYA in Russian No 9, Sep 80 pp 97-104

[Article by N. M. Abramenkov, Central Asiatic Regional Scientific Research Institute, submitted for publication 28 Jan 80]

[Text]

Abstract: The author demonstrates the possibility and some peculiarities of use of the kinetic coagulation equation for describing the formation of small accumulations of frazil ice and slush. Numerical solutions of the kinetic equation are given applicable to the conditions for ice formation in water flows.

The freezing of many rivers begins with the formation of frazil ice, which then with adequate flow turbulence is transformed into slush accumulations. The process of formation of the latter is similar in many respects to the process of coagulation in disperse systems, as was pointed out by S. Ya. Vartazarov in [1]. However, until now the study of the regime of surface slush and frazil ice has been based, as a rule, on the seeking of dependences between the values of elements of the ice regime (density of slush formation, slush discharge) and the heat exchange between the water and slush surfaces with the atmosphere. In some studies the authors have taken into account the hydraulic conditions for the formation of slush but have not numerically described the mechanism for the formation of frazil ice.

In this article we examine some problems relating to the formation of frazil ice, being an important element in the winter regime of many rivers, and on the basis of concepts relating to the coagulation of particles numerically describe this process.

The principal objective of this study was an explanation of the possibility and peculiarities of use of a kinetic equation for describing the process of formation of frazil ice.

We will examine some volume of a mixture of water and ice crystals. Assume in an element of the phase volume $d\Gamma = dxdydzdr$, where r is the size of the particles, the number of particles is characterized by the product of the density of the distribution $f(x, y, z, r, t)$ in a $d\Gamma$ element. The kinetic coagulation equation [2]

can be written in the following form:

$$\frac{\partial f}{\partial t} + \operatorname{div}(f\vec{U}_p) + \dot{r}\frac{\partial f}{\partial r} + f\frac{\partial \dot{r}}{\partial r} = I_+ - I_- + F_p. \quad (1)$$

Expression (1) is the continuity equation, where the internal sources and losses are integrals of the collisions I_+ and I_-, describing coagulation proper, and also the F_p value, representing the rate of entry of newly forming crystals into a unit of phase volume. The $\vec{U}_p$ value in expression (1) denotes the velocity of motion of particles of the size r. The last two terms on the left-hand side of equation (1) take into account the change in size of already existing ice crystals as a result of freezing and thawing.

We introduce the following assumptions:

1. We will examine a one-dimensional case, taking into account only the coordinate of depth of the flow z.
2. We will assume that the changes in the size of the crystals of frazil ice themselves do not occur, but the newly forming crystals, whose appearance is described by the term F_p, have the size r_0.

The latter assumption is entirely admissible if the results of the investigations [1, 5, 6] are taken into account. V. V. Piotrovich [6] indicates that it is impossible even to make an intercomparison of the process of growth of crystals in place (near a body) and the process of combination in the increase of ice accumulations, it being impossible to ascertain the extent to which the combination process predominates over the growth process.

With the mentioned assumptions equation (1) is simplified:

$$\frac{\partial f}{\partial t} + \frac{\partial}{\partial z}(f U_{pz}) = I_+ - I_- + F_p, \quad (2)$$

where U_{pz} is the velocity of movement of particles, I_+ is the number of particles which as a result of collisions (changes in size) enter into a given unit phase volume in a unit time, I_- is the number of particles which as a result of collisions (changes in size) emerge from a given unit phase volume in a unit time.

The collision integrals are adopted here in the form

$$I_+ = \pi\varphi \int_0^{r_1 \sqrt[3]{2}} r^2 (r^3 - r_1^3)^{-2/3} (r_1 + r_2)^2 \, Vf(r_1) f(r_2) \, dr_1, \quad (3a)$$

$$I_- = \pi\varphi f(r) \int_0^{r_{max}} (r + r_1)^2 \, Vf(r_1) \, dr_1, \quad (3b)$$

where $r_2 = (r^3 - r_1^3)^{1/3}$, r is particle radius, φ is the capture coefficient,

$$V = |U(r_1) - U(r_2)|,$$

U is the velocity of motion of particles, r_{max} is the radius of the largest particles participating in coagulation.

Since in thermal investigations of ice the kinetic coagulation equation has not been employed, here it is fitting to cite at least a brief phenomenological validation of the collision integrals (3a), (3b).

Assume that a particle of the radius r_1 moves in a flow with the velocity $\vec{U}_p(r_1)$. The number of its collisions during a unit time with particles with the radius $r_2 + \Delta r_2$, moving with the velocity $\vec{U}_p(r_2)$, is assumed equal to the number of the latter situated in the phase volume $\Delta\Gamma = S_{eff} | U_p(r_1) - U_p(r_2)| \Delta r_2$, where S_{eff} is the effective area of interaction of particles r_1 and r_2, $S_{eff} = \pi (r_1 + r_2)^2$. The number of particles r_2 in the indicated volume $\Delta\Gamma$ is equal to

$$\Delta N = \pi (r_1 + r_2)^2 f(r_2) | U_p(r_1) - U_p(r_2)| \Delta r_2.$$

From the conservation of masses of colliding particles and particles forming as a result of collision we have the obvious relationship $r_1^3 + r_2^3 = r^3$. Then

$$\Delta r_2 = \frac{r^2}{(r^3 - r_1^3)^{2/3}} \Delta r.$$

All further reasonings will be carried out for a unit interval of sizes of the forming particles $\Delta r = 1$.

$$\Delta N = \pi r^2 (r^3 - r_1^3)^{-2/3} (r_1 + r_2)^2 f(r_2) | U_p(r_1) - U_p(r_2)|.$$

The number of collisions of all particles r_1 in the range of sizes dr_1 with particles r_2 in the range of sizes Δr_2 is equal to

$$dN_1 = \pi r^2 (r^3 - r_1^3)^{-2/3} (r_1 + r_2)^2 f(r_1) f(r_2) | U_p(r_1) - U_p(r_2)| dr_1.$$

The number of collisions of particles r_1 and r_2, leading to the formation of a new particle of the size r, equals $dN/\varphi\, dN_1$, where φ is the capture coefficient, determining the percentage of collisions leading to the formation of a new particle of the size r. Then the total number of particles forming in a unit time as a result of all possible collisions is determined by the following expression:

$$I_+ = \pi \int_0^{r/\sqrt[3]{2}} \varphi r^2 (r^3 - r_1^3)^{-2/3} (r_1 + r_2)^2 f(r_1) f(r_2) \times \times | U_p(r_1) - U_p(r_2)| dr_1. \qquad (3a)$$

Thus, equation (3a) was derived. Integration in this equation is carried out for sizes from 0 to the size of a particle having a volume equal to half the volume of a particle r (the radius corresponding to it is equal to $r/\sqrt[3]{2}$) in order not to take into account the same combination of sizes of colliding particles twice. Equation (3b) is derived in a similar way.

In order to exclude from consideration the variations of the instantaneous values f and $\vec{U}_p$, caused by flow turbulence, instead of (2) we will examine the time-smoothed equation

$$\frac{\partial \overline{f}}{\partial t} + \frac{\partial}{\partial z} (\overline{f U_{pz}}) = \overline{I}_+ - \overline{I}_- + \overline{F}_p.$$

The right-hand side of expression (2) will be considered a random value, so that

$$\frac{\partial \overline{f}}{\partial t} + \frac{\partial}{\partial z} (\overline{f U_{pz}}) = I_+ - I_- + F_p. \qquad (4)$$

In accordance with the Schmidt and Keller semi-empirical theory [3]

$$\overline{f U_{pz}} = \overline{f}\,\overline{U_{pz}} - \nu_T \frac{\partial \overline{f}}{\partial z}, \qquad (5)$$

where ν_T is the turbulent viscosity coefficient.

Now understanding by f and U_{pz} their averaged values, and substituting (5) into (4), we obtain

$$\frac{\partial f}{\partial t} + \frac{\partial}{\partial z}\left(f U_{pz} - \nu_T \frac{\partial f}{\partial z}\right) = I_+ - I_- + F_p. \tag{6}$$

Since all further computations are made in a coordinate system moving with the mean flow velocity, by U_{pz} we will understand the hydraulic granularity of the considered particles. The computation of U_{pz} is based on solution of the equation of motion for a particle situated in a fluid medium. The solution of the equation is similar to the solution proposed by Yu. M. Denisov. In contrast to it, in our scheme we have taken Archimedes force into account and have neglected change in the density of the medium with depth. It can be demonstrated that for not excessively large particles (r<1-5 cm) the following expression is correct

$$U_{pz} = -\frac{B}{2C} w^{-1/3}\left(1 - \sqrt{1 - \frac{4AC}{B^2} w}\right),$$

where

$$A = 1 - \frac{\rho}{\rho_p}, \quad B = \frac{6\pi\mu k_\delta}{\rho_p},$$

$$C = \frac{0.22\,\pi k_\delta^2 \rho}{\rho_p},$$

w is the particle volume, ρ is water density, ρ_{ice} is ice density, ρ_p is the density of a particle, in our case the density of accumulations of frazil ice, μ is the coefficient of water viscosity, k_δ is a coefficient characterizing the shape of the particles, for a sphere

$$k_\delta = (3/4\pi)^{1/3} \approx 0.62.$$

The value of the coefficient of turbulent viscosity is computed using the formula [3]

$$\nu_T = \varkappa \sqrt{gHI}\, z\left(1 - \frac{z}{H}\right), \tag{7}$$

where $\varkappa = 0.4$, H is the depth of flow, I is water surface slope.

The rate of entry of newly forming ice crystals into a unit phase volume (F_p) was determined from an expression based on computations of crystallization of supercooled water carried out by V. A. Rymsha [7]

[π = surf; Γ = ground]

$$P = \frac{1}{\sqrt{\eta m}\,\mathrm{sh}\,\frac{H}{\sqrt{\eta m}}}\left[S_n \mathrm{ch}\,\frac{z}{\sqrt{\eta m}} - S_r \mathrm{ch}\,\frac{H - z}{\sqrt{\eta m}}\right], \tag{8}$$

where P is the intensity of release of the heat of crystallization in a unit volume, η is the coefficient of turbulent thermal conductivity, m is a factor for the proportionality between water temperature and P, H is the total depth of the flow, z is the depth from the bottom to the point where P is computed, S_{surf} is the intensity of heat transfer from a unit water surface, S_{gr} is the intensity

of the heat flux from the ground (assumed equal to zero).

According to the investigations of A. N. Chizhov [8], A. G. Kolesnikov [5], V. V. Piotrovich [6] and R. V. Donchenko [4], the sizes of the crystals of frazil ice are 2-3 mm, rarely exceeding 4 mm. Accordingly, in our case the following assumption was made: the sizes (radii) of the newly forming particles have a fixed limiting value r_0, which in our case was assumed equal to 2 mm. The total mass of ice crystals forming in a unit time in a unit volume is equal to

$$M = \frac{P}{\gamma} = N w_0 \rho_p,$$

where $w_0 = (r_0/k\delta)^3$ is the crystal volume, N is the number of crystals forming in a unit time in a unit volume, γ is the latent heat of fusion, ρ_p is the density of the crystals (for convenience in computations assumed to be equal to the density of slush formations).

Hence

$$N = \frac{P k_\delta^3}{\gamma \rho_p r_0^3}.$$

For computing F_p it is necessary to assume that all the newly forming crystals have a size from 0 to r_0. Accordingly,

$$\begin{cases} F_p = \dfrac{N}{r_0} = \dfrac{P k_\delta^3}{\gamma \rho_p r_0^4} & \text{when} \quad r \leqslant r_0 \\ F_p = 0 & \text{when} \quad r > r_0. \end{cases} \tag{9}$$

Substituting (7) into (6), we obtain a final differential equation for the distribution function

$$\frac{\partial f}{\partial t} + \left[U_{pz} - \varkappa \sqrt{gHl}\left(1 - \frac{2z}{H}\right) \right] \frac{\partial f}{\partial z} - \varkappa \sqrt{gHl}\, z \left(1 - \frac{z}{H}\right) \frac{\partial^2 f}{\partial z^2} = \tag{10}$$
$$= I_+ - I_- + F_p,$$

which is fundamental for all numerical computations. I_+, I_- and F_p are computed using formulas (3a), (3b) and (9).

For numerical solution of equation (10) we selected a semi-implicit predictor-corrector scheme; the explicit part of the scheme -- the corrector -- is conservative.

The velocity V in equations (3a), (3b) is the relative velocity of approach of interacting particles to one another; it is equal to the difference in the averaged velocities of the particles and the difference in their "pulsating" additions:

$$V = |(\vec{V}_1 - \vec{V}_2) + (\vec{V}_1' - \vec{V}_2')|.$$

In the first approximation we will examine only the averaged velocities of the particles, which in our case represent the rate of floating up, that is, the hydraulic granularity of the particles. It is therefore clear that in this case only that part of the gravitational coagulation [2] is considered which is caused by the difference in the hydraulic granularity of the particles.

Results of computations. In this article we describe the results of two numerical experiments for computing the coagulation of frazil ice. The radius of the largest particles participating in coagulation was assumed to be 2 cm and the interval of radii is 2 mm. The total depth of the flow was 8 m, the depth interval was 1 m, the time interval was 4 sec. The coefficient of turbulent viscosity was computed using formula (7) for a slope I = 0.0002. The entry of newly crystallizing ice particles corresponded to the heat losses from an open water surface and was about 290 J/(m^2·sec).

The first and second variants of the computations differ only with respect to the capture coefficients φ in formulas (3a), (3b), that is, the effectiveness of collisions of ice particles. For the first variant φ = 1.0, for the second φ = 0.1, that is, in the first case each collision leads to coagulation, whereas in the second -- only one of ten collisions leads to coagulation.

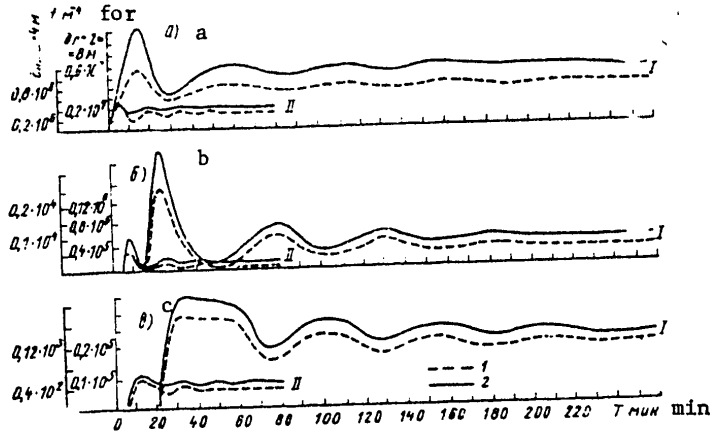

Fig. 1. Chronological variation of distribution function at different depths z with different capture coefficients φ. a) r = 2 mm, b) r = 10 mm, c) r = 20 mm; 1) z = 8 m, 2) z = 4 m; I) φ = 0.1, II) φ = 1.0.

Figure 1 shows the chronological variation of the distribution function (or the concentration of particles) at different depths for particles of different sizes. The variations of the distribution function with time evidently are attributable to the peculiarities of the adopted difference scheme. The variations are attenuating and after some time the solution enters into a stationary regime, despite the constant influx of the finest particles. The existence of such a stationary state is mathematically attributable to the limited range of sizes of the considered particles. Such a limitation is physically valid because the coagulating particles of sufficiently large size float to the surface, forming surface slush, that is, a qualitatively different process begins, which in the described scheme is not taken into account. In our numerical experiments the largest radius of the coagulating ice formations r_{max} is equal to 2 cm. Accordingly, it is assumed that particles whose size, as a result of coagulation, becomes greater

than r_{max} emerge from the limits of the considered spectrum and do not participate in further coagulation. The quantity and total mass of such particles increase with an increase in the number of large formations, and, finally, an equilibrium sets in between the mass of the crystallizing particles and the mass of particles emerging from the limits of the considered spectrum.

The time required for reaching a stationary regime and the period of variations are essentially dependent on the size of the particles and the capture coefficient and virtually do not change with the depth at which the coagulation is considered. The time required for the appearance of an appreciable quantity of large particles is 10-15 min from the time of appearance of the first crystals for $\varphi = 1$ (time of onset of the first maximum for the largest particles) and 30-50 min for $\varphi = 0.1$ (Fig. 1). According to the observations of A. N. Chizhov on the Naryn River [8], slush is collected into individual concentrations already 30-40 min after the time of appearance of the first crystals of frazil ice in the flow.

In order to compare the computed time of appearance of a sufficiently large number of coarse particles with the results of observations we carried out additional computations for hydraulic and meteorological conditions close to those observed [8]. The total depth of the flow was assumed to be 0.48 m, the slope of the water surface was I = 0.037, the depth interval was 0.06 m, and the time interval was 0.2 sec; r_{max} = 1 cm. The computations indicated that with a capture coefficient $\varphi = 0.1$ the time of appearance of a sufficiently large number of the coarsest particles is 5-6 minutes, for $\varphi = 0.01$ -- 17-20 min, and for $\varphi = 0.001$ it increases to 60-70 min.

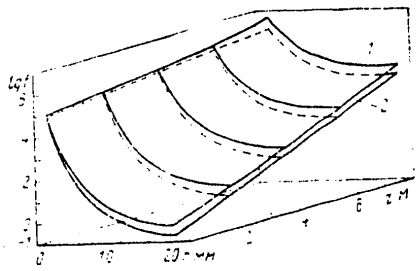

Fig. 2. Solution of coagulation equation after its entry into a stationary regime. 1) $\varphi = 0.1$; 2) $\varphi = 1.0$.

Accordingly, it can be expected that the value of the φ parameter in our scheme for the selected computation conditions falls between 0.001 and 0.01, closer to the lower boundary.

In our computations the concentration of the finest crystals of ice near the flow surface was in the range 10^6-10^8 m^{-3}, which in order of magnitude is close to the observed data [9].

A decrease in the total quantity of both large and small particles with an increase in the capture coefficient φ can be seen in Figures 1 and 2. A decrease in the concentration of small particles is easily attributed to a more intensive coagulation (with a high value of the capture coefficient). After some time this leads to a decrease in the number of large formations because small particles are the initial material for their formation. However, an increase in the concentration of the largest particles, which, it seemed, should be observed under conditions of more intensive coagulation, does not occur due to an increase in the rate of transition of the particles beyond the limits of the considered spectrum. Such, evidently, is the mechanism of the general decrease in the concentration of particles of all sizes with an increase in the capture coefficient.

Figure 2 is a graphic representation of the stationary solutions of the two numerical experiments. The logarithm of the distribution function in dependence on particle size and distance from the bottom z has been plotted along the y-axis.

The computed relationship between large (r = 2 cm), already forming, and the smallest (r = 2 mm) "primary" particles varies in a very wide range. For a capture coefficient $\varphi = 1.0$ the concentration of the largest particles is less than the concentration of small particles by a factor of 220 at the surface and by a factor of $0.48 \cdot 10^6$ at the bottom. With $\varphi = 0.1$ the relationships of large and small particles are 240 and $0.20 \cdot 10^6$. At the same time, the total weight of the large formations at the surface of the flow (for $\varphi = 1$) is 4.5 times greater, whereas at the bottom -- 480 times less than the weight of the small particles. For $\varphi = 0.1$ these relationships are equal to 4.2 and 200 respectively. The computed value of the concentration of particles of all sizes is maximum at the surface of the flow. Whereas the number of the "primary" crystals (for $\varphi = 1$) at the surface is only 17 times greater than at the bottom, for the largest formations this relationship is already $0.37 \cdot 10^5$. The similar relationships of concentrations for $\varphi = 0.1$ are 44 and $0.38 \cdot 10^5$ respectively.

It must be remembered that the results of the numerical experiments cited here are determined entirely by those conditions under which equation (10) was solved. Additional computations indicated that such a parameter as the size of the largest particles taken into account in the scheme (r_{max}) exerts a particularly strong influence on solution of the equation.

Our study indicated the possibility of use of the kinetic coagulation equation for numerical computation of small concentrations of frazil ice or slush.

It was stated above that the adopted scheme makes it possible to compute only gravitational coagulation. In order to take into account other aspects of this process, such as "direct turbulent coagulation" [1], the rate of convergence of particles, determined in the collision intervals (3), must be computed by a different method. A substantial refinement of the scheme can also be obtained by a more detailed description of the capture coefficient φ in (3). In our scheme we assumed $\varphi = \text{const}$. Evidently, the capture coefficient must be dependent both on the degree of supercooling of the water, turbulent mixing or the rate of relative approach of the particles and on their sizes. However, there have been few studies for clarification of such dependences even in regions where the kinetic coagulation equation is used quite extensively. A further improvement of the scheme will possibly require allowance for the processes of destruction of particles.

In the described scheme the "primary" crystals are represented in the form of spheres of the radius r_0, whereas under natural conditions it is possible to observe the most diverse forms of crystals of frazil ice -- from acicular to spherical. It is very common to observe particles in the form of small thin ice disks [7, 8]. The use of the characteristics of form of the particles better corresponding to natural conditions should also lead to a refinement of the numerical scheme.

BIBLIOGRAPHY

1. Vartazarov, S. Ya., "Movement of Frazil Ice in a Flow," IZVESTIYA AN ARMYANSKOY SSR, FIZIKO-MATEMATICHESKIYE, YESTESTVENNYYE I TEKHNICHESKIKH NAUK (News of the Armenian Academy of Sciences, Physical-Mathematical, Natural and Technical Sciences), Vol 2, No 2, 1949.

2. Voloshchuk, V. M., Sedunov, Yu. S., PROTSESSY KOAGULYATSII V DISPERSNYKH SISTEMAKH (Coagulation Processes in Disperse Systems), Leningrad, Gidrometeoizdat, 1975.

3. Grinval'd, D. I., TURBULENTNOST' RUSLOVYKH POTOKOV (Turbulence in Channel Flows), Leningrad, Gidrometeoizdat, 1974.

4. Donichenko, R. V., "Physical Properties of Frazil Ice," TRUDY GGI (Transactions of the State Hydrological Institute), No 55(109), 1956.

5. Kolesnikova, A. G., Belyayev, V. I., Bukina, L. A., "Rate of Formation of Frazil Ice," TRUDY 3-go VSESOYUZNOGO GIDROLOGICHESKOGO S"YEZDA (Transactions of the Third All-Union Hydrological Congress), Vol 3, 1959.

6. Piotrovich, V. V., "Cause of the Selective Formation of Frazil (Bottom) Ice," METEOROLOGIYA I GIDROLOGIYA (Meteorology and Hydrology), No 4, 1949.

7. Ryshma, V. A., "Distribution of the Heat of Crystallization of Supercooled Water With Depth in Flows and Water Bodies," TRUDY GGI, No 93, 1962.

8. Chizhov, A. N., "Formation of Frazil Ice and Formation of Slush Flow in Mountain Rivers," TRUDY GGI, No 93, 1962.

9. Osterkamp, T. E., "Frazil Ice Nucleation by Mass Exchange Processes at the Air-Water Interface," J. GLACIOLOGY, Vol 19, No 81, 1977.

UDC 551.(510.534+590.21)

OZONE AND SOLAR FLARES

Moscow METEOROLOGIYA I GIDROLOGIYA in Russian No 9, Sep 80 pp 105-107

[Article by Professor A. Kh. Khrgian and N. A. Petrenko, Moscow State University, submitted for publication 6 Apr 80]

[Text]

Abstract: The change in the total quantity of atmospheric ozone X in the earth's circumpolar and tropical regions was examined during the time of 80 solar flares during 1972-1977. In the circumpolar region there is a decrease in X on the average by X = -8 d.u., which substantially exceeds the probable error in determining X. In the tropical region the decrease in X is insignificant.

The problem of the influence of change in solar activity on the atmosphere is of great interest. Its influence on the uppermost atmosphere -- the thermosphere above 100 km -- has been well studied and has a clear physical interpretation: there is a considerable heating of the upper atmosphere from its daytime side during periods of great activity, which leads to its expansion, a relative increase in pressure (at a stipulated level in comparison with the nighttime side) and the development of characteristic air circulation.

The situation is more complex with the lower layers of the atmosphere -- the mesosphere and upper stratosphere -- in which these manifestations of activity are not so considerable and are more difficult to explain. Here it is possible to expect an appreciable influence of activity on composition and accordingly on absorption of solar energy and as a result, also on circulation. For the time being the investigation of these processes has only begun.

A special, but the clearest manifestation of activity is so-called solar flares, relatively brief (with a duration of about 1 hour), but yielding a considerable flux of electromagnetic and corpuscular radiation, including relatively fast protons. A single more detailed observation of change in composition -- a change in ozone content in the upper stratosphere -- was made during the large flare of 4 August 1972. At that time a marked decrease in total content was discovered from a satellite in the latitude zone 70-80°N in the layer above 38 km. A reduced concentration then persisted there, almost unchanged, for a period of more than 20 days.

At the present time the idea prevails [1] that such significant flares produce an "explosivelike" formation of considerable quantities of nitrogen oxides NO_x in the mesosphere. Since protons are focused in the high magnetic latitudes under the influence of the earth's magnetic field, the initial effect of the flare should be concentrated specifically there in the annular region of the auroral maximum or somewhat outside it, in the so-called region of "hydrogen auroras." Here NO, it is postulated, enters into a catalytic interaction with ozone and initiates the process of its prolonged destruction.

In order to check this hypothesis we examined the changes in the total quantity of ozone X during a more prolonged period -- during flares occurring in 1972-1977. A study was made of a total of 80 flares of the class 1B and 2B. For these we computed the X values on the day before the flare, on the day of its occurrence and 1-3 days after. In the circumpolar zone, close to the auroral zone, we used X observations at Edmonton, Churchill, Goose Bay and Resolute (Canada), at Leningrad, Murmansk and Yakutsk, and also at Lerwick (Great Britain). Thus, eight observatories were used. The observations were sufficiently regular in order to ensure a uniformity of the data for the mentioned five days in each case. Data on 32 flares were used for 1972, data on 15 for 1973, 17 -- 1974, 3 -- 1975, 4 -- 1976, 9 -- 1977. Thus, this period took in both the time of relatively high activity (1972) and a year of very low activity (1976) when over the course of individual weeks there were no spots on the sun at all.

Table 1

Change in Total Quantity of Ozone X in Dobson Units During Solar Flares of Classes 1B and 2B

Year	n	Circumpolar region					Tropical and equatorial regions				
		−1	0	1	2	3	−1	0	1	2	3
1972	32	382	382	372	370	380	271	264	272	272	274
1973	15	386	380	379	381	382	268	270	269	269	270
1974	17	380	378	376	375	371	273	275	276	275	273
1975	3	327	323	318	318	318	279	280	279	276	280
1976	4	403	401	406	408	410	278	278	278	279	284
1977	9	351	353	355	347	341	267	266	268	268	267
Mean for all flares											
	80	378	376	374	370	374	271	269	272	272	273

Note. n -- number of observations. Days: -1 -- day before; 0 -- day of flare, 1, 2, 3 -- days after flare.

The mean data for all 80 flares for the six-year period are given in Table 1. This table shows that in the circumpolar region at the time of a flare there is evidently a small gradual decrease in X in agreement with the above-mentioned photochemical hypothesis. The decrease in X from the "eve" of the flare to the second day

on the average was $\Delta X = -8$ d.u. (Dobson units). However, it varied from -12 in 1972 (the year of greatest activity) to +4 in 1976 (a year of very low activity). It is possible that the flare effect is dependent both on the flares themselves and on the general activity level.

Table 2

Standard Deviation σ of Mean Daily Data in Dobson Units

	1972	1973	1974	1975	1976	1977	Mean
Leningrad							
April	24.5	51.1	47.2	33.1	39,0	32.3	37.9
August	17,2	16.7	23,3	16.3	22.0	23,7	19,9
Edmonton							
April	33.2	36.0	37.8	31.0	20.6	52,7	35.2
August	26,3	25,1	25,3	40.1	22,4	20,0	26.5

However, on individual days with flares the ΔX values can deviate substantially from these means in both directions. For example, in 1972-1974 we discovered a number of cases when $\Delta X \leqslant -20$. Thus, on 13 January and 7 March 1972 ΔX attained -31; in 1973 and 1975-1977 there were no cases with $\Delta X \leqslant -20$. To be sure, it must be remembered that in a number of our observations there are also values $\Delta X > 0$ and that therefore the correlation of flares and X can be ambiguous or burdened by random deviations.

In order to evaluate the reliability of our data on the mean ΔX we compared them with v -- the value of the probable error in the daily X values. In this case, obviously, the mean error of data from n observatories for N cases of observations is

$$v = 0{,}67\,\sigma\,[\sqrt{nN-1}],$$

where σ is the standard deviation of the daily data for one observatory.

We computed the σ values for two characteristic observatories -- Leningrad and Edmonton, relatively close to the region of "hydrogen" auroras. The computations were made for April and August -- the months with the maximum and minimum ozone variability respectively (see Table 2).

On the other hand, the mean value ΔX for 1976, determined from observations of all four flares, has the probable error

$$v = 0{,}67 \cdot 30\,[\sqrt{4 \cdot 8 - 1}] \approx 3{,}5 \text{ dobson units,}$$

and the $\Delta X = +4$ value therefore in no case can be considered reliable or indicative for the ΔX variation.

It is obvious that rapid photochemical changes over the course of several days can occur only in that upper part of the ozone layer where the mean time for the setting-in of photochemical equilibrium is $\tau = 1$ day. For the usual system of ozone

reactions this will be above 36 km — in the atmospheric layer which was examined, in particular, for the above-mentioned observation of the flare of 1972. In the layer above 36 km (in the high latitudes) there is on the average about 27 d.u. of ozone. Thus, if the ozone changes which we discovered in these latitudes are actually associated with flares, the effect of the latter is a decrease in X by approximately 30%.

However, it is also necessary to examine the change in relaxation time τ of ozone with the postulated (see above) explosivelike formation of NO_x in the mesosphere. It can be somewhat different than with a mean state of the atmosphere and the level with τ = 1 day can be different.

Similarly we studied the changes in X in the tropical and in the equatorial regions. For this purpose we used observational data for Varansi, Mount Eba, Mauna Loa, Kodaykanal and Huancayo (between 23°N and 16°S). There were no progressive changes in X during the flare and for three days thereafter. In individual years the mean ΔX was from +2 to -3, averaging +1. True, in this zone the variability of ozone was small, $\sigma \approx 8$ and accordingly for the five observatories v = 0.3 d.u. However, in this case it is very difficult to ascribe a physical sense and value to ΔX = +1 (see Table 1). It can be surmised that the disturbance of the ozone layer arising during the period of a flare in the circumpolar latitudes during such a short time as three days can be propagated into the low latitudes. In addition, the absence of changes in X in the latter suggests that the electromagnetic radiation of a flare evidently produces a lesser influence on the ozone layer than corpuscular radiation. If the influence of direct irradiation by X- or UV-radiation was substantial and decisive the ozone changes would be far more appreciable in the low latitudes than in the high latitudes.

In the future, evidently, it would be of interest to analyze the influence of flares directly on the basis of observations of the vertical distribution of ozone. For the time being there are few such data.

BIBLIOGRAPHY

1. Dutsch, H. U., OZON IN ATMOSPHARE. GEFAHRDET DIE STRATOSPHARENVERSCHMUTZUNG DIE OZONSCHICHT? Hsg von Naturforschenden Gesellschaft in Zurich, 1980.

UDC 551.510.534

CHANGE IN THE TOTAL CONTENT OF ATMOSPHERIC OZONE DURING THE PASSAGE OF TYPHOONS

Moscow METEOROLOGIYA I GIDROLOGIYA in Russian No 9, Sep 80 pp 107-109

[Article by G. K. Gushchin, Karadagskaya Actinometric Observatory, submitted for publication 25 Feb 80]

[Text]

Abstract: On the basis of measurements from scientific research ships in the northwestern tropical zone of the Pacific Ocean it was possible to obtain the mean characteristic curve for change in the total ozone content in dependence on distance to the center of a typhoon. In the regions of a typhoon adjacent to the center and on its most distant periphery the quantity of ozone is 6-12% greater than in the undisturbed atmosphere. An ozone deficit (4-6%) is noted at distances 1,100-1,500 km from the center of the typhoon. These peculiarities in the distribution of the total ozone content can be explained qualitatively on the basis of vertical air movements noted during observations.

Circulation in a typhoon takes in the entire troposphere and even the lower stratosphere [7]. Intensive ascending and descending air movements, developing in a typhoon and leading, in particular, to fluctuations in the altitude of the tropopause, should also exert a definite influence on the atmospheric distribution of ozone.

The fluctuations of the total content of atmospheric ozone in the tropics are related for the most part to a change in the position of the subtropical anticyclones and have a small amplitude [3]. As an example, the table gives the mean daily values of the total ozone content (Ω) in the region of work of the expeditions "Tayfun-75" and "Tayfun-78," which were obtained on the southern periphery of the North Pacific Ocean subtropical anticyclone and characterize the undisturbed ozonosphere. The mean Ω value here was 0.255 cm and the deviations from the mean did not exceed ±4%.

The disturbed tropical atmosphere is characterized by completely different amplitudes of fluctuations of the Ω values. Intensive flows of stratospheric air from the temperate latitudes are accompanied by marked increases in the total content of

ozone by 30-50% [4]. On the other hand, ascending air movements in the ICZ can lead to a decrease in the Ω values by 60% [1, 2].

Table 1

Mean Daily Values of Total Ozone Content (Ω, 10^{-3} cm) on S and SW Peripheries of Subtropical Anticyclone Characterizing Undisturbed Ozonosphere in Region of "Typhoon" Expeditions (Data for 16th, 18th and 23d Voyages of Research Ships "Akademik Korolev" and 24th Voyage of Scientific Research Weather Ship "Priliv"

Date	Latitude, °	Longitude, °	Ω	Date	Latitude, °	Longitude, °	Ω
			1975 г.				
31 VIII	12.0 с.	113.7 в.	252	14 IX	18.5 с.	145.0 в.	255
11 IX	21.0	148.7	253	15	18.5 N	145.0 E	255
12	18.8	145.8	256	11 X	17.3 N	119.1 E	248
13	18.5	145.0	253	12	12.8	114.6	256
			1976 г.				
4 VIII	21.8 с.	129.7 в.	253	16 VIII	20.0 с.	170.2 з.	258
10	20.0	155.4	252	17	20.0 N	164.0 W	251
11	20.0	160.4	253	20	22.1	161.1	264
12	20.0	165.3	252	21	23.0	162.0	263
13	20.0	170.2	259	22	26.7	165.9	258
14	20.0	175.2	257				
			1978 г.				
22 IX	15.7 с.	148.0 в.	256	5 VIII	23.3 с.	146.2 в.	262
30	11.0	145.0	256	7	23.3	145.3	263
1 X	11.0	145.0	255	11	23.3	145.3	260
2	11.0	145.0	253	15	23.5	145.5	258
10	23.9	131.8	248	16	23.2	145.5	257
11	27.4	132.4	261	17	23.4	144.7	257
24 VI	25.0	149.0	253	18	23.2	144.5	249
25	25.0	145.0	252	24	23.3	131.5	257
26	22.0	143.5	253	19 IX	13.3	147.6	253
30	15.5	148.0	250	22	13.3	147.6	254
11 VII	11.1	149.5	248	25	13.3	147.6	257
3 VIII	22.0	147.8	252			Mean	255

With the passage of typhoons there were appreciable increases in the ozone concentrations in the upper troposphere and lower stratosphere [9] and a considerable decrease in the total ozone content in the region of ascending air movements [5]. Measurements of the total ozone content made on scientific research ships make it possible to trace the Ω distribution at different distances r from the center of typhoons (see Fig. 1). Use was made of observational data for several voyages of the scientific research ship "Akademik Korolev" and the scientific research weather ships "Okean" and "Priliv" in the northwestern tropical zone of the Pacific Ocean. The greatest volume of data was obtained on the 16th voyage of the scientific research ship "Akademik Korolev" during the "Tayfun-75" expedition.

Out of safety considerations the ships did not enter the typhoons and all the observations were made at great distances from the centers of the typhoons. However, a study of the processes even on the distant periphery of typhoons is of undoubted

interest because the influence of a typhoon extends far beyond its limits. For example, observations from a satellite show that the area of spiraling convective cloud cover entrained into a typhoon exceeds the area of the cloud vortex of the typhoon itself by a factor of 20 [6].

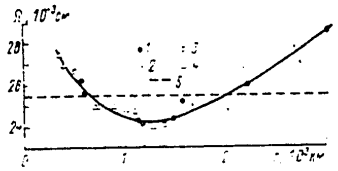

Fig. 1. Dependence of mean daily values of total content of atmospheric ozone Ω on distance r to center of typhoon. 1) typhoons; 2) Typhoon Tess; 3) tropical storm; 4) tropical depression; 5) mean Ω value in undisturbed atmosphere.

Typhoon Tess was tracked for the longest time and ozonometric observations made it possible to determine the trend in the change of Ω with $r > 1000$ km (see Fig. 1). In order to clarify the dependence of Ω on r at distances less than 1000 km observations were made in tropical depressions and on the peripheries of tropical storms. The legitimacy of combining observations relating to different stages of tropical cyclones follows from computations made using data from the "Tayfun-75" expedition and showing that the values characterizing the dynamic and energy state of the atmosphere in this case were completely similar both on the periphery of typhoons and in tropical depressions [8].

In Fig. 1 the curve drawn on the basis of 24 Ω values shows the change in the total ozone content with advance toward the center of the typhoon. The deviations of individual Ω values from the curve for the most part does not exceed 2%. The quantity of ozone is minimum at an average distance of 1300 km from the center of the typhoon and increases both with an increase and with a decrease in distance r. At distances of 1000-1500 km from the center of the typhoon the ozone deficit relative to the mean Ω value in the undisturbed atmosphere (0.255 cm) is 5-6%. With $360 < r < 500$ km and $2500 < r < 3000$ km the total ozone content exceeds the value 0.255 cm by 5-8 and 5-12% respectively.

Since typhoons have a relatively small extent and move tropical air masses rather homogeneous with respect to their ozone content, the advective changes in the values can scarcely be significant. Probably all the peculiarities in the distribution of the total ozone content represented in the figure are related only to the vertical movements of air in typhoon systems. In such a case in the region of ozone deficit (r = 800-1800 km) there should be a predominance of ascending air flows near the tropopause. In actuality, computations of vertical wind velocities made for distances of 800-1000 km from the center of typhoon Tess indicate that there, in a general case, it is possible to observe ascending movements up as far as the tropopause [8].

Observations and computations show that with $r > 300$ km descending movements usually develop [8] which should lead to an increase in the total ozone content. In our case with $r \approx 400$ km there was an increase in the Ω values by 8% relative to the mean value (0.255 cm).

On the most distant periphery of the typhoon ($r > 2000$ km) the total ozone content also increased and accordingly descending air movements predominate there.

Thus, the nature of changes in the Ω values (see Fig. 1) agrees qualitatively with the dynamics of typhoons. More numerous and specially organized observations make it possible to ascertain the quantitative relationships between the total ozone content and individual parameters of typhoons.

BIBLIOGRAPHY

1. Gushchin, G. K., "Latitudinal Variation and Seasonal Fluctuations of Total Content of Atmospheric Ozone in the Indian Ocean," TRUDY GGO (Transactions of the Main Geophysical Observatory), No 279, 1972.

2. Gushchin, G. K., "Correlation Between the Total Content of Ozone and the Quantity of Water Vapor in the Atmosphere Over the Oceans," TRUDY GGO, No 324, 1974.

3. Gushchin, G. K., "Principal Peculiarities in the Distribution of the Total Content of Atmospheric Ozone Over Ocean Areas," TRUDY GGO, No 357, 1976.

4. Kuznetsov, G. I., "Atmospheric Ozone Over the Tropical Zone of the Atlantic Ocean," DOKLADY AN SSSR (Reports of the USSR Academy of Sciences), Vol 171, No 3, 1966.

5. Nguen Tkhi Kiyen, Khrgian, A. Kh., "Some Characteristics of Atmospheric Ozone in the Tropics," VESTNIK MGU, FIZIKA, ASTRONOMIYA (Herald of Moscow State University, Physics, Astronomy), Vol 16, No 4, 1975.

6. Pavlov, N. I., Bel'skaya, N. N., Veselov, Ye. P., Bakushin, A. I., "Tropical Cyclones in the Cloud Cover Field According to Data from Meteorological Satellites and Radar Observations," TAYFUN-75 (Typhoon 75), Vol I, Leningrad, Gidrometeoizdat, 1977.

7. Palmen, E., Newton, Ch., TSIRKULYATSIONNYYE SISTEMY ATMOSFERY (Circulation Systems of the Atmosphere), Leningrad, Gidrometeoizdat, 1973.

8. Petrova, L. I., Nesterova, A. V., "Dynamic and Energy Characteristics of the Troposphere on the Periphery of Typhoons and in Zones of Their Maximum Frequency of Recurrence," TAYFUN-75, Vol I, Leningrad, Gidrometeoizdat, 1977.

9. Penn, S., "Ozone and Temperature Structure in a Hurricane," J. APPL. METEOROL., Vol 4, No 4, No 2, 1965.

UDC 551.510.4

DEPENDENCE OF CONCENTRATION OF TROPOSPHERIC CARBON DIOXIDE ON SURFACE PRESSURE

Moscow METEOROLOGIYA I GIDROLOGIYA in Russian No 9, Sep 80 pp 110-112

[Article by Candidate of Physical and Mathematical Sciences V. F. Belov, Doctor of Geographical Sciences V. D. Reshetov, Doctor of Chemical Sciences B. A. Rudenko and N. P. Shoromov, Central Aerological Observatory, submitted for publication 25 Feb 80]

[Text]

Abstract: This paper presents the results of aircraft measurements of the volumetric concentration of tropospheric CO_2 obtained in November 1978. The results, averaged for all altitudes, are represented in the form of a graphic dependence on atmospheric pressure of the air mass in which the measurements were made. The least squares method is used in finding the linear dependence of the CO_2 concentration on pressure. With an increase in pressure the CO_2 concentration in the troposphere decreases.

During recent years scientific interest in the carbon dioxide problem is increasing [3]. This interest is attributable to the fact that the mean CO_2 content in the atmosphere, beginning with the beginning of the century, is continuously increasing. For example, whereas at the end of the last century the relative volumetric concentration of CO_2 in the atmosphere averaged 290 parts per million parts of air ($mill^{-1}$), by the end of the 1970's it had attained 330 $mill^{-1}$. Thus, during this period the increase in the mean CO_2 content was 13.8%. The rate of increase of CO_2 during the last 20 years has also been increasing and by the end of the 1970's had attained 1.5 $mill^{-1}$/year [5].

This increase in atmospheric CO_2, according to the calculations of climatologists, can cause a warming of climate, which in turn can have such consequences as a thawing of the polar ice, inundation of the coasts of seas and oceans and unpredictable changes in the atmosphere [4]. In order to predict the further change in the atmospheric CO_2 content it is necessary to know the factors exerting an influence on the CO_2 content there.

The first regular observations of the atmospheric content of CO_2 were begun in Sweden and Finland in 1954 [8]. These observations were considerably activated during the period of the International Geophysical Year (1957-1958). The results of observations made in the free atmosphere by Bolen and Bischof for the northern

hemisphere, by Pearman and Garratt for the southern hemisphere [6, 7, 9]. In the Soviet Union such observations of the CO_2 content in the free atmosphere made from an aircraft were initiated in 1973 by the Central Aerological Observatory [1].

Observations during the first years were made with a coulometric gas analyzer. The instrument was installed aboard a flying laboratory -- an IL-18 flying laboratory. The measurement errors were 3-5% of the measured parameter. A preliminary analysis of the results of the measurements indicated that the CO_2 content in the troposphere was subjected to quite great variations attaining 10% or more of its mean content [1].

Table 1

Results of Aircraft Measurements of CO_2 Concentration in Troposphere in Different Air Masses at Different Altitudes Over Territory of Soviet Union in November 1978

Число 1	Высота, км 2										Район измерений 3	Давление, мб 4
	0,5	1	2	3	4	5	6	7	8	9		
2	328	317		335							Чарджоу 5	1000
15				329			327			320	Амдерма 6	970
17		317			310			305	310		Магадан 7	1020
18	338					310				324	Камчатка 8	990
19					317				304		Сахалин 9	1000
21	315		320	330		329		320		320	Сахалин 9	980
22			318	324		329	329		330		Братск 10	970
24		312	318	329				318			Донецк 11	1020
24			333				328		326		Москва 12	980

KEY:

1) Number
2) Altitude, km
3) Measurement region
4) Pressure, mb
5) Chardzhou
6) Amderma
7) Magadan
8) Kamchatka
9) Sakhalin
10) Bratsk
11) Donetsk
12) Moscow

In the analysis of the results it was possible to determine the factors which can be responsible for variability of carbon dioxide in the troposphere. In particular, it was discovered that the mean CO_2 content in the troposphere in clear anticyclonic weather is less than in cyclones [1]. Such facts have been noted earlier by other authors. For example, in determining the CO_2 content in the near-surface and near-water layers of the atmosphere from ships and automobiles it was possible to note a dependence of the CO_2 content in the air mass on its origin [2]. However, no correlation was noted between the CO_2 content in the air mass and cyclonic or anticyclonic circulation. Therefore the objective of this study was a clarification of the dependence between the CO_2 content in the air mass on atmospheric pressure.

For this purpose we analyzed the results of the observations made by the Central Aerological Observatory in November 1978 in the troposphere over the territory of the USSR. The measurements were made employing an improved method aboard an

aircraft employing a new airborne gas chromatographic gas analyzer developed by the Institute of Organic Chemistry imeni Zelinskiy USSR Academy of Sciences in collaboration with the Central Aerological Observatory on the basis of a standard-produced LKhM-8MD gas chromatograph.

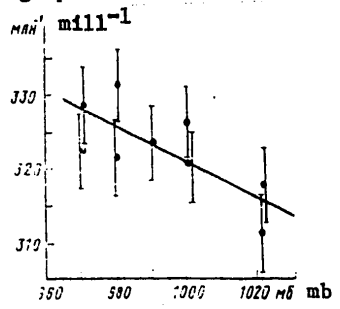

Fig. 1. Dependence of mean volumetric concentration of CO_2 in troposphere on atmospheric pressure at the earth. The graph shows the mean square measurement errors.

The operating principle of the gas analyzer is as follows. The air sample to be analyzed is transported by a helium flow through a chromatographic column filled with an adsorbent of the "polysorb" type. The components of the sample to be analyzed, with their passage through the column, are separated from one another and after emergence from the column are registered by means of a detector on the basis of the change in the thermal conductivity of the passing gases. The signals from the detector are fed to an automatic KSP-4 potentiometer, where they are registered in the form of peaks. The gas concentration in the sample is determined from the value of the peak, for example, from its height. Improvement of the aircraft method for measuring the CO_2 concentration involved the carrying out of regular calibration of the gas analyzer by means of a standard gas mixture with a known CO_2 content, determined with a high accuracy. The time required for the analysis of one sample was 3-5 minutes. The error in an individual measurement was 1-1.5%. The sampling of air for analysis was accomplished from the aircraft air line feeding air into the cabin.

The results of the observations of CO_2 content in the troposphere at different altitudes from 0.5 to 9.0 km, carried out in November 1978, are presented in Table 1 in the form of volumetric relative concentrations. The last column of the table gives the atmospheric pressure at the earth at the center of the air mass in which the observations were made. In order to clarify the dependence of the tropospheric CO_2 content on pressure at the ground level the observational data were averaged for all altitudes and plotted on a graph (Fig. 1). Here along the x-axis we have plotted the pressures at the ground level (see Table 1), and along the y-axis -- the mean CO_2 concentration in the troposphere.

The figure shows that with an increase in pressure at the ground level the CO_2 concentration in the air mass decreases. This fact agrees with the phenomenon, noted earlier in [1], of a lower CO_2 content in the troposphere under anticyclonic conditions. If it is postulated that the dependence of the CO_2 concentration on pressure at the ground level is linear, that is, that the CO_2 concentration is related to pressure P by the formula

$$C = aP - b, \quad (1)$$

then, using the least squares method, it is possible to determine the constants a and b in formula (1) using the experimental values C_i and P_i (see Table 1 and Figure 1).

After computing the coefficients a and b we obtain the following dependence of the volumetric concentration of CO_2 in the air mass on atmospheric pressure in the form

$$C = -0{,}235\,P + 555. \quad (2)$$

This dependence has a preliminary character since it is based on limited statistical data. Nevertheless, it can be of some interest in constructing mathematical models describing the CO_2 content in the troposphere in dependence on atmospheric pressure at the ground level. One of the reasons for the decrease in the CO_2 content with an increase in pressure at the ground level (that is, under anticyclonic conditions) can be a predominance of descending currents under such conditions, bringing from the upper layers air having a lesser CO_2 content, and vice versa, an increased CO_2 content in cyclones can be caused by ascending flows in a cyclone bringing CO_2 from surface sources.

BIBLIOGRAPHY

1. Belov, V. F., Reshetov, V. D., Khamrakulov, T. K., Shlyakhov, V. I., "Preliminary Results of Investigations of CO_2 in the Troposphere," METEOROLOGIYA I GIDROLOGIYA (Meteorology and Hydrology), No 10, 1975.

2. Bruyevich, S. V., Lyutsarev, S. V., "CO_2 Content in the Atmosphere Over the Pacific and Indian Oceans in the Black Sea Region," PROBLEMY KHIMII MORYA (Problems in Marine Chemistry), Moscow, Nauka, 1978.

3. Budyko, M. I., PROBLEMA UGLEKISLOGO GAZA (The Carbon Dioxide Problem), Leningrad, Gidrometeoizdat, 1978.

4. Budyko, M. I., ATMOSFERNAYA UGLEKISLOTA I KLIMAT (Atmospheric Carbon Dioxide and Climate), Leningrad, Gidrometeoizdat, 1973.

5. KHIMIYA NIZHNEY ATMOSFERY: SBORNIK STATEY (Chemistry of the Lower Atmosphere: Collection of Articles), Translated from English, Moscow, Mir, 1977.

6. Bischof, W., "Carbon Dioxide Measurements from Aircraft," TELLUS, Vol 22, No 5, 1970.

7. Bolen, B., Bischof, W., "Variation in the CO_2 Concentration for the Northern Hemisphere," TELLUS, Vol 18, No 1, 1970.

8. Fonselius, S., Koroleff, F., "Microdetermination of CO_2 in the Air, With Current Data for Scandinavia," TELLUS, Vol 7, No 2, 1955.

9. Garratt, J. R., Pearman, G. I., "Large-Scale CO_2 Fluxes in the Southern Hemisphere Troposphere," NATURE PHYS. SCI., Vol 242, No 117, 1973.

UDC 551.508.7

DETERMINATION OF THE WATER VAPOR CONTENT ON NEAR-SURFACE PATHS FROM THE SPECTRAL BRIGHTNESS OF OBJECTS

Moscow METEOROLOGIYA I GIDROLOGIYA in Russian No 9, Sep 80 pp 113-116

[Article by V. N. Marichev, Institute of Atmospheric Optics, Siberian Department USSR Academy of Sciences, submitted for publication 23 Nov 79]

[Text]

Abstract: The author has developed a simple and effective method for determining the integral moisture content of the air layer to an observed object, based on measurement of the intensity of the solar radiation reflected by the object in and outside the water vapor absorption band. The measurement method is described. The paper gives the results of determination of the precipitable layer of water vapor on paths with a length of 0.7-3 km, obtained on the basis of experimental data.

In order to solve a number of problems related to investigation of the physical properties of the atmosphere and also for practical needs it is necessary to have routine information on the integral characteristics of humidity on near-surface paths. In such cases it is of unquestionable interest to develop new, simple and effective methods for the remote determination of moisture content of air layers, as will be considered below.

The essence of the method is as follows. The earth's surface is illuminated by the sun, whose wide-band radiation spectrum takes in the vibrational-rotational absorption spectrum of atmospheric gases. In order to determine the gas content in the air layer to the observed object its spectral brightness is measured. In the measurements use is made of sectors corresponding to the absorption band of gas molecules (λ_2) and the nearest window of atmospheric transparency (λ_1). From a comparison of the signals received in the absorption and transmission sectors it is possible to determine the quantity of gas along the measurement path.

The expression for the sensed brightness of the observed object B(L), in accordance with [2], is written as follows:

$$B(L) = B_0 T(L) + B[1 - T(L)]. \quad (1)$$

where $T(L) = e^{-\gamma L}$ is the transmission function, γ is the extinction coefficient, B is the brightness of an infinitely extended air layer (that is, sky brightness at the horizon), B_0 is the true brightness of the object.

With increasing distance from the observed object the sensed brightness differs from the true brightness for two reasons [2]: first, because there is attenuation of radiation along the path from the object to the observer due to scattering and possible absorption; second, due to the fact that due to the fogging effect of atmospheric haze there is an increase in the brightness of the object proportional to the length of its layer. The first effect in (1) is taken into account by the function T(L) and the second by the second term, following from the Koshmider "light-air" equation. The corresponding spectral brightnesses for the two spectral sectors of interest are written in the form

[π = abs]

$$B_{\lambda_1}(L) = B_{0\lambda_1} T_{p\lambda_1}(L) + B_{\lambda_1}(1 - e^{-\xi_1 L}),$$
$$B_{\lambda_2}(L) = B_{0\lambda_2} T_{p\lambda_2}(L)\, T_{n\lambda_2}(L) + B_{\lambda_2}(1 - e^{-(\xi_2 + \alpha) L}). \quad (2)$$

where $T_{p\lambda 1}$, $T_{p\lambda 2}$ is the transmission function for a layer of the atmosphere with the extent L in the spectral sectors λ_1 and λ_2, determined by radiation scattering; $T_{abs\,\lambda 2}$ is the transmission function in the absorption band, determined by the absorption of radiation; ξ_1, ξ_2 are the coefficients of atmospheric scattering; α is the coefficient of molecular absorption.

The true spectral brightnesses of the object $B_{0\lambda 1}$, $B_{0\lambda 2}$ are determined as

$$B_{0\lambda_1} = g_{\lambda_1} \frac{\varkappa_{\lambda_1}(\theta)}{2\pi} E_{0\lambda_1} T_{p\lambda_1}(\infty),$$
$$B_{0\lambda_2} = g_{\lambda_2} \frac{\varkappa_{\lambda_2}(\theta)}{2\pi} \times E_{0\lambda_2} T_{p\lambda_2}(\infty)\, T_{n\lambda_2}(\infty). \quad (3)$$

Here $g\lambda 1$, $g\lambda 2$ are the spectral albedos of the object; $\varkappa_{\lambda 1}$, $\varkappa_{\lambda 2}$ are the scattering indicatrices for the radiation of objects in the direction of the observer; θ is the angle between the line of sight and the direction to the sun; $E_0\lambda_1$, $E_0\lambda_2$ are the spectral illuminations of the object without allowance for the attenuation of radiation; $T_{p\lambda 1}(\infty)$, $T_{p\lambda 2}(\infty)$, $T_{abs\,\lambda 2}(\infty)$ are the functions of transmission of radiation by the thickness of the atmosphere in the transparency window and the absorption band.

The brightnesses of an infinitely extended atmospheric layer $B_{\lambda 1}$ and $B_{\lambda 2}$, in accordance with [2], are represented as

[π = abs]

$$B_{\lambda_1} = \frac{\varkappa_{\lambda_1}(\theta)}{4\pi} E_{0\lambda_1} T_{p\lambda_1}(\infty),$$
$$B_{\lambda_2} = \frac{\xi_2}{4\pi(\xi_2 + \alpha)} \times E_{0\lambda_2} T_{p\lambda_2}(\infty)\, T_{n\lambda_2}(\infty). \quad (4)$$

where $f_{\lambda_1}(\theta)$, $f_{\lambda_2}(\theta)$ are the indicatrices of scattering of radiation by air in the direction of the observer.

On the basis of [4-6], for the spectral sectors of the visible and IR ranges, spaced several hundredths of a micron, it can be assumed with a high accuracy that

$$\begin{gathered}\xi_1 = \xi_2 = \xi, \quad g_{\lambda_1} = g_{\lambda_2} = g, \\ \varkappa_{\lambda_1} = \varkappa_{\lambda_2} = \varkappa, \\ T_{p\lambda_1} = T_{p\lambda_2} = T_p, \\ f_{\lambda_1}(\theta) = f_{\lambda_2}(\theta) = f(\theta).\end{gathered} \tag{5}$$

We introduce the coefficients f_K and f_Φ, determined as

$$f_K = \frac{B_{0\lambda_2}}{B_{0\lambda_1}}, \quad f_\Phi = \frac{E_{\lambda_2}}{E_{\lambda_1}}. \tag{6}$$

In accordance with the expressions (4), they will be equal to

$$f_K = \frac{E_{\lambda_2}}{E_{\lambda_1}} T_{п\lambda_2}(\infty), \tag{7}$$

[п = abs]

$$f_\Phi = \frac{\xi}{\xi + \varkappa} f_K.$$

The final expression for the transmission function $T_{abs\,\lambda_2}(L)$, which carries information on the gas content along the measurement path, is written as follows:

$$T_{п\lambda_2}(L) = \frac{1}{f_K} \times \frac{B_{\lambda_2}(L) - E_{\lambda_2}\left(1 - e^{-\xi \frac{f_K}{f_\Phi} L}\right)}{B_{\lambda_1}(L) - E_{\lambda_1}(1 - e^{-\xi L})}. \tag{8}$$

For determining $T_{abs\,\lambda_2}(L)$ it is necessary to find seven parameters, specifically B_{λ_1}, B_{λ_2}, E_{λ_1}, E_{λ_2}, f_K, f_Φ, ξ.

Measurement method. The expression for the registered signal in this case has the form

$$U(L) = \mu\Omega S B_{\Delta\lambda}(L)\,\Delta\lambda. \tag{9}$$

where μ is a coefficient including the response and transmission of the receiving system; Ω, S is the solid angle of the field of view and the area of the receiving antenna; $\Delta\lambda$ is the transmission band of the spectral instrument.

Since the useful information ultimately arrives in the form of electric signals, the expression for $T_{abs\,\lambda_2}(L)$ is written more conveniently through the values of these signals:

$$T_{\text{п}\,\lambda_2} = \frac{1}{f_K}\frac{U_{\lambda_2}(L)-\Phi_{\lambda_2}(L)}{U_{\lambda_1}(L)-\Phi_{\lambda_1}(L)} = \frac{1}{f_K}\frac{U^*_{\lambda_2}(L)}{U^*_{\lambda_1}(L)}. \qquad (10)$$

Here the signals $U_\lambda(L)$, $\Phi(L)$ are related to $B_\lambda(L)$ and $E_\lambda(L)$ by expression (9).

$T_{abs\,\lambda\,2}(L)$ is determined by satisfaction of the following operations:

1) The spectral signals $U_{\lambda 1}(L)$, $U_{\lambda 2}(L)$ from the observed object are measured.
2) The signals corresponding to sky brightness at the horizon are determined. Then with $L = \infty$ $U_{\lambda 1}(\infty) = \Phi_{\lambda 1}(\infty)$, $U_{\lambda 2}(\infty) = \Phi_{\lambda 2}(\infty)$, and $f_\Phi = \Phi_{\lambda 2}(\infty)/\Phi_{\lambda 1}(\infty)$.
3) Signals from a near-lying screen ($L = 0$) are registered, this excluding the contribution of haze to the total signal. From these signals we find the coefficient

$$f_K = U_{\lambda_2}(0)\cdot U_{\lambda_1}(0).$$

4) Using the meteorological range of visibility S_M we find the scattering coefficient ξ. For evaluating ξ it is possible to use tables of its dependence on wavelength for different S_M [3].

In cases when the object is situated at a short distance or atmospheric transparency is high, the influence of haze can be neglected.

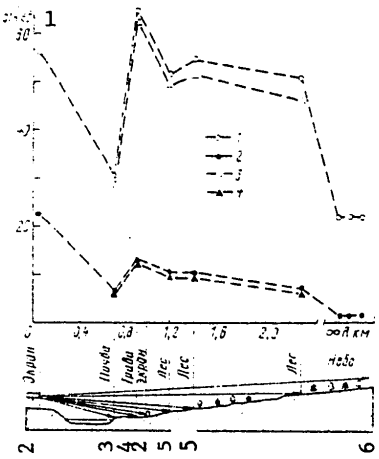

Fig. 1. Signals obtained in observation of some objects at different distances in two parts of spectrum: in band (2, λ = 942 nm) and near band (1, λ = 928 nm) (water vapor absorption band)

KEY:
1) Relative units
2) Screen
3) Soil
4) Grass
5) Forest
6) Sky

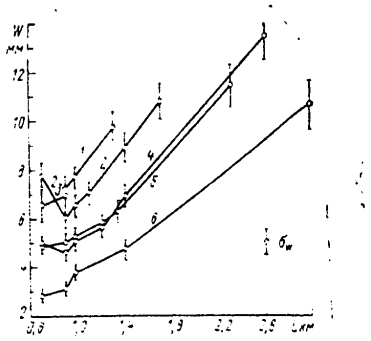

Fig. 2. Results of determination of precipitable layer of water vapor on the basis of measurement of the spectral brightness of objects.

Table 1

Mean Humidity Values $\overline{\rho}$ = W/L on Different Paths, 1977

1 Обозначения на рис. 2	2 Дата	3 Время	$S_м$ км	4 ξ км$^{-1}$	4 $\rho_п$ г/м^3	$p_г$ г/м^2	5 Протяженность до конца трассы, км: 6 берег 0,7	7 полная 0,9	8 экран 0,98	9 лес 1,1	1,2	1,3	1,4	1,7	2,3—3,0
4	28 V	16^{40}—16^{50}	25—30	0,10	5,0	5,4	7,1	5,3	5,2						5,2
5	28	17^{00}—17^{10}	25—30	0,10	5,0	5,5	7,0	5,8	5,4		4,7		5,0		4,9
2	31	17^{10}—17^{20}	22—25	0,12	5,5	6,5	7,9	6,6	6,6	6,4		4,8	6,4	6,3	
6	1 VI	16^{10}—16^{20}	20—25	0,13	3,2	3,6	4,0	3,45	3,8				3,4		3,5
1	2	16^{15}—16^{25}	25—30	0,10	7,5	8,2	9,5		8,0			7,6			
3	7	13^{20}	10	0,4	8,1	8,4	9,3	7,8							

KEY:
1) Notation in Fig. 2
2) Date
3) Time
4) g/m^3
5) Extent to end of path, km
6) Shore
7) Glade
8) Screen
9) Forest

The considered method was checked in the example of sounding of water vapor. We used spectral sectors near λ_1 = 929 nm (transparency window) and λ_2 = 942 (absorption band) with a width $\Delta\lambda$= 6 nm. This gave basis for using the empirical dependence between the precipitated layer of moisture W and the optical thickness $\tau_{abs}(W)$ [1], which we derived earlier, which is more conveniently written in the form

$$W = 9{,}5\tau_{\pi}^{1{,}39}. \qquad (11)$$

[π= abs]

where τ_{abs} is determined through the transmission function $\tau_{abs\,\lambda_2}(W)$: $_1$ abs = 1 $[T_{abs\,\lambda_2}(W)]^{-1}$.

Measurement results. An experiment for determining the integral humidity was carried out in May-June 1977 with solar zenith angles 35-60°. The length of the realized paths was in the range 0.7-3 km. One of the series of measurements is represented in Fig. 1. Here the signals denoted by the figures 1 and 2 relate to measurements λ_1 and λ_2 and the figures 3 and 4 represent signals obtained with allowance for the correction for the influence of haze. In this situation $S_M \simeq 25$ km ($\xi \approx 0.1$ km^{-1}). It can be seen that the signals in the transparency window are considerably stronger than in the absorption band. Their ratio $U_{\lambda_1}(L)/U_{\lambda_2}(L)$ increases with increasing distance of the observed object from 4.8 (L = 0.7 km, river shore) to 7.3 (L = 3 km, forest). The minimum and maximum ratios of the signals, 2.5 and 16.9, were obtained for a nearby screen (L = 0) and with measurement of sky brightness at the horizon ($L = \infty$).

The results of determination of the precipitable layer are given in Fig. 2, which gives the dependence of W on the length of the path on different days and different hours. The W values relating to the same series of measurements are connected by lines and annotated with figures corresponding to the numbers in the table. It can be seen that in general the increase in W is proportional to the length L of the path (with the exception L = 0.7 km, which will be mentioned below). The measurement error σ_w/W is 13-18% with S_M = 20-30 km and 21-27% with S_M = 10 km. The precipitated layers of moisture 4 and 5, determined on the basis of observational data from observations made with a 20 min interval, are in good agreement. The value for the precipitated layers was used in determining the mean humidities on the paths $\rho = W/L$, which are cited in the table. As a comparison, here we have also given the humidities measured with a psychrometer at the reception point (ρ_{rec}) and an optical hygrometer [1] on a path with L = 0.98 km (ρ_{hy}). In all cases it was ascertained that the humidity along the path reception point - shore (see Fig. 1) exceeds the control humidities ρ_{rec} and ρ_{hy}, which surpasses the measurement error. The figure shows that this path then passes closer than the others to the water surface and therefore high mean humidity values should be expected here, as was discovered in the experiment. The humidities measured along one and the same path reception point - screen by the two different methods (also described from the radiation of a thermal source) agree well with one another (the difference does not exceed 10%). On paths rising higher above the river the ρ values are close to ρ_{rec}. A comparison of the data obtained by different methods gives basis for drawing the conclusion that the proposed method can be recommended for determining the integral content of water vapor on paths of different length. An analysis of the accuracy characteristics of the method, not presented here to save space, shows that the accuracy in determining W, considered above, can be improved to 8-15%. Among the merits of the method is its simplicity, ease of use and routineness in making measurements in the surface layer in any azimuthal directions and the possibility of sounding other atmospheric gases.

BIBLIOGRAPHY

1. Borovikov, V. G., Marichev, V. N., "Instrument for Optical Measurement of Atmospheric Humidity," TEZISY DOKLADOV PYATOGO SIMPOZIUMA PO LAZERNOMU I AKUSTICHESKOMU ZONDIROVANIYU ATMOSFERY (Summaries of Reports at the Fifth Symposium on Laser and Acoustic Sounding of the Atmosphere), Tomsk, 1978.

2. Gavrilov, V. A., VIDIMOST' V ATMOSFERE (Atmospheric Visibility), Leningrad, Gidrometeoizdat, 1966.

3. Zuyev, V. V., et al., "Atmospheric Propagation of Laser Radiations," ZARUBEZHNAYA RADIOELEKTRONIKA (Foreign Radioelectronics), No 7, 1977.

4. Zuyev, V. Ye., RASPROSTRANENIYE VIDIMYKH I INFRAKRASNYKH VOLN V ATMOSFERE (Propagation of Visible and IR Waves in the Atmosphere), Moscow, Sovetskoye Radio, 1970.

5. Zuyev, V. Ye., Kabanov, M. V., PERENOS OPTICHESKIKH SIGNALOV V ZEMNOY ATMOSFERE (Transfer of Optical Signals in the Earth's Atmosphere), Moscow, Sovetskoye Radio, 1977.

6. Shifrin, K. S., Zel'manovich, I. L., TABLITSY PO SVETORASSEYANIYU. T. III, KOEFFITSIYENTY OSLABLENIYA, RASSEYANIYA I LUCHEVOGO DAVLENIYA (Tables of Light Scattering. Vol III. Coefficients of Attenuation, Scattering and Ray Pressure), Leningrad, Gidrometeoizdat, 1968.

UDC 551.5:556:46:378.96

FIFTIETH ANNIVERSARY OF THE MOSCOW HYDROMETEOROLOGICAL INSTITUTE AND THE MOSCOW HYDROMETEOROLOGICAL TECHNICAL SCHOOL

Moscow METEOROLOGIYA I GIDROLOGIYA in Russian No 9, Sep 80 pp 117-119

[Article by K. A. Khzmalyan, USSR State Committee on Hydrometeorology and Environmental Monitoring, submitted for publication 7 Feb 80]

[Text] The Moscow Hydrometeorological Institute (MHMI) and the Moscow Hydrometeorological Technical School (MHMTS) were organized in 1930 in the system of the Hydrometeorological Committee of the Council of People's Commissars in the USSR. These were the first specialized hydrometeorological instructional institutions not only in our country, but in the entire world.

The MHMI was organized on the basis of the Department of Geophysics of the Physics Faculty at Moscow State University and the MHMTS was organized on the basis of a nine-year school near Moscow (Saltykovka village) where students in the eighth and ninth years were specially trained for work as observers at meteorological stations.

The organization of the MHMI and the MHMTS was directly associated with the broad development of hydrometeorological investigations and studies necessary for ensuring the grandiose problems of industrialization of the country, uplifting of agriculture and maximum use of the natural resources of the country outlined by the Communist Party in the years of the First Five-Year Plan.

During the first year of existence of the MHMI a total of about 100 students studied in its two faculties (meteorological and hydrological). However, already in 1931 their number had increased to 500 and by 1940 they numbered 1000.

The rapidly growing needs of the hydrometeorological service, scientific, planning-engineering and other organizations for highly qualified meteorologists, hydrologists, oceanographers and agrometeorologists made it necessary not only to expand the MHMI, but also to create the Khar'kov Hydrometeorological Institute, and also to organize the training of specialists with hydrometeorological knowledge at a number of other colleges. Such specialists are now being trained at 14 institutes of higher education in our country. About 8,000 students are in these fields of specialization.

The development of hydrometeorological investigations and the network of hydrometeorological stations also required expansion of the training of professional hydrometeorologists with intermediate qualifications -- meteorological technicians,

aerologists, hydrologists, oceanographers and agrometeorologists. Now technicians with hydrometeorological fields of specialization are being graduated from 11 intermediate specialized academic institutions with a total number of students over 7000.

A great service of the organizers, first directors, professorial and instructional staff of the MHMI and MHMTS has been that from the very beginning the instruction of hydrometeorological specialists has rested on a fundamental formulation of physical-mathematical and special disciplines. It has been carried out with allowance for the prospects of development of hydrometeorological science and practical work. At the same time, much attention has been devoted to both the theoretical and practical aspects of training of students, the creation of an instructional-laboratory base, production of fundamental textbooks and study aids, development of scientific and scientific teaching staffs, improvement in the living conditions for students, their ideological-political education and military-sports training.

A highly important role in all this was played by the attraction of leading scientists to instructional work at the young and relatively small Moscow Hydrometeorological Institute. These included B. P. Apollov, S. L. Bastamov, Ye. V. Bliznyak, V. F. Bonchkovskiy, M. A. Velikanov, N. N. Zubov, P. Ya. Kochina, Ye. S. Kuznetsov, A. I. Kaygorodov, S. S. Kovner, N. A. Lavrent'yev, B. P. Mul'tanovskiy, S. I. Nebol'sin, B. P. Orlov, B. V. Polyakov, N. N. Slavyanov, B. I. Semikhatov, S. P. Khromov, V. V. Shuleykin, V. M. Shul'gin and many other outstanding specialists.

It is impossible to overlook the great work which has been carried out by the military department of the MHMI under the direction of A. A. Samoylo.

A major contribution to the organization and development of the MHMTS was made by its first directors and instructors M. M. Gol'tsov, S. P. Zouloshnov, V. A. Uspenskiy, N. M. Bochkov, Ye. A. Sokolov, V. D. Bykov, A. P. Loidis, Ye. V. Mal'chenko, A. A. Lucheva and other workers at the technical school.

The first director of the Moscow Hydrometeorological Institute, Professor Vasiliy Alekseyevich Belinskiy, who still continues his scientific and teaching activity, devoted many efforts to the organization and realization of the MHMI and the MHMTS. In all stages of development of hydrometeorological education great attention was devoted to it by the directors of the Hydrometeorological Service.

Many of the first instructors and students of the MHMI and MHMTS are no longer alive. Some of them gave up their lives in the struggle with fascism in the years of the Great Fatherland War. The bright memory of these people has been preserved among their friends and comrades; it lives in the modern achievements in hydrometeorology in our country which came about with their participation.

The successful development of the system of hydrometeorological education played a decisive role in providing the hydrometeorological service and other interested organizations with highly qualified scientific, engineering-technical and supervisory personnel.

During the threatening years of the Great Fatherland War the accumulated experience made possible the training and retraining, within a relatively short period of time, of hydrometeorological specialists for the Soviet Army and Navy, the

transformation of the MHMI into the Higher Military Hydrometeorological Institute (HMHMI). After the end of the war the HMHMI was reorganized into a civilian hydrometeorological institute and moved to Leningrad (LHMI -- Leningrad Hydrometeorological Institute).

During the years of its existence the MHMI and its successors (HMHMI and LHMI) trained more than 13,000 highly qualified specialists in hydrometeorological fields and the MHMTS graduated 11,500 hydrometeorological technicians. Graduates of these academic institutions can be encountered in many republics, krays and oblasts of our Motherland, in the Arctic and Antarctica and on far expeditions. A considerable number of them became outstanding scientists and organizers. They are successfully carrying out scientific and pedagogic activity and are heading up major scientific and operational-production groups in the system of the State Committee on Hydrometeorology and other departments; they are working in responsible posts in the central administration and local agencies of the State Committee on Hydrometeorology.

Naturally, with the passing years, in accordance with the new, higher requirements on specialists, there has been a further improvement in the entire system of hydrometeorological education, an intensification of academic and instructional work, an improvement in academic documentation. During recent years the hydrometeorological schools have begun the training of specialists (by means of specialization in the higher courses) in such modern directions as numerical weather forecasting methods, artificial modification of atmospheric processes, long-range weather forecasting, hydrometeorological measurements and instruments. At the Khar'kov Institute of Radioelectronics there is now training of radio engineers with specialization in the field of radar systems used in hydrometeorology and at hydrometeorological technical schools there is training in the field of specialization "hydrometeorological radar apparatus." A special course entitled "Preservation of the Environment" has been introduced at all colleges and technical schools training hydrometeorological specialists and programs in special disciplines have been supplemented. This has required a considerable strengthening of the academic-material base for academic institutions and a re-examination of curricula and programs, the preparation of new and supplementing of earlier published textbooks.

During the last 10 years alone the Hydrometeorological Publishing House has published more than 100 textbooks and study aids for students at colleges and technical schools teaching hydrometeorological fields of specialization. Many of these are original study aids on new disciplines or they are substantially revised and supplemented textbooks on traditional subjects.

In adopting measures for improving hydrometeorological education, Soviet scientists and specialists make extensive use of international communication. They participate in the activity of the WMO, UNESCO and other specialized agencies of the UN for the dissemination of the achievements of the Soviet Union in this field and in study of leading foreign experience. Comparing the status of training of hydrometeorologists in the USSR with the training of similar specialists in the well-developed capitalist countries, it is possible to note with satisfaction the superiority of Soviet hydrometeorological education not only with respect to the number of specialists in training, but what is most important, the high quality

of this training. This is leading to an increase in the interest of foreign scientists in the experience of training hydrometeorological personnel in our country and a constant increase in the number of foreigners coming to the USSR for training and gaining experience in the field of hydrometeorology. During recent years the number of foreign students studying in the colleges and technical schools in the Soviet Union with hydrometeorological fields of specialization has reached 326. They represent 59 countries. They include about 60 scholarship holders of the WMO from 16 countries. In addition, Soviet hydrometeorological experts are doing much work in the training of national personnel in a number of foreign countries.

The development of hydrometeorological investigations and studies increasing the requirements on the hydrometeorological service in connection with the transformation of the Hydrometeorological Service into the USSR State Committee on Hydrometeorology and Environmental Monitoring is making necessary a further improvement in hydrometeorological education, taking into account:

-- the need for satisfying the increasing requirements of agriculture and water management, electric power, transportation, construction and other branches of the national economy for completeness and quality of regime, prognostic and computed hydrometeorological materials;
-- practical introduction of automatic and remote instruments and apparatus, automated systems for the collection and processing of hydrometeorological data, electronic computers, space meteorological systems and other new technical equipment;
-- organization of a system for monitoring the state of the environment, the level and sources of its contamination, as well as the development of investigations in this field;
-- development of investigations and practical work in the field of artificial modification of atmospheric processes;
-- strengthening of international cooperation in the field of hydrometeorological investigations and preservation of the environment.

In accordance with the resolutions of the 25th Congress CPSU and subsequent resolutions of the Party and government, particular attention must be devoted not only to a further increase in the quality of the professional training of specialists, but also a resolute intensification of ideological-educational work at colleges and technical schools.

The formation and development of the system of higher and intermediate special hydrometeorological education played its decisive role and continues to remain one of the most important factors in the successful solution of the problems facing hydrometeorological science and practice.

REVIEW OF MONOGRAPH BY S. L. VENDROV: 'PROBLEMS IN TRANSFORMATION OF RIVER SYSTEMS IN THE USSR' (PROBLEMY PREOBRAZOVANIYA RECHNYKH SISTEM SSSR), Leningrad, Gidrometeoizdat, 1979, 207 pages

Moscow METEOROLOGIYA I GIDROLOGIYA in Russian No 9, Sep 80 p 120

[Review by A. A. Sokolov and V. V. Kupriyanov]

[Text] The second edition of a monograph by S. L. Vendrov, entitled PROBLEMY PREOBRAZOVANIYA RECHNYKH SISTEM SSSR (Problems in the Transformation of River Systems in the USSR), appeared in 1979. It has attracted the attention of scientists and specialists due to the novelty of formulation of the problem. In this monograph the author has set forth his points of view concerning highly complex modern problems related to the use and conservation of water resources of the country.

In his reasonings and conclusions the author relies not only on a deep understanding of hydrological phenomena and processes occurring during the regulation and redistribution of river runoff with time and in space, but also on the basis of his rich personal experience in participation in expert evaluation of many water management processes carried out in the USSR.

The author has an original and extremely successful method of exposition of material, presented in the form of reflections sometimes of a polemic character, and not from the point of view of a disinterested observer, but as a profoundly concerned specialist highly reacting to the by no means always successful intervention of man in natural processes, counseling careful treatment of the environment, every possible protection of nature against exhaustion and contamination.

The book, abounding in factual information, examines a wide range of questions associated with the problems of present-day and long-range reconstruction of the hydrographic network, analysis of changes in the hydrometeorological regime as a result of anthropogenic activity, the need for the redistribution of runoff over the territory of the USSR.

In analyzing the negative phenomena associated with different transformations of water bodies, S. L. Vendrov does not descend to the extremely widespread unfounded condemnations of a number of projects which have been carried out, but examines all aspects of the problem, in his way weighing the resulting socioeconomic effect and expenditures on restoration of the damage inflicted on the environment. The

author uses as a point of departure the correct materialistic idea of the inevitability and necessity of an active transformation of water systems and individual objects. His understanding of the Sevan problem is characteristic in this respect. S. L. Vendrov agrees that the depletion of part of the century-long accumulations of lake water would worsen the entire complex of natural conditions of this unique water body, but the waters of the Razdanskiy cascade were the only initial material base for the economic development of the Armenian SSR during the period of the pre-war five-year plans. Now that the tasks of economic development of the Armenian SSR have to a large extent already been realized, the preservation of Sevan is of primary national importance.

S. L. Vendrov objectively evaluates the rapid "moral aging" of water management principles and schemes for the use of water resources as the economic and social development of the country progresses.

In examining the national economic role of the regulation of runoff of our lowland rivers, S. L. Vendrov also notes the problem of the need, already existing today, for a universal reduction of the areas of reservoirs for the purpose of freeing arable lands for their economic exploitation.

With respect to the problems of redistribution of runoff, S. L. Vendrov uses as a point of departure the historical inevitability and socioeconomic necessity of their solution in our country. However, the means and methods for implementing this, as correctly noted by the author, must be well studied and validated. It is also important to take into account and carefully weigh all the possible ecological changes in the regions from whence water is taken and to which it is redistributed. And indeed, an equally important, and possibly the main circumstance is that it is necessary to make full, economically rational use of water resources without allowing their unnecessary loss.

One can disagree with individual conclusions presented by the author and his evaluations of different projects, but it must be admitted that the general concepts developed in the monograph are characterized by depth and penetration into the essence of the problems involved in the preservation of the environment and its transformation in the interests of a socialist society.

The book will unquestionably find a broad response among specialists working in the field of effective use of water resources, the transformation of river systems and preservation of the environment.

SIXTIETH BIRTHDAY OF SEMEN SAMUILOVICH KAZACHKOV

Moscow METEOROLOGIYA I GIDROLOGIYA in Russian No 9, Sep 80 p 121

[Article by members of the Board of the USSR State Committee on Hydrometeorology and Environmental Monitoring]

[Text] Semen Samuilovich Kazachkov, chief of the Omsk Territorial Administration of Hydrometeorology and Environmental Monitoring, marked his 60th birthday on 28 August.

From the time of his graduation from the Leningrad Hydrometeorological Institute in 1945 all his activity has been associated with the hydrometeorological service. Being deputy chief of the Administration of the Hydrometeorological Service of the Kirgiz SSR, to which S. S. Kazachkov was sent in 1946, he did considerable work on the construction and reconstruction of hydrometeorological structures and development of the hydrometeorological network in the mountainous regions of the Kirgiz SSR.

S. S. Kazachkov became chief of the Omsk Territorial Administration, one of the largest administrations in our country, in 1955. During this time the administration did considerable work on development of the network, which more than doubled, and a service for safeguarding the environment was recreated.

The exploitation of the virgin lands in the southern part of the administration, the petroleum and gas deposits in its northern part, the construction of new cities and settlements, railroads and highways required a radical restructuring of the hydrometeorological servicing of all branches of the national economy, a task with which the personnel headed by S. S. Kazachkov has successfully contended. And servicing continues to improve.

The productive activity of Semen Samuilovich has been repeatedly recognized by departmental awards and valuable presents.

In 1976 Semen Samuilovich was awarded the order of the Red Banner of Labor for implementation of the targets of the Ninth Five-Year Plan and for the successes attained in the hydrometeorological servicing of the national economy.

S. S. Kazachkov has been a member of the CPSU since 1945. His organizational abilities and his high qualifications fruitfully contribute to the development of the meteorological service in our country.

We sincerely wish Semen Samuilovich good health and further successes in work.

SEVENTIETH BIRTHDAY OF VALENTIN DMITRIYEVICH KOMAROV

Moscow METEOROLOGIYA I GIDROLOGIYA in Russian No 9, Sep 80 pp 121-122

[Article by specialists of the USSR Hydrometeorological Scientific Research Center]

[Text] Professor Valentin Dmitriyevich Komarov, Doctor of Geographical Sciences, Meritorious Worker in Science and Technology RSFSR, marked his 70th birthday on 5 July.

The scientific and teaching activity of the outstanding Soviet professional hydrologist V. D. Komarov, who has made a major contribution to the development of hydrological forecasts, has received broad recognition in our country and abroad.

The creative work of Valentin Dmitriyevich began in 1934 at the Central Weather Bureau immediately after his graduation from the Moscow Hydrometeorological Institute. Already in his first scientific studies he laid out the principles of a fundamentally new approach to investigations of the spring runoff of rivers, to study of the physical laws of formation of runoff on the basis of the water balance equation.

This scientific direction is being productively developed by V. D. Komarov himself and by his numerous students.

During the period of the Great Fatherland War V. D. Komarov worked in routine support of the operational army with hydrological forecasts. Since 1943 his creativity has been inseparably associated with the Central Institute of Forecasts, organized in this same year and subsequently reorganized into the USSR Hydrometeorological Center.

There he did much work in creating a general model of formation of high water. His fundamental works, including the monograph VESENNIY STOK RAVNINNYKH REK YEVROPEYSKOY CHASTI SSSR, USLOVIYA FORMIROVANIYA I METODY PROGNOZOV (Spring Runoff of the Lowland Rivers of the European USSR, Conditions of Formation and Forecasting Methods), became reference books for all hydrologists. The deep scientific analysis and sagacity of the researcher enabled him to see broad possibilities of territorially universal dependences in the development of methods for long-range forecasts of runoff for different geographical zones. As a result of these studies we now have methods for predicting the runoff of many rivers in the USSR and the inflow of water into reservoirs. These are being successfully used in the country's economic activity.

Experimental investigations at runoff stations, one of whose founders and organizers was V. D. Komarov, have played a major role in the development of the physical aspect of runoff investigations.

A rigorous formulation of scientific experiments (such as investigation of the phenomenon of infiltration into frozen soil), evaluation of observations, analysis and theoretical generalization of an enormous volume of field observations, enabled V. D. Komarov to detect a series of highly important regularities becoming the basis of our knowledge concerning the process of formation of meltwater runoff. They are used in modern mathematical models describing this process.

The ATLAS SNEZhNOGO POKROVA YEVROPEYSKOY TERRITORII SSSR (Atlas of the Snow Cover of the European USSR), created under his direction, is used extensively in the development of forecasting methods and in hydroengineering planning.

During recent years Valentin Dmitriyevich has been working on the problem of prediction of the runoff of mountain rivers and has engaged in extremely important and responsible public-scientific activity. He is a member of three scientific councils and is deputy chairman of the Expert Council on the Earth Sciences of the USSR Higher Certification Commission.

V. D. Komarov is the author of several monographs and more than 50 articles and one of the authors of a textbook on hydrological forecasting which has been translated into several foreign languages and which enjoys a well-deserved broad fame among hydrologists in our country and beyond its limits.

Teaching activity plays a significant place in the life of Valentin Dmitriyevich and has earned him the love and respect of hundreds of hydrologists with advanced training who attended his lecture courses, profound in their content and clear in their exposition. His graduate students, successfully defending their dissertations, are continuing to develop the Komarov school.

The scientific and humane rectitude of his judgments, high demands on himself and others, soundness in evaluating the results of investigations, enormous capacity for work and his kind relationship to people always create a special climate of productive creative activity and absence of compromise in scientific discussions and in the groups in which his activity takes place.

The services of V. D. Komarov in the development of Soviet hydrological forecasting have received high recognition from the government. He has been awarded two orders and several medals.

Friends, students and colleagues with all their hearts congratulate Valentin Dmitriyevich Komarov on his birthday and wish him good health and new creative successes.

SIXTIETH BIRTHDAY OF GENNADIY PETROVICH GUSHCHIN

Moscow METEOROLOGIYA I GIDROLOGIYA in Russian No 9, Sep 80 pp 122-123

[Article by specialists of the Main Geophysical Observatory]

[Text] Doctor of Technical Sciences Gennadiy Petrovich Gushchin, head of the section on actinometry and atmospheric optics at the Main Geophysical Observatory, marked his 60th birthday on 7 September 1980.

The scientific activity of G. P. Gushchin began in 1946 at the Vorkuta Scientific Research Permafrost Station. In 1954 he completed his graduate work at the Main Geophysical Observatory and in 1958 defended his Candidate's dissertation there. Between 1960 and 1965 he worked as senior scientific specialist at the Main Geophysical Observatory and beginning in 1965 and up to the present time he has been head of the section.

The field of scientific interests of G. P. Gushchin is closely related to the problem of atmospheric ozone. He developed and introduced the integral method for measuring total ozone. He created the M-83 filter ozonometer and introduced it into industrial production and into the network of stations in the USSR. The ozonometric network of the USSR was created under his direction and operates under his supervision. In 1957 G. P. Gushchin developed an airborne ozonometer and introduced it

into practical work and for the first time in the world organized regular observations of total ozone on aircraft and scientific research ships, which are continuing even now. In 1969 Gennadiy Petrovich successfully defended his doctoral dissertation on the theme: "Investigation of Ozone in the Earth's Atmosphere." A series of studies by G. P. Gushchin became well known: in these investigations the phenomenon of deformation of the field of atmospheric ozone by a jet stream was discovered. In 1968, on the basis of computations, for the first time he demonstrated that the presence of nitrogen oxides leads to a decrease in the concentration of atmospheric ozone. Since 1961 G. P. Gushchin has published a series of studies in which for the first time he developed a one-dimensional theoretical model of an ozone layer with a physical interpretation of the latitudinal and annual variations of ozone.

A considerable part of the activity of G. P. Gushchin has been devoted to an investigation of the spectral transparency of the atmosphere and the optical properties of atmospheric aerosol. He developed, and introduced in the network of stations, a method for measuring the spectral transparency of the atmosphere and the characteristics of atmospheric aerosol. An instrument for measuring the spectral transparency of the atmosphere has been developed and introduced. In a number of studies he generalized data from network observations on spectral tmospheric turbidity for the territory of the USSR.

Many of the studies of G. P. Gushchin dealt with investigations of the patterns of transmission of solar UV radiation through the atmosphere. He evolved a physical interpretation of the C. F. Rodionov effect, based on the multiple scattering of light.

During recent years G. P. Gushchin developed, and introduced in the network of stations, a method for measuring the natural UV radiation. A network of stations for measuring UV radiation was established and operates under his direction.

Gennadiy Petrovich has published about a hundred scientific studies, including two monographs, a number of methodological instructions, and has received two author's certificates for inventions. He has been awarded the emblem "Distinguished Worker of the Hydrometeorological Service," a number of diplomas and medals, including the silver medal of the All-Union Exhibition of Achievements in the National Economy.

Over a period of many years G. P. Gushchin has been a member of the International Commission on Atmospheric Ozone, has been a member of a number of international working groups on radiation and ozone and has repeatedly participated in international comparisons and intercalibrations of ozonometric instruments.

We congratulate Gennadiy Petrovich on his birthday and wish him good health and further successes.

CONFERENCES, MEETINGS AND SEMINARS

Moscow METEOROLOGIYA I GIDROLOGIYA in Russian No 9, Sep 80 pp 123-125

[Article by Yu. G. Slatinskiy]

[Text] A scheduled session of the basin section "Indian Ocean and the Southern Seas" of the Scientific Council on the Problem "Study of Oceans and Seas and Use of Their Resources" of the USSR State Committee on Science and Technology was held during the period 12-14 March 1980 at Sevastopol'. The session was attended by 75 persons from 13 scientific research, planning and other organizations whose activity is related to the sea. From the State Committee on Hydrometeorology the session was attended by specialists of the Sevastopol' Division of the State Oceanographic Institute and the sea section of the Crimean Hydrometeorological Observatory. The speakers summarized the preliminary results of a broad complex of scientific research studies carried out by members of the basin section during the Tenth Five-Year Plan. Twenty-eight scientific reports were presented at the session. They were devoted to different aspects of study of the hydrometeorological regime of the Black Sea, an increase in its biological productivity and use of the results for the national economic needs of the country.

In discussing the preliminary results of investigation of the dynamics and thermal parameters of the active layer in the Black Sea, N. K. Shelkovnikov (Moscow State University) noted that difficulties in the interpretation of numerous field observations of temperature, conductivity and current velocities in the coastal zone led to the need for formulating a whole series of laboratory experiments in order to understand better the mechanism and patterns of the considered phenomena. An investigation of the averaged and fluctuating characteristics of the turbulent flow was carried out in a rectangular open chanr l. Data were obtained on the vertical distribution of the velocity of flow, including near the water-air discontinuity.

Yu. M. Belyakov (Marine Hydrophysical Institute) reported on the results of study of inertial currents. On the basis of observational data from numerous buoy stations it was possible to trace the variability of inertial currents from the surface to a depth of 1.5-1.6 km. It was noted that at all depths the rotation of the vector of the inertial current occurs in a clockwise direction and the phase shift from the surface to a depth of 1.5-1.6 km is about 20 hours.

V. B. Titov (Southern Division Institute of Oceanology) told of some results of long-term measurements of currents from a stabilized buoy. An experimental buoy was set out in a polygon along the Caucasus coast at a depth of 70 m; measurements

were made by BPV-2 automatic recorders with a discreteness of 60 min. The results of the observations confirmed the predominance of along-shore flows whose direction varies in the course of the seasonal alternation of winds. Currents of a northwesterly direction prevail for about 7 months per year; currents of other directions prevail about 5 months. The observations also indicated that the current velocities vary from 2-5 to 128 cm/sec. Current velocities of a northwesterly direction are 1.5-2 times greater than for the southeasterly direction.

L. D. Rozman (Institute of Biology of the Southern Seas) discussed some problems relating to study of the structure of mesoscale turbulence in the Black Sea. It was established that the principal dynamic factor determining the turbulent regime is current velocity. The coefficients of turbulent exchange increase proportionally to the values of the velocity vector only to a definite value. The report gives universal dependences of the anisotropy of turbulence and turbulent exchange on the mean current velocity vector obtained for the conditions prevailing in the Black Sea.

G. S. Dvoryaninov (Marine Hydrophysical Institute) reported on investigations of turbulence in the wave mixing layer. A layer whose depth is commensurable with the characteristic wavelength was used in the computations. All the principal characteristics of the layer of wave mixing were analyzed: the field of drift currents, the wave velocity field, the distribution of turbulent energy and the coefficients of turbulent exchange of momentum and heat. The results of the computations agree well with experimental data and field observations.

G. G. Neuymin (Marine Hydrophysical Institute) told about study of optical characteristics in the Black Sea and the prospects for further development of these studies. It was noted that with respect to optical properties the waters of the Black Sea differ sharply from the waters of other internal seas and approach those of highly transparent ocean waters. The uniqueness of the vertical structure of the waters also finds its reflection in the optical properties, as is indicated by the presence of a stable abyssal layer of reduced transparency, as well as an increase in the selective absorption of short-wave radiation with an increase in depth in the western part of the sea. The reports of I. L. Isayev and V. G. Shemtura (Marine Hydrophysical Institute) were devoted to investigations of the mesoscale field of temperature and transparency and the hydrooptical characteristics of waters of the Black Sea. The authors analyzed the results of the summer expedition of 1979 on the scientific research ship "Aytodor." In order to establish a correlation between the optical and biological characteristics the measurement of transparency was accompanied by determination of the concentration of organic carbon.

L. F. Yermakova, O. I. Belyayeva and N. G. Khorolich (Sevastopol' Division of the State Oceanographic Institute) reported on the results of hydrological, hydrochemical and hydrobiological investigations carried out in the open sea and in individual regions of the coastal zone. The observations were made synchronously by four ships in 16 special polygons having the configuration of a square with sides having a length of about 10-12 miles. The investigations which have been made will serve as a basis for optimizing the network of stations and the choice of the most representative observation points.

L. V. Kurakova (Institute of Biology of the Southern Seas) told of new data obtained in the course of study of the variability of the content of phosphates in the coastal waters. It was noted that the observed concentrations of phosphates at the sites of discharge of sewage are considerably greater than should be the case under the condition only of their dilution by sea water. Simultaneous observations of the content of dissolved oxygen indicated that its content in such places is somewhat reduced in comparison with pure sea water. It is postulated that this is caused by inadequate aeration of waters at the time of dilution of effluent and great expenditures of oxygen on the oxidation of entering organic matter.

K. K. Zelenov (Moscow State University) presented a new hypothesis on the reasons for hydrogen sulfide contamination of Black Sea waters. It is postulated that an important source for the entry of hydrogen sulfide into the deep layers of the sea is the anticlinal structures of Upper Cretaceous calcareous rocks lying under recent deposits and emerging at the surface in the neighborhood of Sochi-Matsesta. According to the calculations of the speaker, the "flares" rising from the sea floor contain about 290 million tons of dissolved hydrogen sulfide; its excess corresponds to the quantity annually oxidizing in the zone of contact with oxygen.

A. V. Krotov (Odessa Division Institute of Economics) discussed some problems involved in increasing the biological productivity of the Black Sea. It was noted that the biological resources of the Black Sea are quite great. During 1973-1978 the fish catches in all parts of the basin were from 280,000 to 430,000 tons annually. According to long-range calculations, in the course of the coming decade the fish catch can be increased to 0.5 million tons. In addition, it will be possible to harvest a great quantity of other sea products, including about 200,000 tons of phyllophora and 300,000 tons of mussels from natural fishing areas. In order to maintain stable productivity of the water body there is a need for immediate investigations for optimizing river runoff so that hydroengineering measures which are being taken and which are being planned will not inflict losses on the productivity of the water body.

A. F. Vysotskiy (Institute of Government and Law Ukrainian Academy of Sciences) in his address told of some peculiarities of application of the norms of international law to the Black Sea basin.

G. S. Baskirov (Odessa Division Institute of Economics) reported on the development of long-range development of the productive forces of the southern economic region on the basis of use of the natural resources of the Black Sea.

S. G. Boguslavskiy (Marine Hydrophysical Institute) familiarized specialists at the session with the plan for the basic directions in investigations of the Black Sea during 1981-1985.

The resolution which was adopted contained a formulation of a number of fundamental tasks for the further development of investigations and improvement in the coordination of activity of the marine institutes in the Sea of Azov-Black Sea basin. It was recommended, in particular, that synchronous complex surveys be regarded as the basic method for studying the regime of the Black Sea. In this connection they

should be carried out in a standard network of stations covering the entire sea surface or its individual regions, depending on the formulated tasks. It was deemed desirable that when carrying out synchronous surveys the observations at all the hydrological stations be carried out to the bottom. It was also recommended that work be done in evaluating the effectiveness of environmental protection measures applicable to the Black Sea basin.

AT THE EXHIBITION 'ANALYTICAL INSTRUMENTS-80' (ANALITICHESKIYE PRIBORY-80)

Moscow METEOROLOGIYA I GIDROLOGIYA in Russian No 9, Sep 80, pp 125-126

[Article by I. M. Shenderovich]

[Text] An exhibition entitled "Analytical Instruments-80" was held during the period 11-20 March 1980 at Tallin. This international exhibition was attended by participating firms from 12 countries, including the United States, Great Britain, Japan and Italy.

At this exhibition, in addition to instruments intended for analytical investigations carried out for scientific and industrial purposes, there were also oceanographic instruments and equipment for monitoring the state of the environment.

At the exhibition instruments for investigations of the seas and oceans developed by companies in the United States — "Neil Brown Instrument System, Inc." (NBIS) and "General Oceanics, Inc." (GO) were represented most fully.

The DRSM-1 remote current meter, exhibited by NBIS, is of considerable interest for oceanographers. This instrument consists of a submergible sensor and an on-board reading device, connected with one another by a two-strand cable. In the sensor housing there is a two-contact acoustic converter of flow velocity and an induction-type compass. The depth of sensor submergence is up to 1,000 m.

An on-board unit processes the information arriving from the sensor and feeds out readings of current velocity and direction on two digital displays. At the same time, information in analog form can be fed to an external memory device.

Measurements of flow velocity are ensured by means of two independent high-frequency (1.6 MHz) acoustic emitters situated at a right angle to one another. The phase shift of the acoustic beams reflected from an acoustic mirror is dependent on the direction and flow velocity of the water relative to the sensor housing. The range of measurement of flow velocity with the DRSM-1 instrument falls in the range from 0 to 250 cm/sec, the error is about ±1 cm/sec, or 5% of the velocity value (which is greater), the nonlinearity is not more than 1% of the measurement range, the range in measuring direction is 0-360°, the error is not greater than 2°, the admissible tilt of the sensor housing is 30°.

The NBIS Company demonstrated the Mark III CTD sounding system for measuring temperature, conductivity and depth of instrument submergence. As the water temperature converter use is made of a combination of a low-inertia thermistor and a highly precise platinum thermometer. Such a unit is insensitive to thermistor zero drift. Conductivity is measured with a four-electrode element made with aluminized ceramics with platinum black. The pressure sensor is a wire strain gage sensing element. The system consists of an instrument submergible on a cable and an on-board reading device. A single-strand armored cable ensures instrument submergence to 6,500 m. The transmission of information along the cable is accomplished successively for each measured parameter in digital form.

The ranges of pressure measurement (depending on design) are: 3.2, 6.5, 16.0, 32.0 and 65.0 MPa with an error up to 0.1% of the total scale. The range of temperature measurement is from -3 to +32°C with an error not greater than 0.005°C. The range of measurement of conductivity is from 1 to 65 mmho with an error of 0.005 mmho.

The "GO" Company for the most part is developing different types of bathometers for the sampling of sea water and apparatus for their placement and triggering at a stipulated horizon. Depending on the formulated tasks and operating conditions it is possible to use bathometers of the same design, but with a different volume of the samples taken -- from 1.2 to 4[illegible].0 liters. The design of the bathometer is a cylinder open at both ends which is closed by covers by means of springs passing through the inner part of the cylinder.

The bathometers can be employed either individually or in groups, with 12 or 24 instruments per holder.

When working with bathometers in holders the control of triggering at a stipulated horizon is accomplished by means of electric signals fed by means on an on-board command device through a single-strand power cable.

A sea current meter of the pendulum type (model 6011) developed by this firm is of definite interest. In this instrument the current velocity is determined from the angle of deviation of the housing from the vertical and the direction is determined from the angle between the direction along the magnetic meridian and the longitudinal axis of the current meter housing. The instrument contains a tilt sensor of the weight type and a compass with a three-component sensor for measuring the magnetic field based on the use of the Hall effect. Data on the tilt angle and the compass readings are autonomously registered on a magnetic tape. The processing of data and computation of the current velocity and direction are accomplished using an on-board unit.

The current meter has the following measurement ranges: flow velocity 0-225 cm/sec, housing tilt 0-90°, current direction 0-360°. The error in measuring tilt is ±0.5° and the current direction is 2.0°. The capacity of the magnetic recorder is 38,000 measurements, the frequency of the measurements is from 1 to 512 measurements per hour, the depth of submergence is as great at 6,000 m.

The "KROHNE" Company (West Germany) at the exhibition demonstrated different types of mobile (truckborne) stations for monitoring the state of the environment. The stations ensure measurement of a number of meteorological parameters: wind speed

and direction, temperature and relative humidity, atmospheric pressure and also the air content of carbon monoxide, ozone (oxide and dioxide), sulfur gas, sulfur dioxide, nitrogen and other substances, as well as the dust concentration. The measurement of parameters and the taking of air samples can be accomplished at altitudes up to 10 m using an extensible telescopic mast. Apparatus for both processing and registering data in 20 measurement channels was installed in the truck body. The station ensures measurement of the instantaneous and averaged (for a selected time interval) parameters and also feeds signals when the measured parameter exceeds a threshold value. The processing program can be readily restructured. The registry of the collected data is on teletape, punch tape and magnetic tape.

The company produces a number of variants of a mobile station for monitoring the state of the environment.

The British company "Nuclear Enterprises" exhibited three instruments for measuring soil moisture content and density under natural conditions. Instrument operation is based on measurement of the absorption and scattering of radioactive (γ-rays and neutrons) emission of the soil and the moisture which it contains.

The neutron instrument for measuring soil moisture content consists of a source of fast neutrons, a detector of slow neutrons and an electronic reading unit. The number of moderated neutrons is dependent on the number of light atoms (of the hydrogen type) present in the investigated medium.

An instrument with a source of γ-radiation is used in measuring soil density in general, including the moisture present in it. The density of the medium is judged from the backscattering of the γ-radiation measured with a detector of γ-rays in a case when the source and detector are situated over the soil and from the backscattering and absorption when the source and detector are situated in the soil at some distance from one another.

The exhibited units for measurement of soil density and moisture content are characterized by a high measurement accuracy (about 1%), a short time required for measurements (less than 1 minute), simplified servicing and increased safety in operation because use is made of radioactive sources with a low radiation level.

NOTES FROM ABROAD

Moscow METEOROLOGIYA I GIDROLOGIYA in Russian No 9, Sep 80 p 127

[Article by B. I. Silkin]

[Text] As reported in SCIENCE NEWS, Vol 116, No 7, 1979, an apparatus has been constructed at Purdue University (Lafayette, Indiana) which can be used in physical modeling of tornadoes. The apparatus is used in creating conditions similar to those which lead to tornadoes under the environment of the plains and prairies of the United States Middle West which are natural for them.

The apparatus is a cylindrical chamber with a height of 7 m and a diameter of 4 m. Air is fed into the chamber through a rotating screen, entering there through an opening with a variable diameter which is situated in the bottom. The conditions most suitable for the development of a tornado are thereby created: resistance against a horizontal air flow, its rotation in a circle with a large radius and rapid ascent.

The artificial tornadoes in the chamber attain a height of 145 cm and their velocity is 20 m/sec. Thus, a possibility is created for safe study of the behavior of a tornado from its initial phases of development to the formation of funnels, including several funnels, which under natural conditions results in particularly extensive destructive consequences.

A group of specialists at Purdue University, consisting of K. R. Church, E. M. Agee and J. T. Snow, who constructed this apparatus, the largest of its type among similar apparatuses in the United States, is using it in a series of experiments in which the conditions are recreated corresponding to many really occurring tornadoes. A fact which was established is that during a tornado the maximum velocity is attained by those air masses which are in the surface layer of the atmosphere. Further experiments have the purpose of studying the boundary layer of the cone of air trapped by the rotation and the nature of the small-scale circulation within it.

*****

As reported in SCIENCE NEWS, Vol 116, No 21, 1979, the principal weather-forming factor for a considerable part of Asia and the entire coast of the Indian Ocean is monsoons. However, their role in global atmospheric circulation has not yet been adequately studied.

An attempt at studies of the characteristics of monsoons over a long period of time has been undertaken by the scientific specialists J. L. Kallen (Brown University, Providence, Rhode Island, United States) and J.-K. Duplessis (Radioactivity Study Center, France). A report which they presented at a conference of the American Geological Society, held in San Diego (California) in November, 1979, examined the types of fossil foraminifera, organisms essentially dependent on water salinity, at different times living in the Indian Ocean.

It was established that the salinity of waters in the Bay of Bengal is determined by the intensity of the southwesterly monsoon. A strong monsoon drives into the bay a great quantity of fresh water, lessening its salinity; however, weakening of the monsoon causes an increase in the content of salts. Thus, the nature of deposition of foraminifera in columns of sedimentary rocks is an indirect indicator of the intensity of monsoons at a definite time.

The columns studied by J. L. Kallen and J.-K. Duplessis covered the last 25,000 years, that is, a period which includes the most recent transition from conditions of maximum glaciation to the warm conditions of the interglacial period.

The investigations indicated that during the period of maximum glaciation the monsoons lost their intensity, whereas during the transition to warmer conditions they became stronger. Global circulation, on the other hand, becomes stronger in a glacial epoch. In other words, the cycle of the degree of intensity of monsoons does not coincide with the cycle of glaciations. For the time being the reason for this remains unclear.

*****

As reported in NEW SCIENTIST, Vol 84, No 1186, 1979, a special radar network of four stations has been established in Great Britain for use in weather forecasting. The equipment used at the stations has an effective radius of about 200 km and it makes it possible six hours in advance to determine the characteristics of impending precipitation with an accuracy to 1 mm/hour at a distance of about 100 km.

The data collected by the radar are fed into a computer at the central station. There, as a result of their analysis and comparison with other meteorological information, in particular, with data on wind velocity, a weather map is prepared which shows the location of the rain front. The quantity of moisture present in a cloud is not determined in this system.

In the late 1980's plans call for expanding this network to 12 stations so that it will cover the entire territory of Great Britain.

OBITUARY OF VLADIMIR NIKOLAYEVICH PARSHIN (1919-1980)

Moscow METEOROLOGIYA I GIDROLOGIYA in Russian No 9, Sep 80 p 128

[Article by members of the Board of the USSR State Committee on Hydrometeorology and Environomental Monitoring and specialists of the USSR Hydrometeorological Scientific Research Center]

[Text] Soviet hydrometeorological science has experienced a severe loss. Professor Vladimir Nikolayevich Parshin, Doctor of Geographical Sciences, a leading scientist and organizer of science, CPSU member, deputy director of the USSR Hydrometeorological Center, died on 19 July 1980 in his 62d year.

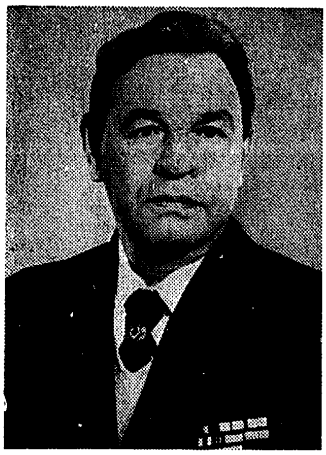

V. N. Parshin was born on 16 January 1919 in Moscow. During the Great Fatherland War he was deputy chief of the hydrometeorological division of the operations staff of the Third Guard Army. Upon completing his combat service in Prague, in 1945 he went to work at the Central Institute of Forecasts, now the USSR Hydrometeorological Center.

Precisely there, working alongside leading professional hydrologists, V. N. Parshin rapidly developed from a novice researcher to a major scientist in the field of general hydrology and hydrological forecasts. His fundamental investigations in

the field of long-range forecasts of river runoff in the zone of inadequate moistening are well known. In particular, the physicostatistical methods which he proposed for the long-range forecasting of the runoff of the most important rivers in the southeastern part of the European USSR, Kazakh and Turkmen SSRs, are still being used effectively in the practical, operational hydrological servicing of the national economy of the country.

V. N. Parshin, for the first time in hydrology, used the method of objective analysis of the fields of meteorological elements for study of the field of spring runoff. The correctness of the theoretical premises which he advanced was convincingly confirmed by the method for predicting water inflow into the reservoir of the Tsimlyanskaya Hydroelectric Station which he developed on the basis of these premises. Engaged in the study of the formation and distribution of the snow cover in the European USSR, V. N. Parshin gave a theoretical validation for the optimum distribution of the network of snow cover observation stations.

The scientific interests of V. N. Parshin were exceedingly broad. It is no accident that during recent years highly important investigations were carried out under his direction in the field of agrometeorology, devoted to the development of methods for the long-range prediction of crop yield and the gross grain harvest.

V. N. Parshin performed exceptionally important services as an organizer of hydrometeorological support of the national economy of the country and he personally participated in the servicing of key Party and government agencies. He has devoted much attention to the popularization of science and hydrometeorological forecasts.

The Party and government have placed a high value on the multisided activity of V. N. Parshin, awarding him the orders of the Red Star, Red Banner of Labor and many medals. He was awarded the gold medal of the All-Union Exhibition of Achievements in the National Economy three times.

Those who for many years worked together with Vladimir Nikolayevich will forever remember him not only as a scientist and leader, but also as a sound Communist, a sensitive and responsive person sincerely interested in the fate of each of us.

[2-5303]

5303
CSO: 1864

-END-